Spatial periodic solutions of the extended Cahn-Hilliard equation

UNIVERSITY *of* LIMERICK

OLLSCOIL LUIMNIGH

SPATIAL PERIODIC SOLUTIONS OF THE EXTENDED CAHN–HILLIARD EQUATION

By

Roman Olegovich Sedakov

SUBMITTED IN FULFILLMENT OF THE
REQUIREMENTS FOR THE DEGREE OF
DOCTOR OF PHILOSOPHY
AT
UNIVERSITY OF LIMERICK
LIMERICK, IRELAND
MAY 2012

UNIVERSITY OF LIMERICK
DEPARTMENT OF
MATHEMATICS AND STATISTICS

The undersigned hereby certify that they have read and recommend to the Faculty of Informatics and Electronics for acceptance a thesis entitled "**Spatial periodic solutions of the extended Cahn–Hilliard equation**" by **Roman Olegovich Sedakov** in fulfillment of the requirements for the degree of **Doctor of Philosophy**.

Dated: May 2012

External Examiner: _____
Dr. Edward Cox

Research Supervisor: _____
Prof. Eugene S. Benilov, Dr. William Lee

Internal Examiner: _____
Dr. Jean Charpin

UNIVERSITY OF LIMERICK

Date: **May 2012**

Author: **Roman Olegovich Sedakov**

Title: **Spatial periodic solutions of the extended Cahn–Hilliard equation**

Department: **Mathematics and Statistics**

Degree: **Ph.D.** Convocation: **June** Year: **2012**

I hereby declare that this thesis is entirely my own work and that it has not been submitted for any other academic award.

Signature of Author

Table of Contents

Abstract

The present thesis studies the problem of existence and stability of spatial periodic solutions of the extended Cahn–Hilliard equation. The extended Cahn–Hilliard equation is a well-known model that describes the process of phase transition in diblock copolymer melts and can be derived using the general Landau theory of phase separations together with some approximations for a short range and long range interactions in copolymer subchains [7], [31], [35].

In this thesis we will present studies of the existence of periodic steady states of the extended Cahn–Hilliard equation in a full parameter space. We will analytically describe steady states in the case of weak nonlinearity (solutions are close to trivial) using perturbation theory. Besides single-wave solutions, described by Liu and Goldenfeld in [32], we found regions where two-wave solutions coexist along with the general type solutions. Numerical studies were done to find periodic steady states in general situation without any assumptions regarding parameters.

We will also present linear stability analysis of described above steady states for bounded disturbances using Floquet boundary conditions. Stability diagram will be shown and comparison with the results of [32] will be presented.

Acknowledgements

I would like to thank my supervisors Prof. Eugene S. Benilov and Dr. William Lee for their relentless support, scientific guidance and warm advice. I have benefitted enormously from our many discussions.

I would like to express my gratitude to Dr. Jean Charpin, Dr. Michael Vynnycky and Dr. Andrei Korobeinikov, whom I often approached with scientific questions. Their advice and stimulating discussions were greatly rewarding.

Also, I would like to thank all the members of MACSI who welcomed me as a part of the group and helped with my research-related and general-life queries and problems. I am grateful to my fellow PhD students and especially to Vladimir Lapin. Finally, I would like to thank my close friends and family for their caring, support and warm encouragement. Special thanks to my dear friend Ivan, whose illustrations were used in this thesis and to my beloved sister Julia.

I gratefully acknowledge the financial support of the Science Foundation Ireland and MACSI (Mathematical Applications Consortium for Science and Industry).

Chapter 1

Introduction

1.1 Thesis motivation

Originally the problem of phase separation of diblock copolymers came to our attention via the 62nd European Study Group with Industry, where it has been presented by CRANN (for references see [13] [30]). The main goal was to model the phase separation process for block copolymers, with a particular interest in how block copolymers self-organize in a corner geometry. The problem happened to be as interesting as it is vast. Now, we will give an introduction to diblock copolymers (BCP) and phase separation in BCP melts.

Block copolymers are synthesized by chemically combining blocks of several dissimilar homopolymers along a chain backbone. Thus, a diblock copolymer is a chain molecule consisting of two different subchain molecules A and B attached to each other. Each subchain A and B consists of different unit monomers a and b, respectively (See Fig. 1.1). In that kind of system even weak repulsion of different monomers leads to a strong repulsion between subchains A and B. In the slow quenching of a melt of such BCPs, at some critical temperature segregation of different type submolecules occurs. But since A and B submolecules are chemically bonded, even strong repulsion between subchains cannot lead to full phase separation. However local microphase separation is present (See Fig. 1.2). Copolymers tend to self assemble in various microstructures, where A– or B– rich domains can

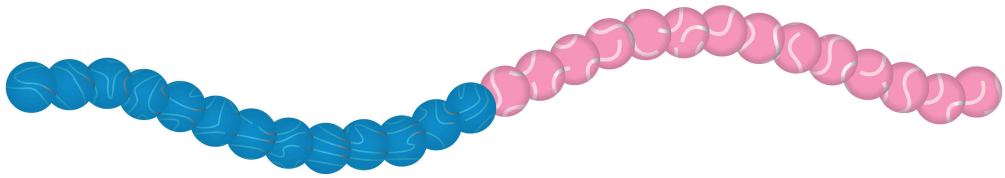

Figure 1.1: A schematic diblock copolymer molecule. A and B subchains are shown in different color. Each of the subchains consists of different unit monomers.

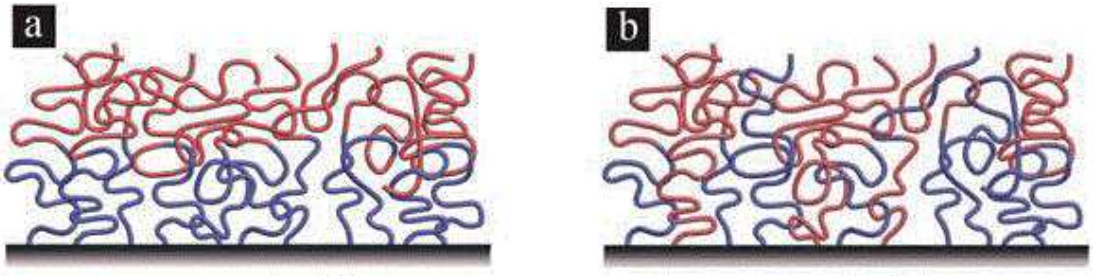

Figure 1.2: Ordered and disordered structures of diblock copolymers.

be formed. This microphase formation produces a large number of different periodic spatial patterns. In experiments, such systems form, for instance, periodic lamellar, spherical, cylindrical structures depending on the relative chain length of two cobonded polymers and on the amount of solvent present in the mixture (for references see [14], [20] and [21]) (See Fig. 1.3). As was pointed out before, such ordered structures are of great technological interest (for references see [15], [16]), for example to produce nanowires. Not to mention the great scientific interest in understanding the process of phase transitions.

There are several ways to proceed from here and examine such phase transitions. Firstly, there is the atomistic Monte-Carlo simulation based on molecular dynamics of unit monomers. Such method is the most accurate one, but computationally intensive and low on insight (to understand the process of phase transition molecular

dynamics studies should be carried out, but since such studies can be very specific and definitely have to imply a lot of chemical theory we did not use it in our work). The second one is mesoscopic Monte–Carlo simulation [25, 29, 30]. The papers referenced above deal with phase separation in binary alloys, which is a preface to studies of phase separation in BCP. One of the main advantages of Monte–Carlo simulations is that in contrast to real experiments one can work with generic systems and avoid the complexities that are often present in the real ones. Thus, Monte–Carlo simulations are easy to setup and run and they are good for insight, but it was impossible to use them for non rectilinear geometries (corner geometries), that were studied during the Study Group. Finally, analysis of PDE models are always available. They provide a good insight and they are much easier to set up in a complex geometry. A valid model to describe phase transition in BCP melts is a widely known extension of a Cahn-Hilliard equation. It is important to look at the origins of the theory of phase transitions, which goes back to Landau general theory of second-order phase transitions (for reference see [26]) and Cahn and Hilliard's theory of non-uniform melts [7, 8, 9]. At some point we realized that the problem of corner geometry of spatial patterns of BCP, as it was presented on the Study Group is not a fundamental one, and, therefore we decided to study the extended Cahn–Hilliard equation on its own. In the present thesis we consider spatial periodic solutions of both Cahn–Hilliard equation and its extension, as the solutions that are related to the periodically patterned mesophases of phase segregation in BCP.

1.2 Previous work

In this section we will briefly provide reviews of some relevant previous works. Interest in the extended Cahn–Hilliard equation is mainly connected to studies of phase separation in BCP melts. Therefore, understanding of the present theory of processes of phase separation, as well as analysis of studies of the extended Cahn–Hilliard equation that had been done in the light of phase transition, will be an objective of the sections of this chapter.

As both industrial and scientific interest in BCP was growing in the 1970's a number of studies of the process of phase transition in polymers started to appear

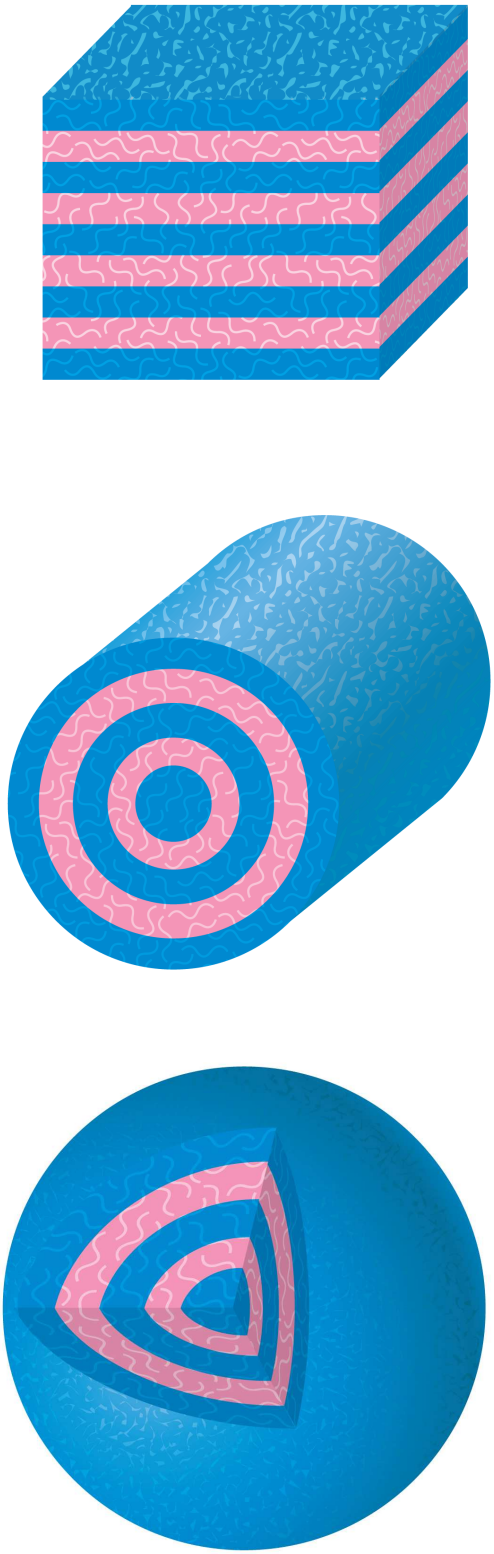

Figure 1.3: Various types of BCP structures: lamellar, cylindrical, spherical.

during this period. In 1975 Helfand [18] and then in 1976 in collaboration with Wasserman [19] proposed an interesting way of modeling such a process by calculating the free energy and concentration distribution from a modified diffusion equation. They start by defining two different regimes of microphase segregation: strong–segregation limit and weak–segregation limit. Structured BCP periodic domain patterns are characterized by a large amount of interfaces between A and B rich zones. If the dimension of such an interface is compared to the average size of domain D (by domain here is assumed the length of the entire phase) then the polymer melt is said to be in the weak-segregation limit. On contrary if the interface is smaller than D, then strong-segregation limit takes place and that would mean that distinct A– or B–rich phases are present. The interphase free energy is considered to be similar to the energy of an interface tension, which is the result of the excess energy of unavoidable A and B contacts as well as losses of entropy to avoid such contacts in the process of segregation [17]. However, there is another component of the free energy determined by the following: one can find out that the situation where a polymer's joint is situated in the interphase is energetically more favorable but that would result in loss of entropy, as the degree of freedom of such joints is limited to the interfaces, thus, to limited regions, which results in entropy losses. One should consider another aspect. Since joints are rather to be found in the interfaces, there is a tendency to have a greater density there. But for such a media as BCP, with very small compressibility, this inhomogeneity is strongly opposed. This would result in straightening the BCP molecules in the direction normal to interface boundary, which leads to further loss of conformational entropy. Here are stated the main aspects to be considered by mathematicians working on defining of the free energy of BCP melts.

Helfand and Wasserman reduced their studies to the strong-segregation limit mainly. They used the analogy between the conformation of a polymer molecule and the trajectory of a Brownian particle. If the Brownian particle is enclosed between two parallel walls with perfectly elastic collision that would impose periodic boundary condition for polymer molecules. Then the free energy of the ordered state of BCP is the following

$$F = c_1 \frac{N}{D} + c_2 \left(\frac{D}{N^{\frac{1}{2}}} \right)^{\omega}, \tag{1.1}$$

where D is the domain size (size of an A–rich phase), N is a polymerization index or a number of unit monomers in a polymer, c_1 and c_2 are numerical constants. The first term of (1.1) is the interfacial energy. The second term is the conformational entropy. The exponent ω was found numerically [19]

$$\omega \simeq 2.5.$$

Minimization of F with respect to D gives an equilibrium which was found to be at

$$D \sim N^{0.636},$$

for a lamellae structure. Their result is in a good agreement with experiments. As it was briefly mentioned before, they have also studied spherical and cylindrical structures [20, 21].

Several years later Leibler [31] proposed quite a different method to define the free energy of BCPs. According to him complete understanding of the phase separation in melted block copolymers requires not only a statistical study of microdomain structures appearing after the transition, but also a study of the homogeneous (disordered) phase. A question of great importance is to find a quantity which may be used to introduce an order parameter of phase transition. The order parameter was chosen to be a local field of density difference of two unlike monomers. It can be given by the following

$$\phi(\mathbf{r}) = \langle (1-f)\rho_A(\mathbf{r}) - f\rho_B(\mathbf{r}) \rangle,$$

here f is the fraction of monomers A in copolymer chain. It is justified to consider the zero of limit compressibility and assume

$$\rho_A(\mathbf{r}) + \rho_B(\mathbf{r}) = 1,$$

for any $\mathbf{r}$, ρ_A, ρ_B reduced densities, local density of corresponding monomers at a point to the overall monomer average density throughout the melt. Taking into account incompressibility and $\langle \rho_A(\mathbf{r}) \rangle = f$ we have

$$\phi(\mathbf{r}) = \langle \delta\rho_A(\mathbf{r}) \rangle = \langle \rho_A(\mathbf{r}) - f \rangle,$$

average deviation from the uniform A, B polymer distribution. Another great advantage is that Leiber's free energy has only two parameters relevant to characterization of phase equilibrium in BCP melts: the composition f (the fraction of monomers A in a polymer chain) and the product χN (where N is the polymerization index and χ is the Flory parameter). The Flory parameter characterizes the energy of interaction in polymers melt and can be defined as the following

$$\chi = \frac{1}{k_B T} \left(\epsilon_{AB} - \frac{1}{2} \left(\epsilon_{AA} + \epsilon_{BB} \right) \right),$$

where k_B is a Boltzmann's constant, T is a temperature, ϵ_{ij} is the energy of interaction between 'i'–type and 'j'-type monomers. It is worth mentioning that χ happens to be a controlling parameter of segregation. Experiments show that χ is positive. Since χ is positive there is a tendency to avoid $A - B$ contacts, as such contacts increases the free energy and avoiding $A - B$ contacts apparently leads to phase separation. Speaking in terms of entropy, such organized structures are not favorable as they diminish entropy which leads to increasing of the free energy. Segregation occurs for χ greater than some critical value. On the other hand if χ is close to zero and, hence, repulsion between unlike monomers is not big enough or attraction between alike monomers is greater, entropy effects are dominant in such situations and homogenous distribution (disordered phase) of A– and B–like chains is favorable and, hence, segregation never occurs. So there are two driving 'forces' and depending on which is stronger there is or there is not phase separation present. The transition between disordered and ordered states occur when $\chi N \gtrsim 10$, when χN is of order 10, $A - B$ interactions are still weak and polymer molecules remain unperturbed (coiled), however, segregation is present and that is what is called the weak–segregation limit. Strong–segregation limit occurs when $\chi N \gg 10$ (for references see [2]).

Leibler studied phase separation in a weak–segregation limit where $\phi(\mathbf{r})$ changes smoothly over its domain and no sharp interface exist. He has obtained (f, χ)–phase diagrams that show when segregation occurs. He also figured out that the domain

D is proportional to the radius of gyration R_G of a copolymer molecule and has the following relation with polymerization

$$D \sim R_G \sim N^{\frac{1}{2}}.$$

This result differs from the one obtained by Helfand and Wasserman and can be explained by the fact that different approaches were used to model the case of strong–segregation and the case of weak–segregation limits, and, thus, a quantative difference in the domain of a phase is present for different regimes. There is another consideration that might verify the difference in the exponent laws for weak– and strong–segregation limits. In the disordered state the energetically favorable state of a BCP molecule is spherical, this is also the case in the weak–segregation limit. Molecules start to straighten a little already in the weak-segregation limit but they only elongate normal to interfaces in the strong–segregation limit and this fact can justify difference in the size of domains in the two cases. Leibler has also proposed a theory of constructing the free energy functional based on Landau theory. This approach was used a lot later on, for example by Ohta and Kawasaki in their own investigations of the phase separation of BCP.

From 1986 Ohta and Kawasaki released a number of papers studying phase separation of BCP using the extended Cahn–Hilliard equation (for references see [35]). They derived the free energy functional in terms of the order parameter $\phi(\mathbf{r})$,

$$F = F_S\{\phi\} + F_L\{\phi\}$$

which consists of two parts. One is the well known Ginzburg–Landau type free energy in the theory of phase transitions F_S. The other is the long-range interaction relating to the fact that two unlike subchains are chemically bonded F_L. The free energy functional takes form (we will discuss the parameters of the following equation in the next chapter, where we will derive the free energy functional)

$$F = \int \left[-\frac{b}{2}\phi^2 + \frac{u}{4}\phi^4 + \kappa(\nabla\phi)^2 \right] d\mathbf{r} + B \int\int G(\mathbf{r}, \mathbf{r}')\phi(\mathbf{r})\phi(\mathbf{r}')d\mathbf{r}d\mathbf{r}',$$

where $G(\mathbf{r}, \mathbf{r}')$ is a Green function of

$$-\nabla^2 G(\mathbf{r}, \mathbf{r}') = \delta(\mathbf{r} - \mathbf{r}').$$

It was shown that in the weak–segregation limit the free energy can be reduced to the form obtained by Liebler previously. In the strong-segregation limit they solved the Euler equation which is, as a matter of fact, an extended Cahn–Hilliard equation for this particular form of free energy and obtained solutions for lamellae, spherical and cylindrical structures. They also have phenomenologically proven that the exponent law in the strong segregation limit by considering and minimizing the free energy of the system

$$D \sim N^{\frac{2}{3}},$$

which is very similar to the result obtained numerically by Helfand and Wasserman.

Oono and collaborators (for references see [1], [36], [37], [38]) decided to abandon the continuous model developed by that time due to its high computational inefficiency. They proposed to use a discretized time–space lattice and a conventional model explicitly imposed on it. Of course this model should be analogue of the continuous model used before and should be based on the same physical background and general understanding of phase separations in BCP that has been developed. In the latter case the general form of such cell–dynamics system for the order parameter ϕ in each cell is following

$$\phi(t+1, n) = \phi(t, n) + \Phi(t, n) - \langle\langle \Phi(t, n) \rangle\rangle,$$

where

$$\Phi(t, n) = f(\phi(t, n)) + d\left[\langle\langle \phi(t, n) \rangle\rangle - \phi(t, n)\right] - \phi(t, n),$$

where $\phi(t, n)$ is the order parameter in the n^{th} cell at time t, $d > 0$ is proportional to the diffusion constant, function f is a one–to–one map on R with two hyperbolic sinks and one hyperbolic source. In their studies it was chosen to be $f(\phi) = A \tanh(\phi)$ with $A < 1$ above critical temperature and $A > 1$ below . Operation $\langle\langle \cdot \rangle\rangle$ is the isotropic spatial average, which for the $2D$ square lattice was chosen

of form

$$\langle\langle\phi(t,n)\rangle\rangle = \frac{1}{6}\sum(\phi \text{ in the nearest-neighbor cells})$$
$$+\frac{1}{12}\sum(\phi \text{ in the next-nearest-neighbor cells}).$$

The authors performed a number of numerical simulations. The results for an equilibrium thickness agree with the previous results of Leibler and Ohta and collaborators. Phase separation patterns were also observed.

Brown and Chakrabarti [4, 5] have done numerical studies of BCP melts based on an extended Cahn–Hilliard model. They solved the extended Cahn–Hilliard equation in $2 - D$ and confirmed the previously known result in the strong-segregation limit $R \sim N^{0.6}$ for symmetric BCP with presence of chemically active surfaces that bound the melt [4]. Later on Chen and Chakrabarti [10] performed numerical experiments in $3 - D$. They found out that if phase separation is happening between two rigid walls, then the walls induce the segregation process and their configuration impacts on the time of segregation, as well as configuration of periodic patterns that occur [5]. Among typical configurations of such chemically active walls, Brown, Chen and Chakrabarti have studied, are:

- one wall is neutral and another wall attracts one type of BCP monomers;
- both walls attract one kind of monomers (case of symmetric walls);
- antisymmetric walls (one attracts monomers of type A, another monomers of type B);
- one of wall is neutral, the other has periodic pattern with the domain size of order of the linear size of a BCP molecule [10].

They have also performed some experiments for asymmetric BCP [4], but since our model is restricted to symmetrical case only we will not go into details of their studies.

We would like to address the work of Novick–Cohen and Segel [34]. They studied steady states of Cahn–Hilliard equation in 1–D for an extended form of the free

energy functional, which was considered to be a fourth degree polynomial

$$F = \int_V \left[a_0 + a_1\phi + a_2\phi^2 + a_3\phi + a_4\phi^4 + \kappa(\nabla\phi)^2 + \ldots\right] dV, \tag{1.2}$$

here a_i are constant coefficients of a Taylor expansion of the free energy near critical temperature of segregation T_c (compare the above form with (2.9)). We obtained very similar results to [34] and will compare them later in the corresponding chapter.

A very important work was done by Liu and Goldenfeld [32]. They studied periodic solutions of the 1–D extended Cahn–Hilliard equation numerically. They considered the free energy functional of the BCP melt in a form

$$F_\lambda = \frac{4}{\lambda}\int_0^{\frac{\lambda}{4}} \left[\frac{\alpha}{2}\left(\frac{d\phi}{dx}\right)^2 - \frac{1}{2}\phi^2 + \frac{1}{4}\phi^4\right] dx - \frac{1}{\lambda}\int_0^{\frac{\lambda}{4}}\int_0^{\frac{\lambda}{4}} \left[|x-x'| + x + x' - \frac{\lambda}{2}\right] dxdx', \tag{1.3}$$

where λ is a rescaled period of a steady state $\lambda = \lambda_{\text{unscaled}}\sqrt{\alpha}$ and α is a controlling parameter of the problem. Eq.(1.3) is an integral form of the 1–D extended Cahn–Hilliard equation. Note, that due to symmetries in the system integration was reduced to a quarter of a period. It can be shown that free energy functional decreases with time. They minimized free energy F_λ with respect to a period of steady states with fixed α and claimed that solutions with such λ are stable. They confirmed exponential laws in weak– and strong–segregation limits. They also studied periodic pattern formation by propagating fronts. In the last chapter of this thesis we will give a throughout comparison of the results obtained by Liu and Goldenfeld with ours.

Matsen and Schick [33] using the mean field theory studied the existence and stability of different microphases such as lamellar, hexagonal, cubic phases (well-know before), as well as additional stable gyroid phase. They present a phase diagram showing existence of such phases depending on parameters of the system.

Choksi, Maras, Peletier and Williams [11, 12] have done studies considering minimizers of the free energy functional of diblock copolymer melts (the extended Cahn–Hilliard model) in 2-D. Such minimizers can be various structures either showing phase segregation or homogenous disordered states. They use different from [25] scaling of the free energy functional. With the help of numerical simulations they

present phase diagrams, that show dependence of such minimizers on parameters of the problem.

1.3 Thesis organization

The objective of our work is to study the special solutions of the extended Cahn–Hilliard equation – spatial periodic steady states.

The specific content of the chapters is as follows.

- **Chapter 2: Mathematical Model.** We present the general mathematical formulation of the extended Cahn–Hilliard equation and non-dimensionalize it.

- **Chapter 3: Cahn-Hilliard equation. Periodic spatial solutions.** We consider Cahn–Hilliard equation. We examine existence of spatial periodic steady states in the full parameter space analytically in the 'linear–limit' case and numerically in general case. We classify the regions of existence. Finally, we examine stability of found solutions using various mathematical methods (analysing a Lyapunov's functional and solving an eigenvalue problem).

- **Chapter 4: The extended Cahn-Hilliard equation. Periodic spatial solutions.** In this chapter we consider the extended Cahn–Hilliard equation. We study existence of spatial periodic steady states depending on the parameters of the equation. A number of different modes of steady states is defined. We obtain solutions of the equation analytically in the case of 'weak nonlinearity' and perform numerical simulations for the general case. Classification of found solutions is given.

- **Chapter 5: Stability of periodic solutions of extended Cahn–Hilliard equation.** We investigate the stability of the steady states of the extended Cahn–Hilliard equation by solving an eigenvalue problem. Analytical investigations are done in the case of 'weak nonlinearity' and numerical calculations are done in the general case. We present a diagram of stability. We also compare the results to those, obtained for the Cahn–Hilliard equation.

- **Chapter 6: Conclusions.** In this chapter we summarize the work of the present thesis and discuss the results. Some possible improvements and directions for future work are suggested.

Chapter 2

Mathematical model

In this chapter we will derive one of the models used to describe phase separation in BCP melts– the extended Cahn–Hilliard equation. This model is based on theoretical works of Landau, Lifshitz, Cahn, Hilliard, Leibler, Ohta, Kawasaki and many others and is well-known for at least 25 years and is not in any sense an achievement of the author of this thesis.

2.1 Free Energy of a Nonuniform System

In this chapter we will show the derivation of a free energy functional for an isotropic binary mixture as it was done by Cahn and Hilliard [7]–[9]. We consider an isotropic binary system having a spatial variation of density (or as a matter of fact any other intensive scalar property other than temperature or pressure). In their work Cahn and Hilliard referred to such system as "nonuniform" system. The relative fraction of one of the two components $\phi(\mathbf{r})$ was chosen to be the nonuniform property. We now follow the work of Cahn and Hilliard. It has been assumed that the free energy is a continuous functional of $\phi(\mathbf{r})$ and its derivatives. Free energy can be expanded in a Taylor series about f_0– free energy per molecule of the system with composition $\phi(\mathbf{r})$. To the leading terms of the expansion we have

$$f(\phi, \nabla\phi, \nabla^2\phi, \ldots) = f_0(\phi) + \sum_{i=1}^{3} L_i \frac{\partial\phi}{\partial x_i} + \sum_{i,j=1}^{3} \kappa_{i,j}^{(1)} \frac{\partial^2\phi}{\partial x_i \partial x_j} + \frac{1}{2} \sum_{i,j=1}^{3} \kappa_{i,j}^{(2)} \frac{\partial\phi}{\partial x_i} \frac{\partial\phi}{\partial x_j} + \ldots, \tag{2.1}$$

where $\mathbf{r}$ is a vector in Cartesian coordinates $\{\mathbf{x}_1, \mathbf{x}_2, \mathbf{x}_3\}$ and for $i, j = \overline{1,3}$

$$\begin{aligned} L_i &= \left[\frac{\partial f}{\partial(\partial\phi/\partial x_i)}\right]_0, \\ \kappa_{i,j}^{(1)} &= \left[\frac{\partial f}{\partial(\partial^2\phi/\partial x_i\partial x_j)}\right]_0, \\ \kappa_{i,j}^{(2)} &= \left[\frac{\partial^2 f}{\partial(\partial\phi/\partial x_i)\partial(\partial\phi\partial x_j)}\right]_0. \end{aligned} \tag{2.2}$$

In the theory of crystals tensors $\kappa_{i,j}^{(1)}$ and $\kappa_{i,j}^{(2)}$ are tensors relating to symmetries of crystals and vector (L_1, L_2, L_3) is a polarization vector in a polar crystal. In the current situation an isotropic medium is considered and, hence, the free energy must be invariant to the symmetry operations of reflection $(x_i \to -x_i)$ and rotation $(x_i \to x_j)$. Assuming these, the following can be obtained from (2.2), for $i, j = \overline{1,3}$

$$\begin{aligned} L_i &= 0, \\ \kappa_{i,j}^{(1)} &= \kappa_1 = \left[\frac{\partial f}{\partial(\nabla^2\phi)}\right]_0 \qquad \text{for } i = j, \\ \kappa_{i,j}^{(1)} &= 0 \qquad \text{for } i \neq j, \\ \kappa_{i,j}^{(2)} &= \kappa_2 = \left[\frac{\partial^2 f}{(\partial(\nabla\phi))^2}\right]_0 \qquad \text{for } i = j, \\ \kappa_{i,j}^{(2)} &= 0 \qquad \text{for } i \neq j. \end{aligned} \tag{2.3}$$

Now the free energy (2.1) with (2.3) takes form

$$f(\phi, \nabla\phi, \nabla^2\phi, \ldots) = f_0(\phi) + \kappa_1\nabla^2\phi + \kappa_2(\nabla\phi)^2 + \ldots. \tag{2.4}$$

After integrating (2.4) over a volume V of the system the free energy of this system can be obtained

$$F = N_V \int_V f dV = \int_V \left[f_0(\phi) + \kappa_1\nabla^2\phi + \kappa_2(\nabla\phi)^2 + \ldots\right] dV, \tag{2.5}$$

where N_V is the number of molecules in the volume V. Using Gauss–Ostrogradsky's theorem one can evaluate the term $\int_V(\kappa_1\nabla^2\phi)dV$ of the integral in (2.5)

$$\int_V(\kappa_1\nabla^2\phi)dV = -\int_V \frac{d\kappa_1}{d\phi}(\nabla\phi)^2 dV + \int_S(\kappa_1\nabla\phi\cdot\mathbf{n})dS \tag{2.6}$$

Surface integral in (2.6) can be put to zero. Since we did not specify the boundary of V and are not considering effects on the external surface, we can choose such boundary in the manner that $\nabla\phi \cdot \mathbf{n}$ is zero on S. Doing so and using modified (2.6) we can eliminate term $\kappa_1 \nabla^2 \phi$ from the free energy (2.5) and obtain the following expression for it

$$F = N_V \int_V f dV = \int_V \left[f_0(\phi) + \kappa (\nabla \phi)^2 + \ldots \right] dV, \tag{2.7}$$

where

$$\kappa = -\frac{d\kappa_1}{d\phi} + \kappa_2 = -\left[\frac{\partial^2 f}{\partial\phi \partial(\nabla^2 \phi)} \right]_0 + \left[\frac{\partial^2 f}{(\partial(\nabla\phi))^2} \right]_0 .$$

The term f_0 represents the free energy per molecule in the system. Landau theory of phase transitions suggests that free energy is an analytic function of the order parameter and, thus, one can write a Taylor expansion for the order parameter. Free energy must also be invariant under all symmetries of the Hamiltonian. Therefore, the terms in a Taylor expansion are restricted by symmetry considerations of the medium (reflection ($x_i \to -x_i$) and rotation ($x_i \to x_j$)). This suggests to take f_0 of the form

$$f_0 = -\frac{b}{2}\phi^2 + \frac{u}{4}\phi^4 + \ldots, \tag{2.8}$$

here b and u are phenomenological positive parameters. The coefficient of ϕ^2 is proportional to $T - T_C$, difference between the current temperature of the melt during segregation and the critical temperature at which segregation can occur, this difference is obviously negative. Taking into account (2.8) the free energy functional becomes

$$F = \int_V \left[-\frac{b}{2}\phi^2 + \frac{u}{4}\phi^4 + \kappa (\nabla \phi)^2 + \ldots \right] dV, \tag{2.9}$$

A free energy functional of this form is suitable to describe phase separation in two–component melts. The situation with BCP melts is quite different as full segregation cannot occur there, but expression (2.9) is a part of free energy of BCP melts. It describes the main “driving forces” of segregation.

2.2 Free energy of a BCP melt

Following Ohta and Kawasaki [35] we will discuss the main steps of deriving the free energy functional for BCP molecules, for which the main difference from two-component melts is that subchains forming different phases are attached to each other and, thus, cannot be separated in a global sense. The mean field treatment applied by Ohta and Kawasaki [35] is based on a similar one of Leibler [31]. Here we will just give an idea of their deductions as the detailed calculations are quite lengthy.

We first start by defining a Hamiltonian for a BCP melt

$$H(\mathbf{r}_i) = \frac{1}{2}\sum_{i=1}^{n}\int_0^N \left(\frac{d\mathbf{r}_i(\tau)}{d\tau}\right) d\tau + V(\mathbf{r}_i), \tag{2.10}$$

here n is a number of polymer molecules in the melt, $\mathbf{r}_i(\tau)$ is the coordinate vector of the monomer on a position τ in the i–th copolymer chain, N is polymerization index. The potential of short- and long-range interactions $V(\mathbf{r}_i)$ can be given by the following

$$\begin{aligned} V(\mathbf{r}_i) \;=\; & \frac{\epsilon_{AA}}{2}\sum_{i,j=1}^{n}\int_0^{\widehat{f}}\int_0^{\widehat{f}} \delta(\mathbf{r}_i(\tau)-\mathbf{r}_j(\tau'))d\tau d\tau' \\ & +\frac{\epsilon_{BB}}{2}\sum_{i,j=1}^{n}\int_{\widehat{f}}^{N}\int_{\widehat{f}}^{N} \delta(\mathbf{r}_i(\tau)-\mathbf{r}_j(\tau'))d\tau d\tau' \\ & +\frac{\epsilon_{AB}}{2}\sum_{i,j=1}^{n}\int_{\widehat{f}}^{N}\int_0^{\widehat{f}} \delta(\mathbf{r}_i(\tau)-\mathbf{r}_j(\tau'))d\tau d\tau', \end{aligned} \tag{2.11}$$

where ϵ_{ij} is the energy of interaction between 'i'–type and 'j'-type monomers. It has been assumed that for A–subchain $\tau, \tau' \in [0, \widehat{f}]$, and for B–subchain $\tau, \tau' \in [\widehat{f}, N]$ for each chain. For simplicity it has been also assumed that Kuhn statistical lengths of both type monomers are the same and equal to 1.

The next step is to introduce the monomer densities

$$\begin{aligned}\rho_A(\mathbf{r}) &= \sum_{i=1}^{n}\int_0^{\widehat{f}}\delta(\mathbf{r}-\mathbf{r}_i(\tau))d\tau,\\ \rho_B(\mathbf{r}) &= \sum_{i=1}^{n}\int_{\widehat{f}}^{N}\delta(\mathbf{r}-\mathbf{r}_i(\tau))d\tau.\end{aligned}$$

BCP melts are incompressible, which can be written in a form

$$\rho_A(\mathbf{r})+\rho_B(\mathbf{r})=\rho_0=const$$

or in a dimensionless form

$$\rho_{A\_\text{new}}(\mathbf{r})+\rho_{B\_\text{new}}(\mathbf{r})=1,$$

where $\rho_{I\_\text{new}}(\mathbf{r})=\frac{\rho_I(\mathbf{r})}{\rho_0}$ for $I\in\{A,B\}$ and subscript $\_\text{new}$ is further omitted. The order parameter $\phi(\mathbf{r})$– the local concentration difference between monomers of two types was defined as following

$$\phi(\mathbf{r})=\rho_A(\mathbf{r})-c\widehat{f}=-\rho_B(\mathbf{r})+c(N-\widehat{f}), \tag{2.12}$$

here $c=\frac{\rho_0}{N}$ polymer number density. Now the potential of short-range interactions $V(\mathbf{r}_i)$ (2.11) in terms of $\phi(\mathbf{r})$ takes the form

$$V(\mathbf{r}_i)=-\chi\rho_0\int(\phi(\mathbf{r}))^2d\mathbf{r}+const,$$

where χ is the Flory–Huggins' parameter(see Section 1.2) defined by

$$\chi=\frac{1}{k_BT}\left(\epsilon_{AB}-\frac{1}{2}\left(\epsilon_{AA}+\epsilon_{BB}\right)\right),$$

we also rescale $\chi_\text{new}=\chi\frac{\rho_0}{k_BT}$. Segregation occurs for the values of $\chi>0$ (see Section 1.2).

Following Leibler, Kawasaki and Ohta (for reference see [31], [35]), we write the

free energy functional in the form

$$F(\phi) = \frac{1}{2c}\int\int \Gamma(\mathbf{r},\mathbf{r}')\phi(\mathbf{r})\phi(\mathbf{r}')d\mathbf{r}d\mathbf{r}' - \chi\int \phi(\mathbf{r})^2 d\mathbf{r} + W(\phi), \tag{2.13}$$

where $W(\phi)$ contains higher order powers of ϕ and $\Gamma(\mathbf{r},\mathbf{r}')$ is a vertex function. The Fourier transform of $\Gamma(\mathbf{r},\mathbf{r}')$ was approximated by the following function [35]

$$\Gamma_q = \frac{1}{2N^2 f(1-f)}\left(\frac{q^2 N}{2} + \frac{6}{q^2 N f(1-f)} + \frac{s(f)}{f(1-f)}\right), \tag{2.14}$$

where f is a fraction of monomers A in a polymer molecule, i.e. $f = \frac{\widehat{f}}{N}$. Function $s(f)$ is an empirical function, found to have the following values at certain points [35]

$$s(0.5) = 0.9, \qquad s(0.3) = 1.0, \qquad s(0.1) = 1.33.$$

Substituting the form (2.14) into the bilinear term in the free energy (2.13) we obtain(in case of $3-D$)

$$\widehat{F} = \frac{1}{(2\pi)^3 2\rho_0 N}\int \left[B(f)q^2 + A(f)q^{-2} - \overline{\chi}\right]\phi_{\mathbf{q}}\phi_{-\mathbf{q}}d\mathbf{q} + \widehat{W}, \tag{2.15}$$

where

$$B(f) = \frac{N}{4f(1-f)}, \tag{2.16}$$

$$A(f) = \frac{3}{Nf^2(1-f)^2}, \tag{2.17}$$

and

$$\overline{\chi} = \frac{2\rho_0 N\chi - s(f)}{2f^2(1-f)^2}.$$

Using the inverse Fourier transform, we obtain the free energy functional in the form

$$F(\phi) = \frac{1}{2\rho_0 N}\int B(f)(\nabla\phi)^2 d\mathbf{r} + \int \widehat{W}d\mathbf{r} + \frac{A(f)}{2\rho_0 N}\int\int G(\mathbf{r}',\mathbf{r})\phi(\mathbf{r})\phi(\mathbf{r}')d\mathbf{r}d\mathbf{r}', \tag{2.18}$$

where $G(\mathbf{r}',\mathbf{r})$ is the Green's function of Laplace's equation

$$-\nabla G(\mathbf{r}',\mathbf{r}) = \delta(\mathbf{r}-\mathbf{r}'),$$

under suitable boundary conditions. The first two terms are a different form of Cahn–Hilliard's free energy (2.13). Note that, $\widehat{W}(\phi_{\mathbf{q}})$ contains higher order powers of the order parameter. The term with factor $\overline{\chi}$ of (2.15) has been absorbed in $\widehat{W}(\phi_{\mathbf{q}})$. Substituting

$$B = \frac{A(f)}{2\rho_0 N} \tag{2.19}$$

and using (2.15) we have the free energy functional of BCP melt

$$F = \int \left[-\frac{b}{2}\phi^2 + \frac{u}{4}\phi^4 + \kappa(\nabla\phi)^2 \right] d\mathbf{r} + B \int\int G(\mathbf{r}', \mathbf{r})\phi(\mathbf{r})\phi(\mathbf{r}')d\mathbf{r}d\mathbf{r}'. \tag{2.20}$$

It is easy to show using (2.17) and (2.19), that factor B has the following form

$$B = \frac{3}{2f^2(1-f)^2\rho_0 N^2}, \tag{2.21}$$

and, thus, $B \sim N^{-2}$, which was first pointed out by Liebler [31].

One can see that the following condition in the integral form can be obtained from the definition of the order parameter (2.12)

$$\int \phi d\mathbf{r} = 0. \tag{2.22}$$

2.3 Extended Cahn–Hilliard equation

Once we know the free energy functional of the system of BCP, we want to study kinetics of the process of phase separation. We now go back to studies on spinoidal decomposition by Cahn [6] and Hillert [23]. We want to write an equation that gives a kinetic measure of the time needed for a system to go from one microstructure to another. We also want that such change in the microstructure decreases the free energy as much as possible. For these reasons the equation is written as a diffusion equation written for the free energy functional of diblock copolymers. It relates a spontaneous flux of the order parameter to a change in composition. Such spontaneous fluxes can be associated with the gradient of a local difference in chemical potential μ.

$$\frac{\partial\phi}{\partial t} = M\nabla\cdot(\nabla\mu) \tag{2.23}$$

here M is mobility. The chemical potential of the system is the variation of the free energy functional, thus, the relation between them is the following

$$\mu = \frac{\delta F}{\delta \phi}.$$

Finding μ from the expression for the free energy for a BCP melt (2.20) and substituting it into Eq.(2.23), also changing $\kappa_{new} = 2\kappa$ and omitting $_{new}$, we obtain the extended Cahn–Hilliard equation

$$\frac{\partial \phi}{\partial t} = M\nabla^2 \left(-b\phi + u\phi^3 - \kappa\nabla^2\phi\right) - B\phi \tag{2.24}$$

2.4 Rescaling

We want to find a suitable rescaling of the concentration field, time, space and the problem's parameters to rewrite (2.24) in more convenient form. Coefficients of the free energy expansion (2.9) b, u and κ are of the same order for BCP melts near the phase transition temperature [7, 8].

We now introduce the following dimensionless variables:

$$\phi^* = \phi \left(\frac{b}{u}\right)^{\frac{1}{2}}, \tag{2.25}$$

$$t^* = t\frac{Mb^2}{\kappa}, \tag{2.26}$$

$$x^* = x \left(\frac{b}{\kappa}\right)^{\frac{1}{2}}, \tag{2.27}$$

$$\alpha = B\frac{Mb^2}{\kappa}. \tag{2.28}$$

Substituting (2.25)–(2.28) into Eq.(2.24), we obtain the following

$$\frac{\partial \phi}{\partial t} = \nabla^2(-\phi + \phi^3 - \nabla^2\phi) - \alpha\phi, \tag{2.29}$$

which is the basic dynamical equation of the model for the bulk system. Coefficient

α is the controlling parameter of the phase transition. From (2.21) and (2.28) it follows that α is proportional to the square of the polymerization index N.

Condition (2.22) on the order parameter holds

$$\int \phi d\mathbf{r} = 0. \tag{2.30}$$

We now have an equation with only one controlling parameter α. In the next chapters we will describe families of spatial periodic steady states of Eq.2.29 in 1-D and examine their stability.

2.5 Conclusions

In Chapter 2 we highlighted the main aspects that should be considered to model a process of phase separation in diblock copolymers and to derive the extended Cahn–Hilliard equation. We considered ideas of Cahn and Hilliard, who, using the Landau theory of phase transitions, proposed a way to describe the free energy of isotropic binary mixtures. Later Ohta, Kawasaki, Leibler and others will extend this theory to a more complex situation considering both short– and long–term interactions between molecules in block copolymer mixtures. We followed the main steps in derivation of a free energy functional for BCP melts. Finally, we considered an evolution equation showing the kinetic of microstructural changes, when a system of block copolymers undergoes the process of phase transition. Such equation is the extended Cahn–Hilliard equation. The aim of this thesis is to study spatial periodic steady states of the equation as being related to periodic patterns that occurs in the process of phase separation. We start our study with Cahn–Hilliard equation, considering it as a simplification of the extended one. Cahn–Hilliard equation governs the process of spinoidal decomposition in binary alloys [22, 34] and is not suitable for BCP melts. Nevertheless, we find it helpful to start our research with an easier model and then move to a more general and complicated one – the extended Cahn–Hilliard equation.

Chapter 3

Cahn-Hilliard equation. Periodic spatial solutions.

3.1 Introduction

We now discuss periodic spatial solutions of the Cahn–Hilliard equation regarding its parameters. We do not aim here to carry out a comprehensive research of the Cahn–Hilliard equation. We will obtain some results, which are not original, referring them to existing works. The goals we pursue are to start with a simpler model, train on it, build up enough of methodology to find periodical solutions and examine their stability, and later employ it for analyzing the extended Cahn–Hilliard. Cahn–Hilliard equation ($\alpha = 0$) has a form

$$\frac{\partial \phi}{\partial t} = \nabla^2(-\phi + \phi^3 - \nabla^2\phi). \tag{3.1}$$

We start with considering a system that defines steady periodic solutions $\frac{\partial \phi}{\partial t} = 0$, and for simplicity we examine a one–dimensional case, thus, $\phi = \phi(x)$. Eq.(3.1) now reduces to the following equation

$$\frac{\partial^2}{\partial x^2}\left(\phi - \phi^3 + \frac{\partial^2 \phi}{\partial x^2}\right) = 0. \tag{3.2}$$

we also deploy periodic boundary conditions for $\phi(x)$

$$\phi(x+\lambda) = \phi(x), \tag{3.3}$$

where λ is the period of steady state. Now we can integrate equation (3.2) over x two times

$$\phi - \phi^3 + \frac{d^2\phi}{dx^2} = a + a_1 x.$$

We are looking for periodic solutions. To satisfy condition(3.3) we need to put $a_1 = 0$. We now obtain

$$\phi - \phi^3 + \frac{d^2\phi}{dx^2} = a. \tag{3.4}$$

Eq.(3.4) with boundary condition (3.3) describes stationary regimes of Eq.(3.1) in one–dimensional case.

3.2 Phase portrait

We now examine a phase portrait of Eq.(3.4). We can obtain the first integral of the equation. We multiply (3.4) by $\frac{d\phi}{dx}$, which is not zero, and integrate with respect to x

$$\frac{1}{2}\phi^2 - \frac{1}{4}\phi^4 + \frac{1}{2}(\frac{d\phi}{dx})^2 = a\phi - \frac{1}{2}h, \tag{3.5}$$

where h is a constant of integration. From (3.5) we can find relation between phase variables $\frac{d\phi}{dx}$ and ϕ

$$\frac{d\phi}{dx} = \pm\sqrt{\frac{1}{2}\phi^4 - \phi^2 + 2a\phi - h}. \tag{3.6}$$

We now introduce the effective potential of the system (3.4), (3.3)

$$V(\phi) = (-\phi^{(0)} + \phi^{(0)3})\phi + \frac{\phi^2}{2} - \frac{\phi^4}{4}, \tag{3.7}$$

where, for convenience calculations, $\phi^{(0)}$ is such that $a = \phi^{(0)} - \phi^{(0)3}$. The phase portrait of (3.4) can be found in Fig. 3.1. Periodic solutions correspond to closed trajectories. Solving $\frac{\partial V(\phi)}{\partial \phi} = 0$, we find equilibrium points. Separatrices intersect ϕ – axis at the two unstable equilibrium points $\phi = \frac{1}{2}(\pm\sqrt{4 - 3\phi^{(0)2}} - \phi^{(0)})$. It can be

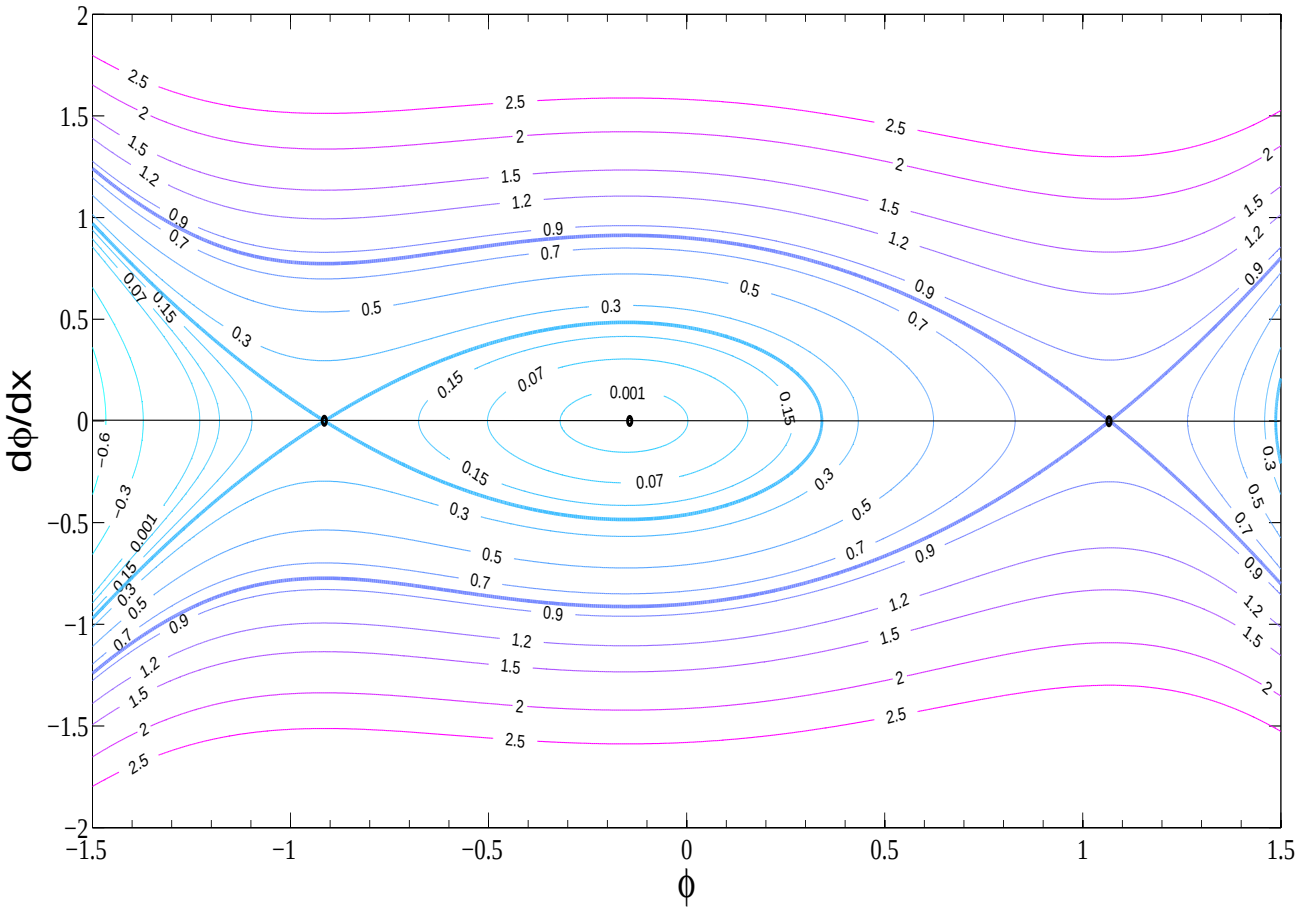

Figure 3.1: Phase portrait of (3.4), $a = 0.15$. Periodic solutions correspond to closed trajectories. Separatrices are shown with thick lines. Equilibrium points are shown with dots. Energy levels h are shown on corresponding lines.

shown that closed trajectories (or periodic solutions) can only exist for $\phi \in [-1, 1]$, or in other words the smallest of two maximums of $V(\phi, a)$ belongs to $[-1, 1]$ interval for any a. All of those non-closed trajectories correspond to solutions for which phase coordinate and phase velocity tends to $\pm\infty$, due to initial conditions. The first integral (3.5), without specific periodic conditions, can be thought of one that describes a mechanical system where a 'particle' is sliding without friction along the effective potential (3.7) curve (Fig. 3.2). Vertical trajectories correspond to those situations when the energy of the 'particle' is too small to reach the nearby maximum. Horizontal trajectories, on the other hand, correspond to the cases with excess of the energy to form periodical solutions, so the 'particle' passes both of the peaks. Another type of trajectories are those that come from $-\infty$ and after passing the point at which $\frac{d\phi}{dx} = 0$ they tend to $-\infty$ again, for these cases the 'particle' has only enough energy to overcome the smallest of the maxima, but cannot overcome the largest one. And at last, the situation where the 'particle' is swinging between two peaks infinitely in time.

As it was mentioned before, there are two unstable equilibrium points and a stable one, corresponding to extremes of the effective potential (they are shown on Fig. 3.1 and 3.2).

We now examine the function of the effective potential (See Fig. 3.2). We can find the extremes of the effective potential from the following equation

$$\frac{\partial V}{\partial \phi} = -\phi^{(0)} + \phi^{(0)3} + \phi - \phi^3 = 0.$$

This equation has three different real roots in nontrivial case (we do not consider situations when there are complex roots). Without loss of generality $\tilde{\phi}_1 = \phi^{(0)}$, which is the minima of V,

$$\tilde{\phi}_2 = \frac{1}{2}(\sqrt{4 - 3\phi^{(0)2}} - \phi^{(0)}) \tag{3.8}$$

and

$$\tilde{\phi}_3 = \frac{1}{2}(-\sqrt{4 - 3\phi^{(0)2}} - \phi^{(0)}) < \tilde{\phi}_2,$$

both maxima (for $\phi^{(0)} \epsilon [-\frac{2}{\sqrt{3}}, -1] \cup [0, 1] : V(\tilde{\phi}_3) > V(\tilde{\phi}_2)$, but for other values of $\phi^{(0)}$ we swap subscripts $_2$ and $_3$). An apparent condition on $\phi^{(0)}$ is that $\phi^{(0)} \epsilon [-\frac{2}{\sqrt{3}}, \frac{2}{\sqrt{3}}]$.

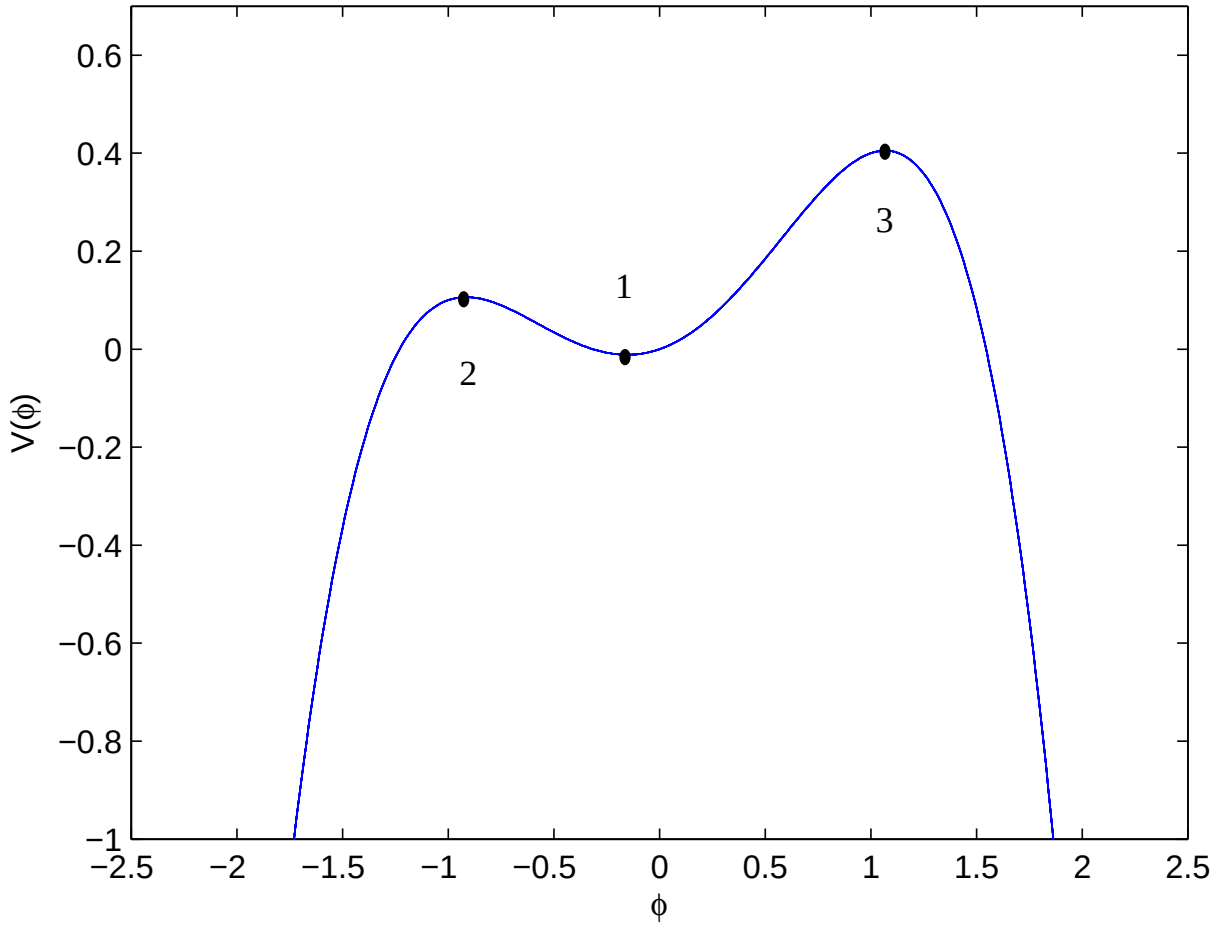

Figure 3.2: Effective potential $V(\phi)$, $a = 0.15$. Points $1, 2, 3$ are critical points $\tilde{\phi}_1$, $\tilde{\phi}_2$, $\tilde{\phi}_3$ respectively.

3.3 Existence of periodic solutions

In this section we will examine existence of periodic solutions of (3.3), (3.4) in the full parameter space. Any of these solutions can be characterized by three parameters: the period λ, the mean value of the order parameter or the concentration field $\bar{\phi}$ and the amplitude of ϕ or maximum deviation from the mean $\bar{\phi}$. Thus, it happens that the above parameters are not independent and one can be expressed in terms of other two. We decided to treat λ and $\bar{\phi}$ as independent ones. And thus, we will illustrate the existence of periodic solutions on ($\bar{\phi}$,λ)-plane.

In order to proceed, we expand ϕ and a around some constant zeroth-order solution $(\phi^{(0)}, a^{(0)})$,

$$\phi = \phi^{(0)} + \epsilon\phi^{(1)} + \epsilon^2\phi^{(2)} + \epsilon^3\phi^{(3)} + ... \tag{3.9}$$

$$a = a^{(0)} + \epsilon a^{(1)} + \epsilon^2 a^{(2)} + \epsilon^3 a^{(3)} + ...$$

where ϵ is a small parameter (for example an amplitude of the highest–order non-trivial oscillation of the expansion above). Then, a relation between zeroth-order coefficients is

$$a^{(0)} = -\phi^{(0)} + \phi^{(0)3}.$$

The first order contribution in Eq.(3.4) has the form,

$$\phi^{(1)\prime\prime} + k^2\phi^{(1)} = a^{(1)},$$

where phase frequency is

$$k^2 = 1 - 3\phi^{(0)2} \geq 0,$$

and to satisfy periodic condition (3.3), or

$$\phi^{(1)}(x + \lambda) = \phi^{(1)}(x),$$

it yields $a^{(1)} = 0$. Therefore, we find

$$\phi^{(1)} = c_1 \cos(kx) + c_2 \sin(kx).$$

We can choose the initial conditions in a way that, $c_1 = 1$, $c_2 = 0$, and hence

$$\phi^{(1)} = \cos(kx), \tag{3.10}$$

$$\lambda_l = \frac{2\pi}{\sqrt{1 - 3\phi^{(0)2}}}. \tag{3.11}$$

We call $\phi^{(1)}$ the linear limit solution, then λ_l is the period of a linear limit solution.

We have to notice here that, $\phi^{(0)}$ is close, but not equal to the mean $\bar{\phi}$, because higher-order terms of series (3.9) also contribute to the mean. We now calculate the next term of expansion (3.9) to estimate the difference between $\phi^{(0)}$ and $\bar{\phi}$.

The second order contribution has the form

$$\phi^{(2)\prime\prime} + k^2\phi^{(2)} = 3\phi^{(0)}\phi^{(1)2} + a^{(2)},$$

$$\phi^{(2)}(x + \lambda) = \phi^{(2)}(x),$$

after substituting (3.10), we have

$$\phi^{(2)\prime\prime} + k^2\phi^{(2)} = 3\phi^{(0)} \cos^2(kx) + a^{(2)}.$$

Hence, we obtain the solution $\phi^{(2)}$

$$\phi^{(2)} = b_1 \cos(kx) + b_2 \sin(kx) + 3\phi^{(0)} \left(\frac{1}{2k^2} - \frac{1}{6k^2} \cos(2kx) \right) + \frac{a^{(2)}}{k^2}.$$

Without loss of generality we let $b_1 = 0$, $b_2 = 0$.

$$\phi^{(2)} = 3\phi^{(0)} \left(\frac{1}{2k^2} - \frac{1}{6k^2} \cos(2kx) \right) + \frac{a^{(2)}}{k^2} \tag{3.12}$$

To find $a^{(2)}$ we need to write down the third order of the expansion, which has the form

$$\phi^{(3)\prime\prime} + k^2\phi^{(3)} = \phi^{(1)3} + 6\phi^{(0)}\phi^{(1)}\phi^{(2)} + a^{(3)},$$

$$\phi^{(3)}(x+\lambda) = \phi^{(3)}(x).$$

Substituting both (3.10) and (3.12), we obtain

$$\phi^{(3)\prime\prime} + k^2\phi^{(3)} = \cos^3(kx) + 18\phi^{(0)2}\cos(kx)\left(\frac{1}{2k^2} - \frac{1}{6k^2}\cos(2kx) + \frac{a^{(2)}}{3\phi^{(0)}k^2}\right) + a^{(3)},$$

simplifying, we obtain the following

$$\phi^{(3)\prime\prime} + k^2\phi^{(3)} = \cos(kx)\left(\frac{3}{4} + \frac{15\phi^{(0)2}}{2k^2} + \frac{6a^{(2)}\phi^{(0)}}{k^2}\right) + \left(\frac{1}{4} - \frac{3\phi^{(0)2}}{2k^2}\right)\cos(3kx) + a^{(3)},$$

Eq.(3.4) has periodic solution only if the summand with $\cos(kx)$ is zero, which means that

$$\frac{3}{4} + \frac{15\phi^{(0)2}}{2k^2} + \frac{6a^{(2)}\phi^{(0)}}{k^2} = 0,$$

from where we find

$$a^{(2)} = -\frac{5\phi^{(0)}}{4} - \frac{k^2}{8\phi^{(0)}}. \tag{3.13}$$

Let us calculate the mean value of ϕ over its period

$$\bar{\phi} = \frac{1}{\lambda}\int_0^\lambda \phi dx \simeq \frac{1}{\lambda}\int_0^\lambda \phi^{(0)} + \epsilon\phi^{(1)} + \epsilon^2\phi^{(2)}dx,$$

substituting (3.10), (3.12) for $\phi^{(2)}$ and $\phi^{(2)}$, we have

$$\bar{\phi} = \phi^{(0)} + \epsilon^2(3\phi^{(0)}\frac{1}{2k^2} + \frac{a^{(2)}}{k^2}),$$

finally, using (3.13) we obtain

$$\bar{\phi} = \phi^{(0)} + \frac{\epsilon^2}{8k^2\phi^{(0)}}(2\phi^{(0)2} - k^2).$$

Substituting $k^2 = 1 - 3\phi^{(0)2}$, we obtain the formula for the mean value in terms of $\phi^{(0)}$

$$\bar{\phi} = \phi^{(0)} + \frac{\epsilon^2(5\phi^{(0)2} - 1)}{8(1 - 3\phi^{(0)2})\phi^{(0)}} + O(\epsilon^3).$$

This equality can be used to express $\phi^{(0)}$ via $\bar{\phi}$

$$\phi^{(0)} = \bar{\phi} + \frac{\epsilon^2(1 - 5\bar{\phi}^2)}{8(1 - 3\bar{\phi}^2)\bar{\phi}} + O(\epsilon^3). \tag{3.14}$$

We can obtain a formula for the period of a steady state in terms of $\phi^{(0)}$. After substitution (3.14) into the formula for the period (3.11), we have

$$\lambda = \frac{2\pi}{\sqrt{1 - 3\bar{\phi}^2}} \left[1 + \frac{3\epsilon^2(1 - 5\bar{\phi}^2)}{8(1 - 3\bar{\phi}^2)^2\bar{\phi}} + O(\epsilon^3) \right] \tag{3.15}$$

One can see that, depending on the sign of the coefficient of ϵ^2

$$\frac{3(1 - 5\bar{\phi}^2)}{8(1 - 3\bar{\phi}^2)^2\bar{\phi}},$$

period λ may be greater or smaller than the linear-limit solution's period λ_l,

$$\lambda_l = \frac{2\pi}{\sqrt{1 - 3\bar{\phi}^2}}, \tag{3.16}$$

note, that for the linear–limit case(and only for the linear–limit case) $\bar{\phi} = \phi^{(0)}$.

The point where the coefficient of ϵ^2 in (3.15) changes its sign is $\bar{\phi} = \frac{1}{\sqrt{5}}$. One can see from (3.15), that λ is greater than λ_l, given by (3.16) when $\bar{\phi} < \frac{1}{\sqrt{5}}$, which means that periodic solutions can exist only above the linear limit curve (3.16). On the other hand, for $\bar{\phi} > \frac{1}{\sqrt{5}}$ periodic solutions can also exist below this curve (λ might be smaller than λ_l), which was also confirmed by numerical calculations (See Fig. 3.3).

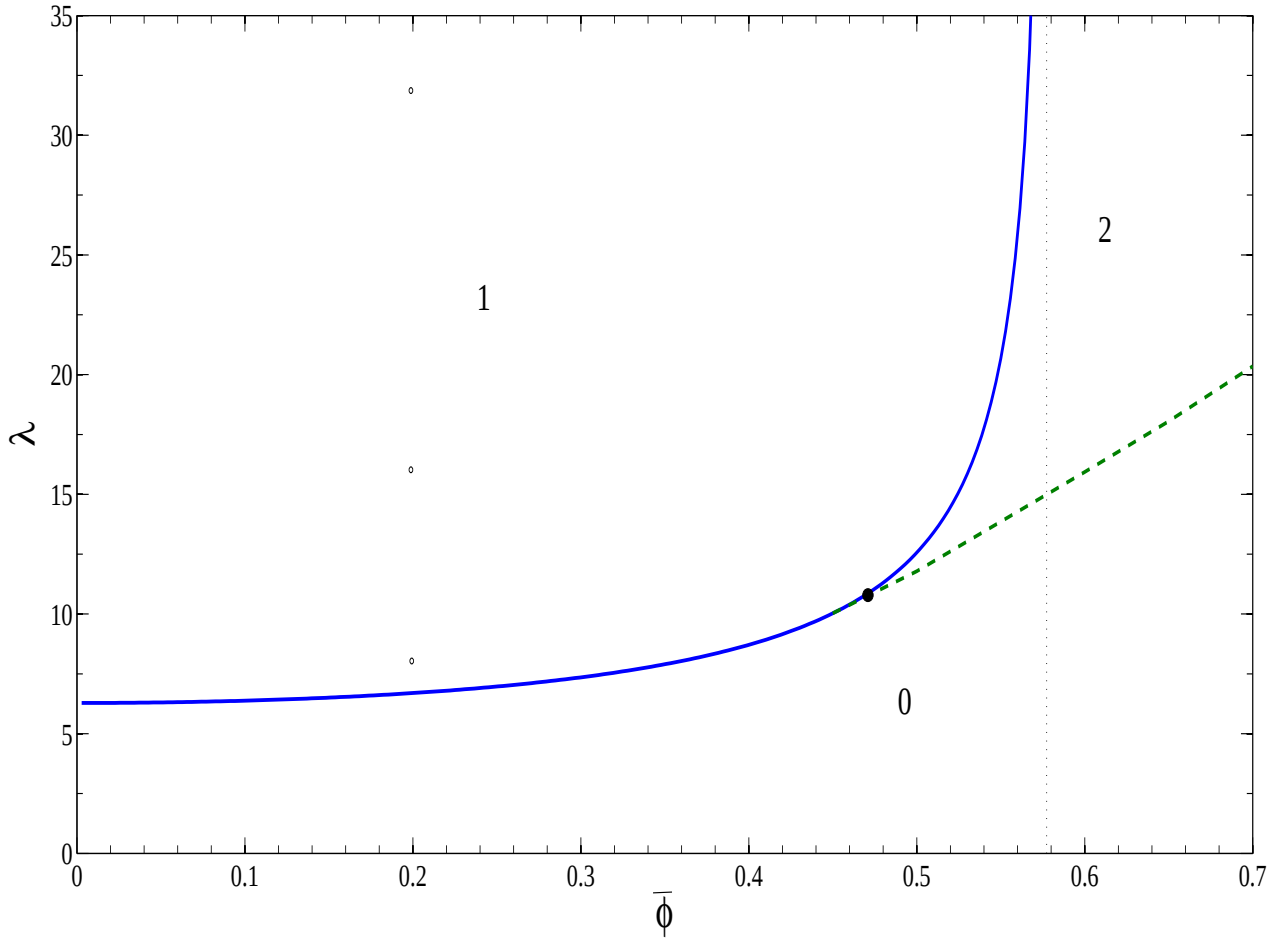

Figure 3.3: The existence of periodic solutions depending on the mean $\bar{\phi}$ and period λ. Regions marked 0, 1, 2 correspond to regions with 0, 1 and 2 nontrivial steady states existing for the same $(\lambda, \bar{\phi})$. The solid line corresponds to the linear-limit relationship (3.16) between λ and $\bar{\phi}$. The vertical line is an asymptote $x = \frac{1}{\sqrt{3}}$ for this curve. The doted borderline of 2–solution region was found numerically. The dot indicates the point where bifurcation occurs. Circles indicate solutions from Fig. 3.4

3.4 Existence of periodic solutions. Numerical results

In this section we will discuss numerical experiments, that have been carried out to find periodic steady states of the Cahn–Hilliard equation. Problem (3.3), (3.4) is a boundary value problem. The shooting method was used to find its solutions. We would like to notice here, that it was more convenient to look for solutions on a half-period. The boundary conditions and the condition for the mean are the following

$$\phi'(0) = 0, \qquad \phi'(\frac{\lambda}{2}) = 0, \tag{3.17}$$

$$\bar{\phi} = \frac{2}{\lambda}\int_0^{\frac{\lambda}{2}} \phi(x)dx, \tag{3.18}$$

here we used the fact that any of the steady states is invariant to the operation of shifting along the x–axis, i.e. $\phi(x) \to \phi(x+c)$.

The shooting method that was used, has two known parameters: λ and $\bar{\phi}$, and two unknown shooting parameters: $\phi(0)$ and a. To construct solutions the Runge-Kutta 4-5 method implemented in MatLab was used. The procedure is the following. For a fixed pair $(\bar{\phi}, \lambda)$ we integrate (3.4), with initial conditions $\phi(0) = \phi_{guess}$, $a = a_{guess}$ and $\phi'(0) = 0$ to match conditions given by the second of (3.17) and (3.18).

For quite large values of λ ($\lambda \gtrsim 25$) the system started to show extreme sensitivity on the initial conditions and, thus, the shooting method stopped to converge. Due to this problems, for lager domains a relaxation method was used, moreover we could verify those solutions obtained with shooting by comparing to ones obtained using relaxation. The discreet problem for Eq.(3.4) looks as the following

$$-\phi_i^{n+1} + 3(\phi_i^n)^2\phi_i^{n+1} - \frac{\phi_{i-1}^{n+1} - 2\phi_i^{n+1} + \phi_{i+1}^{n+1}}{h^2} - a = 2(\phi_i^n)^2,$$

boundary conditions are implemented using "imaginary points"

$$\phi_0^{n+1} - \phi_2^{n+1} = 0,$$

$$\phi_{N-1}^{n+1} - \phi_{N+1}^{n+1} = 0,$$

and condition for the mean of ϕ

$$\frac{1}{N}\sum_{i=1}^{N}\phi_i^{n+1} = \frac{1}{2}\bar{\phi}.$$

Where for space discretisation $\{x_i\}_{i=1,\bar{N}}$, $x_i = h(i-1)$, with step $h = \frac{\lambda}{2(N-1)}$. Discrete analog of the function $\phi(x)$ is $\phi_i^n = \phi(x_i)$, superscript n here is the number of an iteration.

Numerical simulation has shown that periodic solutions exist in region I (See Fig. 3.3), above the linear-limit curve and the amplitude of the solutions is growing from 0, for parameters close to this curve, becoming larger, with λ increasing. The dependence of the solutions' shapes on their periods is illustrated in the Fig. 3.4, as λ increases, as one can see, a periodic profile becomes more staggered.

For small $\bar{\phi}$, when $\bar{\phi} \in [0, \frac{1}{\sqrt{5}}]$, nontrivial periodic solutions do not exist in region II, below the linear limit curve. However, for $\bar{\phi} \in [\frac{1}{\sqrt{5}}, \frac{1}{\sqrt{3}}]$, the second order term contribution in the expansion for λ in (3.15) changes its sign, allowing nontrivial solutions exist below the linear–limit curve as well($\lambda < \lambda_l$). For $\bar{\phi} > \frac{1}{\sqrt{5}}$ two different solutions with the same $(\bar{\phi}, \lambda)$ can coexist. One of the solutions is a small–amplitude and another one is a high–amplitude. This region is bounded by the linear-limit curve from above. Both of the solutions, high– and small–amplitude, vanish when approaching this curve. The curve bounding the two-solution region from below was found numerically. On this curve two solutions become one.

3.5 Stability of periodic solutions. Lyapunov theory.

The simplest way to clarify stability properties of periodic solutions is to examine them using a suitable Lyapunov functional. In our case it is a functional of density of energy of the system.

Let's rewrite the initial equation (3.1) for one-dimensional case:

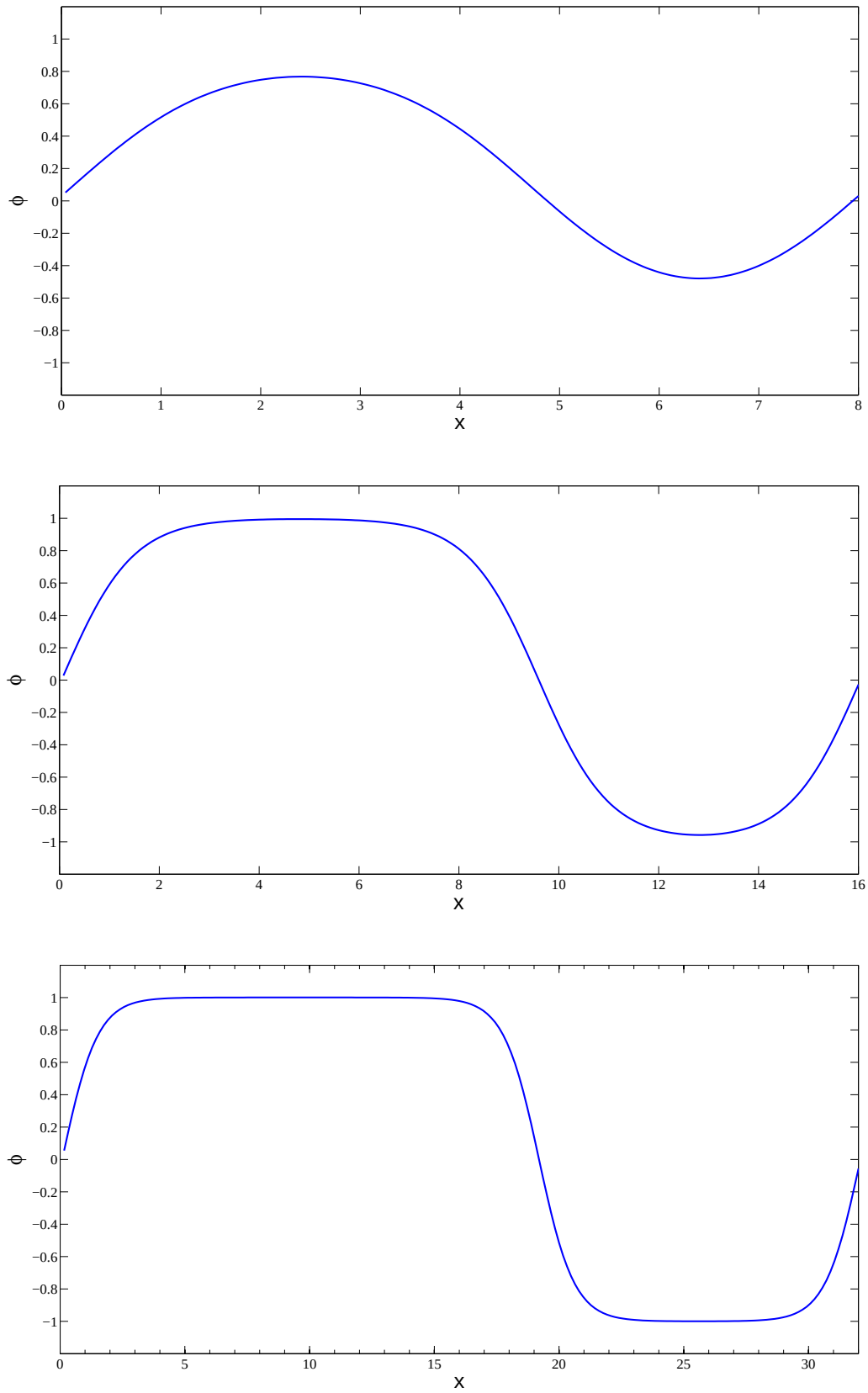

Figure 3.4: The periodic solutions for $\bar{\phi} = 0.2$ and $\lambda = 8, 16, 32$.

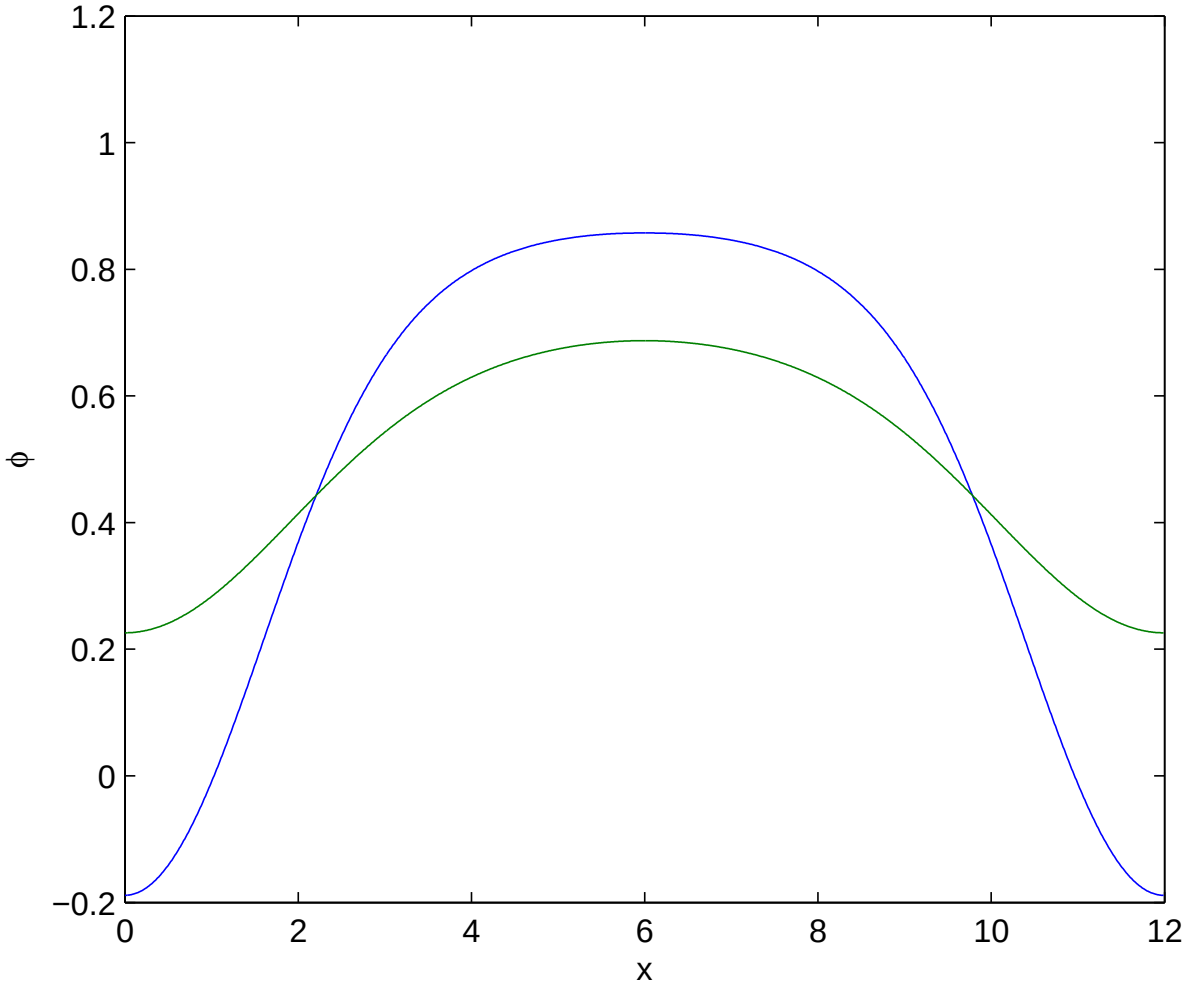

Figure 3.5: An example of a pair of solutions with the same mean and period. Parameters are the follow $\bar{\phi} = 0.5$ and $\lambda = 12$.

$$\frac{\partial \phi}{\partial t} = \frac{\partial^2}{\partial x^2}\left(-\phi + \phi^3 - \frac{\partial^2 \phi}{\partial x^2}\right) \tag{3.19}$$

One can see that the steady states satisfy

$$-\phi + \phi^3 - \frac{\partial^2 \phi}{\partial x^2} = a \tag{3.20}$$

where a is a constant of integration (we obtained this equation above). We also shall impose the condition of periodicity,

$$\phi(x + \lambda) = \phi(x), \tag{3.21}$$

and also require that the mean value of $\phi(x)$ takes a prescribed value $\bar{\phi}$,

$$\frac{1}{\lambda}\int_0^\lambda \phi dx = \bar{\phi}. \tag{3.22}$$

There has been some work done on analysis of a Lyapunov functional of the Cahn–Hilliard equation, proving instability of spatial periodic steady states (for reference see [24]). Here we provide details of the stability analysis found in [24] and confirm instability of all periodic steady states. A Lyapunov functional of one dimensional Cahn–Hilliard equation has the form

$$E = \frac{1}{\lambda}\int_0^\lambda \left[\frac{1}{2}(\frac{\partial \phi}{\partial x})^2 - \frac{\phi^2}{2} + \frac{\phi^4}{4}\right] dx. \tag{3.23}$$

Physically, E represents van der Waal's free energy [24]. We first show that it does not grow in time. Indeed, differentiating E with respect to time and using (3.19), we can show that

$$\frac{dE}{dt} = \frac{1}{\lambda}\int_0^\lambda \left[\frac{\partial \phi}{\partial x}\frac{\partial^2 \phi}{\partial x \partial t} + (-\phi + \phi^3)\frac{\partial \phi}{\partial t}\right] dx$$

Using integration by parts we can show that ,

$$\frac{dE}{dt} = \frac{1}{\lambda}\int_0^\lambda \left(-\frac{\partial^2 \phi}{\partial x^2} - \phi + \phi^3\right)\frac{\partial \phi}{\partial t} dx.$$

Using initial equation (3.19) and integration by parts we have

$$\frac{dE}{dt} = -\frac{1}{\lambda}\int_0^\lambda \left[\frac{\partial}{\partial x}\left(-\frac{\partial^2\phi}{\partial x^2} - \phi + \phi^3\right)\right]^2 dx.$$

Note, that $\frac{dE}{dt} = 0$, if only $-\phi+\phi^3-\frac{\partial^2}{\partial x^2}\phi = \text{const}$, which is a steady state condition. If it is not a steady state solution, then

$$\frac{dE}{dt} < 0.$$

We proved that functional E does not increase with time, so it satisfies the definition of a Lyapunov functional. Following Lyapunov theory, a steady state is stable if and only if it corresponds to a minimum of E. Any given steady state is an extremum of E. To prove that a steady state is unstable, we need to show that it does not minimize the energy even locally. Let us consider a steady state, we fix parameter $\bar{\phi}$, i.e. its 'mass' or an integral of ϕ over a period cannot be changed. The only parameter of such steady state that can be changed, is the period. We assume there exist such disturbances that can change the period of a steady state without changing its 'mass'. If we can show that such disturbances also reduce the steady state's energy, that would mean that this steady state is unstable. To do so we will show that for a family of steady states with fixed mean $\bar{\phi}$, the energy E is a monotonically decreasing function of λ and, hence, there are solutions close to periodic, but with smaller energy, which proves instability.

To examine $E(\lambda)$ we make the following substitution

$$\xi = \frac{x}{\lambda}$$

which from (3.20), (3.21), (3.22) yields

$$-\phi + \phi^3 - \frac{1}{\lambda^2}\frac{\partial^2}{\partial \xi^2}\phi = a \tag{3.24}$$

$$\phi(\xi + 1) = \phi(\xi) \tag{3.25}$$

$$\int_0^1 \phi d\xi = \bar{\phi} \tag{3.26}$$

Substituting steady state into expression for energy (3.23), we rewrite it in terms of ξ,

$$E = \int_0^1 \left[\frac{1}{2\lambda^2} \left(\frac{\partial \phi}{\partial \xi} \right)^2 - \frac{\phi^2}{2} + \frac{\phi^4}{4} \right] d\xi$$

Differentiating E with respect to λ, we have

$$\frac{dE}{d\lambda} = \int_0^1 \left[-\frac{1}{\lambda^3} \left(\frac{\partial \phi}{\partial \xi} \right)^2 + \frac{1}{\lambda^2} \frac{\partial \phi}{\partial \xi} \frac{\partial^2 \phi}{\partial \xi \partial \lambda} - \phi \frac{\partial \phi}{\partial \lambda} + \phi^3 \frac{\partial \phi}{\partial \lambda} \right] d\xi$$

Integrating by parts, and using (3.19), we obtain

$$\frac{dE}{d\lambda} = -\frac{1}{\lambda^3} \int_0^1 \left(\frac{\partial \phi}{\partial \xi} \right)^2 d\xi + a \int_0^1 \frac{\partial \phi}{\partial \lambda} d\xi$$

After differentiation (3.26) with respect to λ, we show that

$$\int_0^1 \frac{\partial \phi}{\partial \lambda} d\xi = 0.$$

From where it follows, that

$$\frac{dE}{d\lambda} = -\frac{1}{\lambda^3} \int_0^1 \left(\frac{\partial \phi}{\partial \xi} \right)^2 d\xi < 0$$

as required. Hence, all periodic steady states of Eq.(3.19) are unstable. A very similar analysis was done in [3] for a different set of equations.

3.6 Stability with periodic disturbance

Here we perform another technique of stability analysis. We examine the stability of periodic solutions of (3.19) with respect to multiple-period perturbations.

$$\frac{\partial \phi}{\partial t} = \frac{\partial^2}{\partial x^2} \left(-\phi + \phi^3 - \frac{\partial^2}{\partial x^2} \phi \right) \tag{3.27}$$

We are looking for a solution of the above equation with a disturbance of the following form

$$\phi = \Phi(x) + \phi'(x,t), \tag{3.28}$$

where Φ is a base solution, found from

$$\Phi - \Phi^3 + \frac{\partial^2 \Phi}{\partial x^2} = \text{const.}$$

With periodic boundary conditions on the base solution

$$\Phi(x+\lambda) = \Phi(x).$$

After substituting (3.28) into (3.27) and linearizing (the disturbance $\phi'(x,t)$ here is a small parameter), we obtain

$$\frac{\partial \phi'}{\partial t} = \frac{\partial^2}{\partial x^2}\left(-\phi' + 3\Phi^2\phi' - \frac{\partial^2 \phi'}{\partial x^2}\right) \tag{3.29}$$

We consider a harmonic disturbance

$$\phi'(x,t) = \psi(x)e^{st}, \tag{3.30}$$

where s is a growth/decay rate.

Let the periodic boundary conditions for the factor $\psi(x)$ of disturbance (3.30) be

$$\psi(x+n\lambda) = \psi(x) \tag{3.31}$$

Substitution of (3.30) into (3.29) yields

$$s\psi = -\frac{d^2}{dx^2}(\psi - 3\Phi^2\psi + \frac{d^2}{dx^2}\psi) \tag{3.32}$$

We shall also require that the disturbance be localized near the base solution,

$$|\psi| < const \tag{3.33}$$

for any x. We have (3.32), (3.33) an eigenvalue problem, where $\psi(x)$ plays a role of an eigenfunction and s, in turn, plays a role of an eigenvalue.

We now introduce a differential operator

$$D(\bullet) = \frac{d^2}{dx^2}(\bullet - 3\Phi^2 \bullet + \frac{d^2}{dx^2}\bullet),$$

which is nonlinear, not self-adjoint differential operator of the order four. It complicates the problem as $D(\bullet)$ is not self-adjoint, but if we introduce $\eta(x)$ such that

$$\psi = \frac{d\eta}{dx}, \qquad |\eta| < const \text{ for any } x. \tag{3.34}$$

We substitute (3.34) into (3.32) and have

$$s\frac{d\eta}{dx} = -\frac{d^2}{dx^2}((1 - 3\Phi^2)\frac{d\eta}{dx} + \frac{d^3\eta}{dx^3}), \tag{3.35}$$

After integration (3.35), yields

$$s\eta = -\frac{d}{dx}((1 - 3\Phi^2)\frac{d\eta}{dx}) - \frac{d^4\eta}{dx^4}, \tag{3.36}$$

now the operator on the right-hand side of (3.36) is a self-adjoint operator. We can show that by multiplying (3.36) by η^*, the complex conjugate of η. Then integrating by parts appropriate number of times with respect to x over $(-\infty, +\infty)$ with periodic boundary conditions, we show that

$$(D'\eta, \eta^*) = (D'\eta^*, \eta),$$

where D' is a differential operator on the right-hand side of (3.36) and $(\centerdot, \centerdot)$ is a product in L_2 for example.

The following properties for the eigenvalue problem (3.36) can be pointed out now

1. The eigenvalue problem (3.36) can have only real eigenvalues.

2. All of the eigenfunctions corresponding to different eigenvalues are linearly independent.

Laugesen and Pugh in [28] studied linear stability of a Cahn–Hilliard like equation, which is more generalized situation than the Cahn–Hilliard equation. They studied a self-adjoint differential operator (which is a more general form of the operator in 3.36) coming from linearization of the equation with respect to small perturbations. They provided a complete analytical study of the stability of periodic steady states. One of their results, that we will confirm in our studies, is instability of all periodic steady states with respect to perturbations with wavelengths greater then the wavelength of the steady state.

Analytically we were able to examine the stability of periodic solutions with periodic disturbances in a case of linear-limit solution only. We have an eigenvalue problem (3.36). In the linear–limit case the disturbance is limited to simple cosine–like waves, thus,we seek a solution of the form

$$\psi = e^{ikx}, \tag{3.37}$$

where k is a wavenumber. Substitution of (3.37) into (3.36) gives us

$$s = k^2(1 - 3\bar{\Phi}^2 - k^2), \tag{3.38}$$

we can rewrite k in terms of λ

$$k = \frac{2m\pi}{n\lambda},$$

n here is a quotient of periods of a perturbation with period Λ and a base function with period λ, m is a sequence number of a corresponding eigenfunction.

One can see that the growth rate s might be non-positive (which corresponds to stable state) for all k, if only

$$1 - 3\bar{\Phi}^2 \geq 0, \tag{3.39}$$

which is a trivial condition for our system. Generally, instability occurs for

$$k < \sqrt{1 - 3\bar{\Phi}^2}, \tag{3.40}$$

which is unconditionally true, unless perturbation has the same period as the base

solution.

But these results are true only for the linear-limit case. For the general situation numerical simulations were done.

3.7 Stability with periodic disturbance. Numerical results.

We want to examine stability of periodic solutions of (3.27) with respect to multiple-period perturbations numerically.

Calculating the spectrum of the corresponding eigenvalue problem (actually we need just the greatest eigenvalue) we can check the stability of solutions. If all of the eigenvalues are less than zero, then the disturbance stabilize the solution. If there is even one eigenvalue greater then zero, that entails instability.

The discrete operator for eigenvalue problem (3.32), (3.33) is the following

$$\frac{1}{h^4}[\psi_{i-2} - 4\psi_{i-1} + 6\psi_i - 4\psi_{i+1} + \psi_{i+2}]+$$

$$+\frac{1}{12h^2}[-\psi_{i-2}(1 - 3\Phi_{i-2}^2) + 16\psi_{i+1}(1 - 3\Phi_{i-1}^2)- \tag{3.41}$$

$$-30\psi_i(1 - 3\Phi_i^2) + 16\psi_{i+1}(1 - 3\Phi_{i+1}^2) - \psi_{i+2}(1 - 3\Phi_{i+2}^2)],$$

where for space discretisation $\{x_i\}_{i=1,\bar{n}N}$, $x_i = h(i-1)$, with step $h = \frac{\lambda}{N-1}$, discrete analogs of the functions $\psi(x)$ and $\Phi(x)$ are $\psi_i = \psi(x_i)$, $\Phi_i = \Phi(x_i)$ respectively. Parameter n here is a quotient of perturbation period Λ and base function period λ

$$n = \frac{\Lambda}{\lambda}.$$

We can find the spectrum of discrete operator (3.41) numerically, using corresponding methods implemented in MatLab. Separating true eigenvalues of continuous operator D' from eigenvalues of the discrete operator we find the maximum eigenvalue and an eigenfunction which corresponds to it. In the linear-limit case, analytical (3.38) and numerical results were compared. Numerical experiments show

that for $n > 1$ instability occurs. The trivial case $n = 1$ gives stability. In the picture below you can find graphs of the maximum eigenvalue versus mean $\bar{\phi}$ for different periods λ (close to linear-limit case and greater than the linear-limit period), calculated both analytically and numerically (See Fig. 3.6). One can see that in the linear-limit case, analytical results agree with numerical results, which is not true for periods different from linear-limit case for corresponding $\bar{\phi}$. In the figure 3.7 these low frequency eigenfunctions for different n are shown.

Howard in [22] has studied periodic steady states of the Cahn–Hilliard equation using spectral analysis. For instance, he stated in Theorem 1.5 of [22] that periodic steady states are unstable with respect to multiple period disturbances and are stable with respect to disturbances of the same period as a given steady state has. He also carried out a stability analysis of two other type of solutions of the Cahn–Hilliard equation, so-called pulse-type and reversal solutions (for references see [22]). We can confirm his stability results for periodic steady states. Solutions of other types are not examined in this thesis.

3.8 Conclusions

In the present chapter we found spatial steady states in the process of spinoidal decomposition. This results are not new and such solutions were obtained previously using different approaches: minimizing the free energy functional of the system (for reference see [27]), studying the Cahn–Hilliard equation [34], which they did for the more general form of the free energy per molecule in the system f_0 given by (2.8). Our results agree well with ones presented in the above mentioned papers. Moreover, we carried out a complete analysis of periodic steady states regarding the parameters of the system $\bar{\phi}$ and λ and found a region of existence of a pair of solutions with different amplitudes but the same mean and period. We also verified the results of [27], [34] regarding the stability of the system using the energy integral (3.23) as a Lyapunov functional and solved and eigenvalue problem corresponding to the system with applied periodic disturbances. The main aim of this work was to develop a methodology and to train on a simple equation before getting to the main objective of this thesis: periodic steady states of the extended Cahn–Hilliard

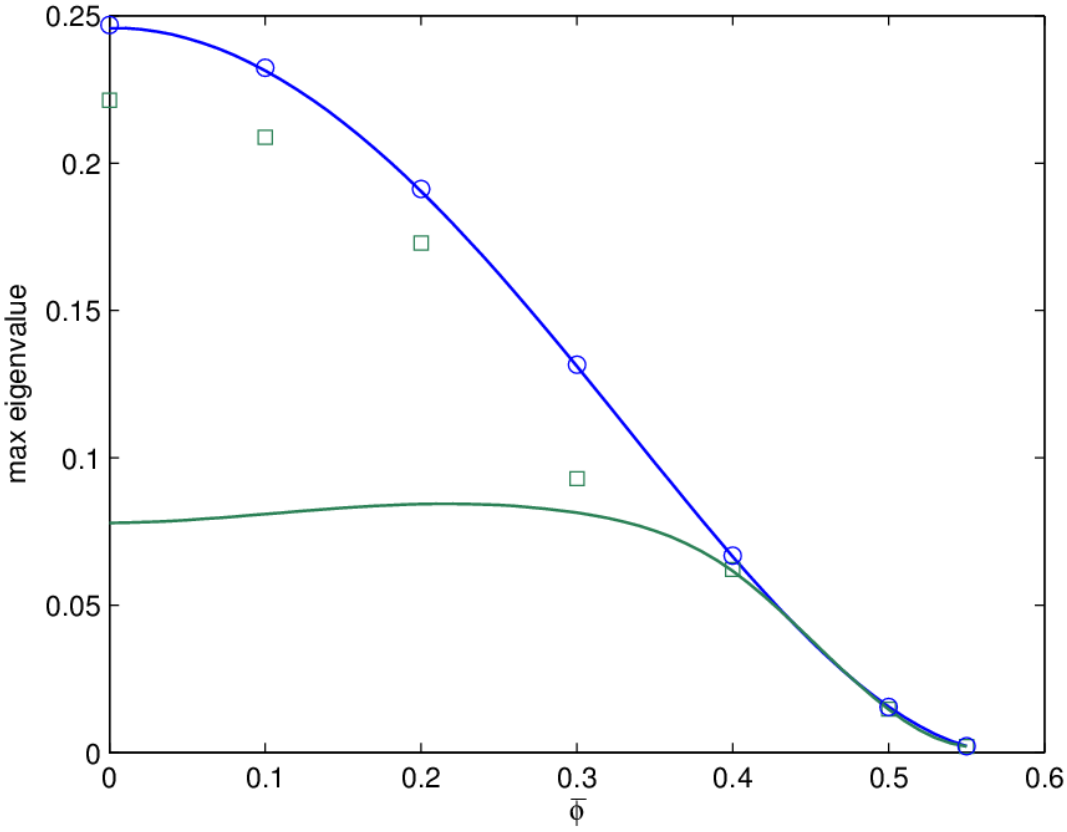

Figure 3.6: Maximum eigenvalue versus mean $\bar{\phi}$ for different periods, calculated numerically (solid lines) and analytically (dots). The top line corresponds to solutions with λ close to the linear-limit case.

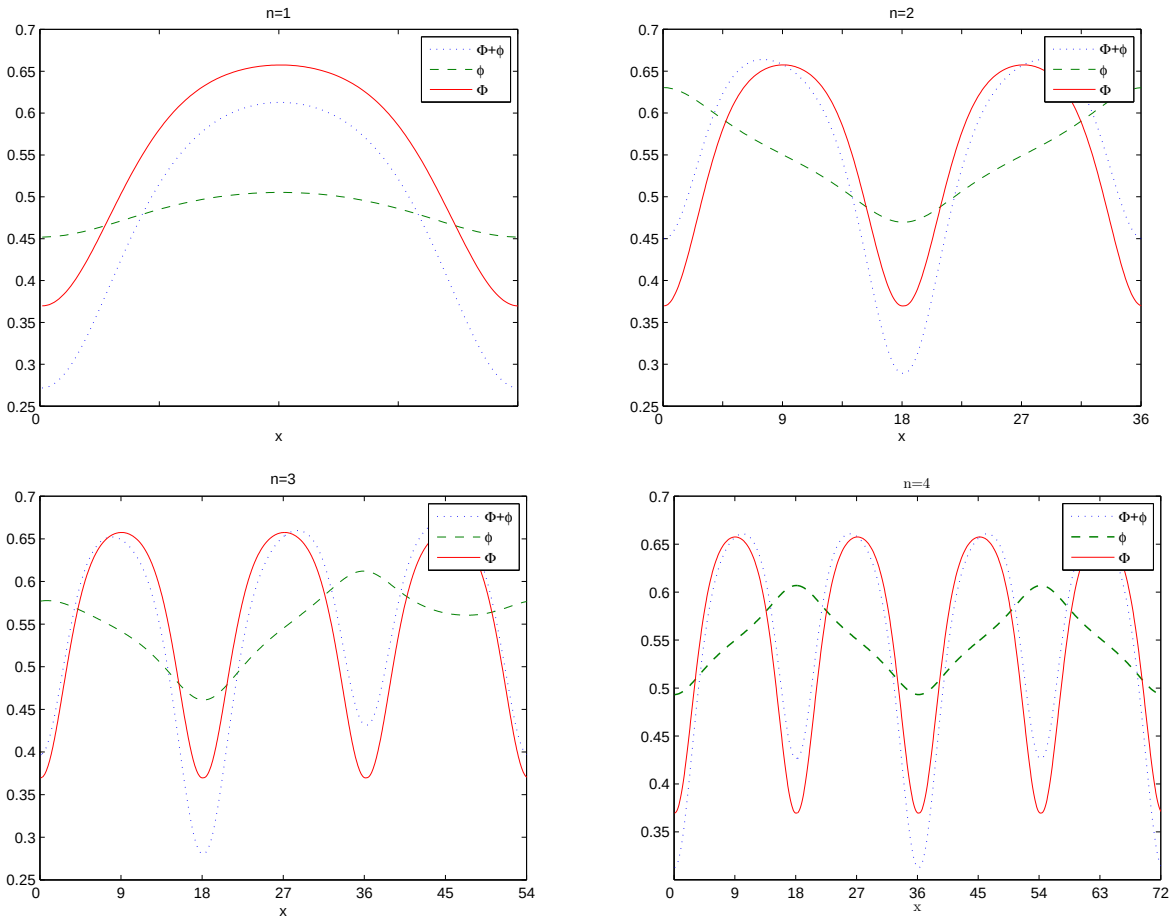

Figure 3.7: Base periodic solutions $\Phi(x,t)$ versus periodic disturbances(shifted by the mean of Φ) $\phi(x,t)$ (correspond to dashed lines) at initial moment for $n = 1,2,3,4$. Dotted lines are disturbed solutions at the same moment. Disturbances are given by the eigenfunctions corresponding to the largest eigenvalues.

equation.

Chapter 4

Extended Cahn-Hilliard equation. Periodic spatial solutions.

4.1 Introduction

In the present chapter we shall consider an extension of the Cahn-Hilliard equation (2.29). The difference of an extended Cahn-Hilliard equation is the presence of the linear term with the constant controlling parameter α. This term in fact makes a global segregation impossible, leaving liability to a local segregation only (for reference see Chapter 2). This property of the extended equation makes it applicable in specifying periodic spatial patterns in BCP phase separation, in which we see the main reason of studying that type of equation. The work that has been done was to describe the entire family of spatial periodic solutions of Eq.(2.29) for all parameter domain of the system and to perform a stability analysis of solutions that have been found.

We consider a one-dimentional extention of Cahn–Hilliard equation

$$\frac{\partial \phi}{\partial t} + \frac{\partial^2}{\partial x^2}(\phi - \phi^3 + \frac{\partial^2}{\partial x^2}\phi) + \alpha\phi = 0. \tag{4.1}$$

As for Cahn-Hilliard equation, a spatial periodic solution of extended Cahn-Hilliard equation depends on three parameters: the period of a solution λ, the amplitude of a solution A and controlling parameter α. The mean value of the solution $\overline{\phi}$ is

always zero for $\alpha \neq 0$,

$$\overline{\phi} = \int_0^\lambda \phi \, \mathrm{d}x = 0. \tag{4.2}$$

And similarly, only two of the specified parameters are independent. They are chosen to be λ and α. We are looking for steady states, that implies time independence. For simplicity the one-dimentional case was examined. An equation of a stationary one-dimentioinal regime is

$$\frac{\partial^2}{\partial x^2}(\phi - \phi^3 + \frac{\partial^2}{\partial x^2}\phi) + \alpha\phi = 0, \tag{4.3}$$

with spatial periodic boundary conditions

$$\phi(x + \lambda) = \phi(x). \tag{4.4}$$

In order to find the boundaries of the region where nontrivial periodic steady states exist we expand the unknown function ϕ and all of the parameters into series with some small ε around a zero solution. Again one can think of ε as of an amplitude of a solution close to a trivial $\phi(x) = 0$ one.

$$\phi = 0 + \varepsilon\phi^{(1)} + \cdots, \tag{4.5}$$

$$\alpha = \alpha^{(0)} + \varepsilon\alpha^{(1)} + \cdots, \tag{4.6}$$

$$\lambda = \lambda^{(0)} + \varepsilon\lambda^{(1)} + \cdots. \tag{4.7}$$

Substituting (4.5)–(4.7) into (4.3)–(4.4), in the first order we have

$$\frac{\partial^2}{\partial x^2}(\phi^{(1)} + \frac{\partial^2}{\partial x^2}\phi^{(1)}) + \alpha^{(0)}\phi^{(1)} = 0,$$

$$\phi^{(1)}(x + \lambda) = \phi^{(1)}(x).$$

solving which we obtain a relation between $\alpha^{(0)}$ and $\lambda^{(0)}$

$$\lambda^{(0)} = \frac{2\pi}{\sqrt{\frac{1}{2} \pm \sqrt{\frac{1}{4} - \alpha^{(0)}}}}, \tag{4.8}$$

which describes a borderline of the region of existence of periodic solutions. This result was previously obtained in [32]. Calculating coefficients of the next order we will show later that

$$\frac{2\pi}{\sqrt{\frac{1}{2}+\sqrt{\frac{1}{4}-\alpha}}} < \lambda < \frac{2\pi}{\sqrt{\frac{1}{2}-\sqrt{\frac{1}{4}-\alpha}}}. \tag{4.9}$$

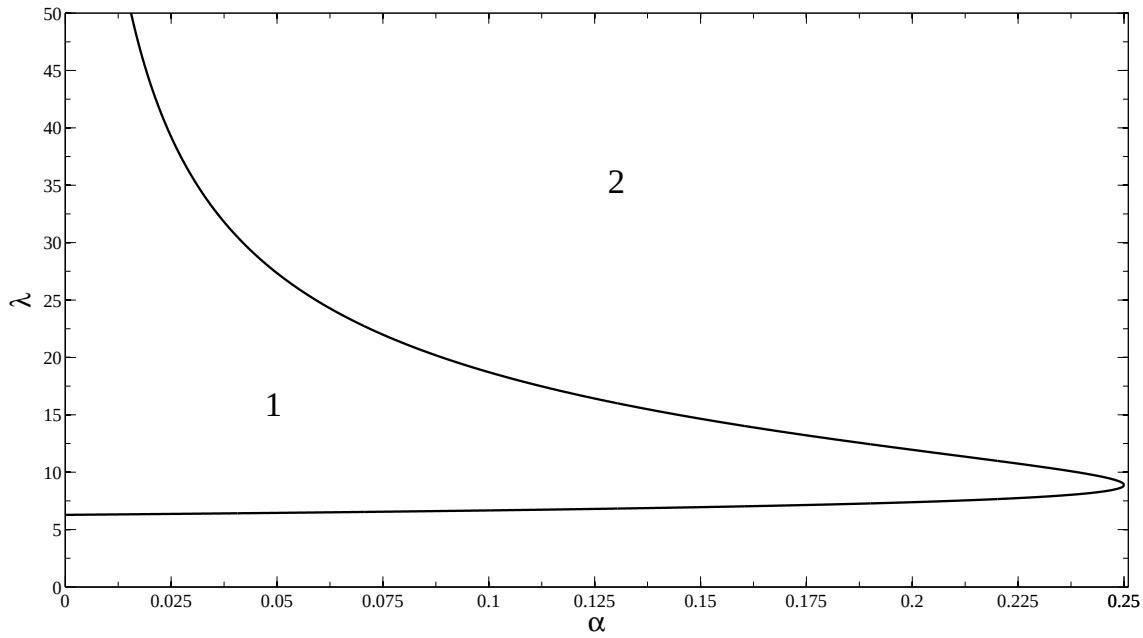

Figure 4.1: Existence region boundaries are given by (4.8). Nontrivial periodic solutions exist in the region 1, in the region 2 only trivial solutions ($\phi(x) = 0$) exist.

Nontrivial periodic solutions exist to the left from the curves (4.8), see Fig. 4.1. We will show later using numerical simulations that the amplitude of such solutions decreases approaching to the borderline and they become zero on it. The nonlinear term in Eq.(4.3) is small compare to other terms in the left neighborhood of the lines (4.8). This fact allows us to use perturbation theory to obtain analytical solutions there. We call such a regime the case of weak nonlinearity.

4.2 Weak nonlinearity

We first introduce a new ϕ

$$\phi = \varepsilon^{1/2}\phi_{new}(x), \tag{4.10}$$

where ε is a small parameter greater than zero. Then Eq.(4.3) yields, $_{new}$ omitted

$$\frac{\partial^2}{\partial x^2}\left(\phi + \frac{\partial^2}{\partial x^2}\phi\right) + \alpha\phi = \varepsilon\frac{\partial^2}{\partial x^2}\phi^3, \tag{4.11}$$

The boundary conditions (4.4) and the condition (4.2) for the mean value of ϕ hold.

Now we will rewrite Eq.(4.11) as a system of two equations of the second order. Differential operator on the left side of (4.11) may be written in a form

$$D(\cdot) = \left(\frac{\mathrm{d}^2}{\mathrm{d}x^2} + a_+\right)\left(\frac{\mathrm{d}^2}{\mathrm{d}x^2} + a_-\right)(\cdot), \tag{4.12}$$

where a_+ and a_- are taken to be

$$a_+a_- = \alpha, \qquad a_+ + a_- = 1.$$

Hence, in terms of α they are

$$a_\pm = \frac{1}{2} \pm \sqrt{\frac{1}{4} - \alpha}.$$

Now we introduce new functions ϕ_+ and ϕ_-, such that

$$\phi = \phi_+ + \phi_-, \tag{4.13}$$

and let ϕ_- satisfy the following

$$\left(\frac{\mathrm{d}^2}{\mathrm{d}x^2} + a_-\right)\phi_- = \varepsilon\left[b_1\phi^3 + b_2\frac{\partial^2}{\partial x^2}\phi^3\right], \tag{4.14}$$

where b_1, b_2 are some unknown constants. Substituting (4.12)–(4.14) into Eq.(4.11)

we can obtain the following equation

$$\left(\frac{\mathrm{d}^2}{\mathrm{d}x^2}+a_+\right)\left(\frac{\mathrm{d}^2}{\mathrm{d}x^2}+a_-\right)\phi_+=-\varepsilon\left[b_2\frac{\mathrm{d}^4}{\mathrm{d}x^4}+\left(b_1+b_2a_+-1\right)\frac{\mathrm{d}^2}{\mathrm{d}x^2}+b_1a_+\right]\phi^3. \tag{4.15}$$

Choosing b_1, b_2 differential operator on the right-hand side of (4.15) can be written in the form

$$b_2\frac{\mathrm{d}^4}{\mathrm{d}x^4}+\left(b_1+b_2a_+-1\right)\frac{\mathrm{d}^2}{\mathrm{d}x^2}+b_1a_+=\left(\frac{\mathrm{d}^2}{\mathrm{d}x^2}+a_-\right)\left(b_2\frac{\mathrm{d}^2}{\mathrm{d}x^2}+b_1a_-\right). \tag{4.16}$$

where b_1, b_2 are required to be

$$b_1=0, \qquad b_2=\frac{1}{a_+-a_-}, \tag{4.17}$$

here we want to notice, that we assume a_+-a_- to be different from zero, and hence, $\alpha\neq\frac{1}{4}$. We will carry out a solution for the case when $\alpha=\frac{1}{4}$ later on. Using (4.16) and (4.17) and integrating (4.15) with conditions (4.4) we obtain

$$\left(\frac{\mathrm{d}^2}{\mathrm{d}x^2}+a_+\right)\phi_+=-\varepsilon\left(b_2\frac{\mathrm{d}^2}{\mathrm{d}x^2}\right)\phi^3+c\cos\left(\sqrt{a_-}x+\theta\right). \tag{4.18}$$

Making a substitution

$$\epsilon=\frac{\varepsilon}{a_+-a_-}=\varepsilon b_2, \qquad k_\pm=\sqrt{a_\pm},$$

and, taking into account (4.13), we rewrite (4.18) in a form

$$\phi_+''+k_+^2\phi_+=-\epsilon\left[\left(\phi_++\phi_-\right)^3\right]''+c\cos\left(k_-x+\theta\right), \tag{4.19}$$

where prime denotes differentiation with respect to x. Now Eq.(4.14) with (4.16), (4.17) and (4.13) takes form

$$\phi_-''+k_-^2\phi_-=\epsilon\left[\left(\phi_++\phi_-\right)^3\right]''. \tag{4.20}$$

Changing variables both in (4.19) and (4.20)

$$\begin{aligned}\phi_+ &= \phi_{+new} + \frac{c}{k_+^2 - k_-^2}\cos\left(k_- x + \theta\right),\\ \phi_- &= \phi_{-new} - \frac{c}{k_+^2 - k_-^2}\cos\left(k_- x + \theta\right),\end{aligned}$$

and omitting $_{new}$, we derive a system

$$\phi_+'' + k_+^2\phi_+ = -\epsilon\left[\left(\phi_+ + \phi_-\right)^3\right]'' \tag{4.21}$$

$$\phi_-'' + k_-^2\phi_- = \epsilon\left[\left(\phi_+ + \phi_-\right)^3\right]'' \tag{4.22}$$

Rescaling space variable x and wavenumbers $k_\pm$ as following

$$x = \frac{\lambda}{2\pi}x_{new}, \qquad k_{\pm new} = \frac{\lambda}{2\pi}k_\pm,$$

and omitting $_{new}$, we obtain from (4.21)–(4.22) a system of two second order equations

$$\phi_+'' + k_+^2\phi_+ = -\epsilon\left[\left(\phi_+ + \phi_-\right)^3\right]'', \tag{4.23}$$

$$\phi_-'' + k_-^2\phi_- = \epsilon\left[\left(\phi_+ + \phi_-\right)^3\right]'', \tag{4.24}$$

with 2π-periodic boundary conditions

$$\phi_\pm(x + 2\pi) = \phi_\pm(x). \tag{4.25}$$

System (4.23)–(4.25) has a number of advantages. Second order equations are easier to work with, there are certain similarities between equations and, thus, between their solutions. Besides we eliminated parameter λ from the boundary conditions. New parameters of the system (4.23)–(4.25) $k_\pm$ have the following relation with the parameters λ, α of the original system (4.3), (4.4)

$$k_\pm = \frac{\lambda}{2\pi}\sqrt{\frac{1}{2} \pm \sqrt{\frac{1}{4} - \alpha}}. \tag{4.26}$$

The relation between the original unknown function ϕ and $\phi_\pm$ is given by (4.13).

4.3 Single–wave solution

In this section we will discuss the most general type of periodic solutions of (4.23)–(4.25), which we called a single-wave solution, as only one of the functions $\phi_\pm$ has a nontrivial term in a leading order. We using perturbation theory to find solutions of system (4.23), (4.24) with periodic boundary condition (4.25).We seek a solution of the form (not to confuse with (4.5))

$$\phi_\pm = \phi_\pm^{(0)} + \epsilon\phi_\pm^{(1)} + \cdots , \tag{4.27}$$

$$k_\pm = k_\pm^{(0)} + \epsilon k_\pm^{(1)} + \cdots , \tag{4.28}$$

To the leading order of Eq.(4.23), (4.24) and condition (4.25) with (4.27) it follows

$$\phi_\pm^{(0)\prime\prime} + k_\pm^{(0)2}\phi_\pm^{(0)} = 0, \tag{4.29}$$

$$\phi_\pm^{(0)}(x + 2\pi) = \phi_\pm^{(0)}(x). \tag{4.30}$$

System (4.29) allows shifting along the x–axis as well as linear rescaling of $\phi_\pm^{(0)}(x)$. Without loss of generality we choose initial conditions for $\phi_+^{(0)}$ to be such, that

$$\phi_+^{(0)} = \cos k_+^{(0)} x, \tag{4.31}$$

and $\phi_+^{(0)}$ should satisfy (4.30), we find

$$k_+^{(0)} = n, \qquad n \in \mathbb{N}. \tag{4.32}$$

For completeness of the analysis we present an existence diagram for solutions with $k_+^{(0)} = 1, 2, 3, 4$. (for reference see Fig.4.2). One should keep in mind, that for $k_+^{(0)} > 1$ the period of a steady state can be reduced to a corresponding solution with $k_+^{(0)} = 1$ and, therefore, we carry out analysis for $k_+^{(0)} = 1$ only further on. At the points where boundaries of the regions of existence for different $k_+^{(0)}$ intersect, bifurcations of so-called 'two-wave' solutions appear, which we will discuss later on.

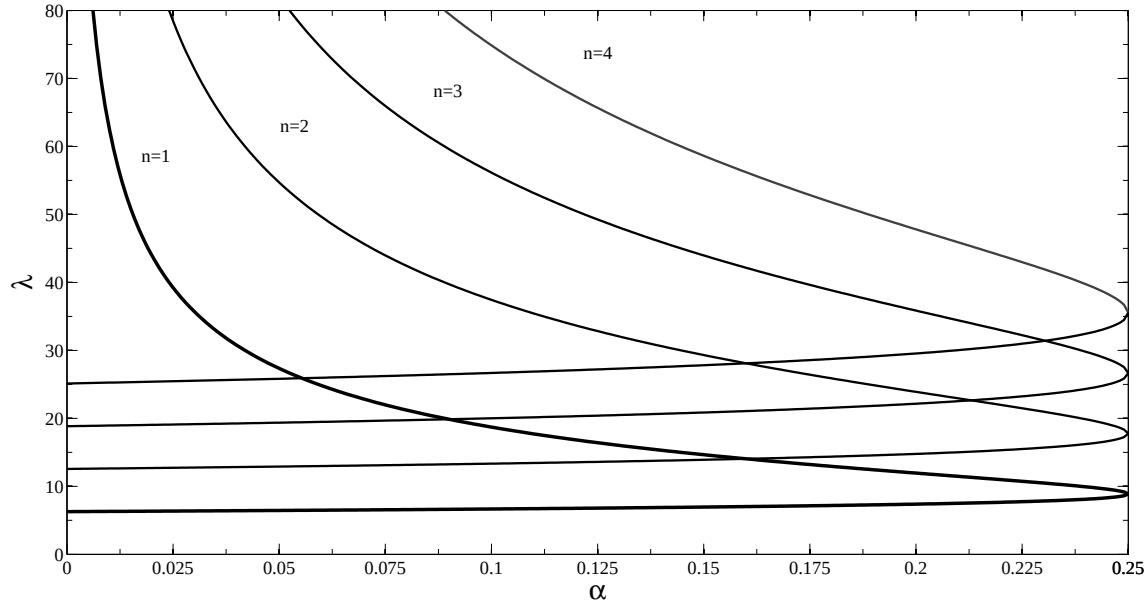

Figure 4.2: Existence regions boundaries of single-wave solutions corresponding to different $k_+^{(0)} = 1, 2, 3, 4$. Bifurcations of 'two-wave' solutions occur at intersections of boundaries of existence of different multiple period solutions.

We now consider

$$k_+^{(0)} = 1. \tag{4.33}$$

Condition (4.26) should state, hence

$$k_-^{(0)} = \sqrt{\frac{\frac{1}{2} - \sqrt{\frac{1}{4} - \alpha}}{\frac{1}{2} + \sqrt{\frac{1}{4} - \alpha}}}, \tag{4.34}$$

that implies

$$\phi_-^{(0)} = 0, \tag{4.35}$$

for an arbitrary α in order to keep solution $2\pi-$periodic.

In the first order we have, substituting (4.27), (4.28), (4.31)–(4.35) into Eq.(4.23), (4.24)

$$\phi_+^{(1)\prime\prime} + \phi_+^{(1)} + 2k_+^{(1)} \cos x = -\left(\cos^3 x\right)'', \tag{4.36}$$

$$\phi_-^{(1)\prime\prime} + k_-^{(0)2}\phi_-^{(1)} = \left(\cos^3 x\right)''. \tag{4.37}$$

We are looking for 2π–periodic bounded solutions. That means that all terms producing growing oscillations in the Eq.(4.36)–(4.37) (those containing $\cos x$ or $\sin x$ in (4.36) and those containing $\cos k_-^{(0)}x$ or $\sin k_-^{(0)}x$ in (4.37)) should be eliminated. We can choose parameter $k_+^{(1)}$ in order to meet this requirement. Hence, we find

$$k_+^{(1)} = \frac{3}{8}, \tag{4.38}$$

and, that yields,

$$\phi_+^{(1)} = -\frac{9}{32}\cos 3x, \tag{4.39}$$

$$\phi_-^{(1)} = -\frac{1}{4}\left(\frac{3}{k_-^{(0)2}-1}\cos x + \frac{9}{k_-^{(0)2}-9}\cos 3x\right). \tag{4.40}$$

It follows from (4.34) that $k_- < 1$ – hence, $k_-^{(0)} \neq 1, 3$ – hence, $\phi_-^{(1)}$ always exists.

Now we can show that periodic solution exist in the region above from the curve $\lambda(\alpha) = \frac{2\pi}{\sqrt{\frac{1}{2}+\sqrt{\frac{1}{4}-\alpha}}}$ or, equally, that the first inequality of (4.9) holds. Using (4.26) and (4.38) we have

$$\frac{\lambda^{(1)}}{2\pi}\sqrt{\frac{1}{2}+\sqrt{\frac{1}{4}-\alpha}} = \frac{3}{8},$$

hence,

$$\lambda = \frac{2\pi\left[1+\frac{3}{8}\epsilon+\mathrm{O}(\epsilon^2)\right]}{\sqrt{\frac{1}{2}+\sqrt{\frac{1}{4}-\alpha}}}.$$

Similarly we examine the case where

$$\phi_-^{(0)} = \cos x, \qquad k_-^{(0)} = 1, \tag{4.41}$$

again without loss of generality we can choose $\phi_-^{(0)}$ to be such as (4.41) and, hence,

$$\phi_+^{(0)} = 0, \tag{4.42}$$

and

$$k_+^{(0)} = \sqrt{\frac{\frac{1}{2} + \sqrt{\frac{1}{4} - \alpha}}{\frac{1}{2} - \sqrt{\frac{1}{4} - \alpha}}}. \tag{4.43}$$

Using the same ideas, we find

$$k_-^{(1)} = -\frac{3}{8},$$

to ensure the periodicity, which yields

$$\phi_+^{(1)} = \frac{1}{4}\left(\frac{3}{k_+^2 - 1}\cos x + \frac{9}{k_+^2 - 9}\cos 3x\right), \tag{4.44}$$

$$\phi_-^{(1)} = \frac{9}{32}\cos 3x. \tag{4.45}$$

Solution (4.9) exists only when $k_+ \neq 1, 3$. Similarly we show that

$$\lambda = \frac{2\pi\left[1 - \frac{3}{8}\epsilon + \mathrm{O}(\epsilon^2)\right]}{\sqrt{\frac{1}{2} - \sqrt{\frac{1}{4} - \alpha}}},$$

hence, periodic solutions belong to the region below $\lambda(\alpha) = \frac{2\pi}{\sqrt{\frac{1}{2} - \sqrt{\frac{1}{4} - \alpha}}}$, or, that the second inequality of (4.9) holds.

In the present section we have found so-called single wave solution, that are given by (4.31)–(4.35), (4.39), (4.40) and (4.41)–(4.45). It has one dominant oscillation with period 2π and exists everywhere in the neighborhood of the curve (4.8) but a point where $\{k_+, k_-\} = \{3, 1\}$. Solution (4.41)–(4.45) becomes invalid for this values of $k_\pm$. This special case will be examined later. The critical value of $\{\alpha, \lambda\}$ for such situation is $\{\frac{9}{100}, 2\pi\sqrt{10}\}$.

4.4 Two–wave solution

Considering a situation from the previous section, one can see that there are certain values of α, and hence, $k_+^{(0)}$, for which $\phi_+^{(0)}$ can be different from zero (see (4.42)) and 2π– periodic at the same time. This situation occurs when k_+ and k_- do not have a common divisor. We call such solution a two-wave solution because there are two different frequency oscillations present in the leading order. Apparently, there is an

infinite number of such extra solutions coexisting along with a general single-wave solution at some neighborhoods of certain points on a $(\lambda, \alpha)-$ plane. In this section we shall examine solutions of this type. We are solving the system (4.23), (4.24) with periodic boundary condition (4.25) We seek a solution in the form of series

$$\phi_{\pm} = \phi_{\pm}^{(0)} + \epsilon\phi_{\pm}^{(1)} + \cdots, \tag{4.46}$$

and we also expand into series all the parameters of the problem

$$\lambda = \lambda^{(0)} + \epsilon\lambda^{(1)} + \cdots, \tag{4.47}$$

$$\alpha = \alpha^{(0)} + \epsilon\alpha^{(1)} + \cdots, \tag{4.48}$$

$$k_{\pm} = k_{\pm}^{(0)} + \epsilon k_{\pm}^{(1)} + \cdots, \tag{4.49}$$

To the leading order of (4.23), (4.24), with (4.46)–(4.49), we have

$$\phi_{\pm}^{(0)\prime\prime} + k_{\pm}^{(0)2}\phi_{\pm}^{(0)} = 0, \tag{4.50}$$

From (4.26) we can also obtain

$$k_{\pm}^{(0)} = \frac{\lambda^{(0)}}{2\pi}\sqrt{\frac{1}{2} \pm \sqrt{\frac{1}{4} - \alpha^{(0)}}}, \tag{4.51}$$

boundary condition takes form

$$\phi_{\pm}^{(0)}(x + 2\pi) = \phi_{\pm}^{(0)}(x).$$

Let

$$k_{\pm}^{(0)} = n_{\pm}, \tag{4.52}$$

where $n_{\pm} \in \mathbb{N}$ and $n_{\pm}$ have no common divisor. Without loss of generality, due to linearity of (4.50) and the fact that there is no explicit dependence on x, we can write the solution of the above system in the form

$$\phi_{+}^{(0)} = a\cos\left(n_{+}x + \theta\right), \qquad \phi_{-}^{(0)} = \cos n_{-}x, \tag{4.53}$$

here $n_\pm$ play roles of wavenumbers, θ is a phase difference between two oscillations, a is a relative amplitude of this oscillations. From (4.51) we obtain the following

$$\frac{n_+}{n_-} = \frac{\sqrt{\frac{1}{2} + \sqrt{\frac{1}{4} - \alpha^{(0)}}}}{\sqrt{\frac{1}{2} - \sqrt{\frac{1}{4} - \alpha^{(0)}}}}, \qquad n_+ n_- = \frac{\lambda^{(0)2}}{4\pi^2}\sqrt{\alpha^{(0)}},$$

and, hence,

$$\alpha^{(0)} = \frac{n_+^2 n_-^2}{\left(n_+^2 + n_-^2\right)^2}, \qquad \lambda^{(0)} = 2\pi\sqrt{n_+^2 + n_-^2}. \tag{4.54}$$

At the next order of (4.23)–(4.24) we have

$$\phi_+^{(1)\prime\prime} + n_+^2\phi_+^{(1)} + 2n_+k_+^{(1)}a\cos\left(n_+x+\theta\right) = -\left\{\left[a\cos\left(n_+x+\theta\right) + \cos n_-x\right]^3\right\}'', \tag{4.55}$$

$$\phi_-^{(1)\prime\prime} + n_-^2\phi_-^{(1)} + 2n_-k_-^{(1)}\cos n_-x = \left\{\left[a\cos\left(n_+x+\theta\right) + \cos n_-x\right]^3\right\}'', \tag{4.56}$$

with boundary conditions

$$\phi_\pm^{(1)}(x+2\pi) = \phi_\pm^{(1)}(x). \tag{4.57}$$

From (4.26) we find

$$k_\pm^{(1)} = \frac{\lambda^{(1)}}{2\pi}\sqrt{\frac{1}{2} \pm \sqrt{\frac{1}{4} - \alpha^{(0)}}} \mp \frac{\lambda^{(0)}}{2\pi}\frac{1}{2\sqrt{\frac{1}{2} \pm \sqrt{\frac{1}{4} - \alpha^{(0)}}}}\left(\frac{\alpha^{(1)}}{2\sqrt{\frac{1}{4} - \alpha^{(0)}}}\right), \tag{4.58}$$

now, substituting (4.54) into (4.58), we have

$$k_\pm^{(1)} = \frac{\lambda^{(1)}}{2\pi}\frac{n_\pm}{\sqrt{n_+^2 + n_-^2}} \mp \frac{\alpha^{(1)}\left(n_+^2 + n_-^2\right)^2}{2n_\pm\left(n_+^2 - n_-^2\right)}. \tag{4.59}$$

Like the previous case of a single-wave solution, we are looking only for bounded (or periodic, which is the same in some sense) functions and, therefore, there should be no terms producing growing oscillations, or in other words those with $\cos n_\pm x$ or $\sin n_\pm x$. Simplifying right-hand sides of (4.55) and (4.56) we obtain

$$
\begin{aligned}
\left[a\cos\left(n_+x+\theta\right)+\cos n_-x\right]^3 &= \frac{3}{2}a\cos\left(n_+x+\theta\right)\\
&+\frac{1}{4}a^3\left[3\cos\left(n_+x+\theta\right)+\cos 3\left(n_+x+\theta\right)\right]\\
&+\frac{3}{4}a^2\left\{\cos\left[\left(2n_+-n_-\right)x+2\theta\right]+\cos\left[\left(2n_++n_-\right)x+2\theta\right]\right\}\\
&+\frac{3}{4}a\left\{\cos\left[\left(n_+-2n_-\right)x+\theta\right]+\cos\left[\left(n_++2n_-\right)x+\theta\right]\right\}\\
&+\frac{3}{2}a^2\cos n_-x+\frac{1}{4}\left(3\cos n_-x+\cos 3n_-x\right). \qquad (4.60)
\end{aligned}
$$

If $n_+ \neq 3n_-$, (4.55)–(4.57) have a bounded solution if and only if

$$2n_+k_+^{(1)}a = \left(\frac{3}{2}a+\frac{3}{4}a^3\right)n_+^2,$$

$$2n_-k_-^{(1)} = -\left(\frac{3}{2}a^2+\frac{3}{4}\right)n_-^2,$$

or

$$k_+^{(1)} = \left(\frac{3}{4}+\frac{3}{8}a^2\right)n_+, \qquad (4.61)$$

$$k_-^{(1)} = -\left(\frac{3}{4}a^2+\frac{3}{8}\right)n_-. \qquad (4.62)$$

Taking into account (4.59), (4.61) and (4.62) take form

$$\frac{\lambda^{(1)}}{2\pi}\frac{n_+}{\sqrt{n_+^2+n_-^2}}-\frac{\alpha^{(1)}\left(n_+^2+n_-^2\right)^2}{2n_+\left(n_+^2-n_-^2\right)} = \left(\frac{3}{4}+\frac{3}{8}a^2\right)n_+, \qquad (4.63)$$

$$\frac{\lambda^{(1)}}{2\pi}\frac{n_-}{\sqrt{n_+^2+n_-^2}}+\frac{\alpha^{(1)}\left(n_+^2+n_-^2\right)^2}{2n_-\left(n_+^2-n_-^2\right)} = -\left(\frac{3}{4}a^2+\frac{3}{8}\right)n_-. \qquad (4.64)$$

Solving (4.63), (4.64) we find $\lambda^{(1)}$ and $\alpha^{(1)}$, in terms of $n_\pm$ and a

$$\lambda^{(1)} = \frac{3\pi}{4\sqrt{n_+^2+n_-^2}}\left[a^2\left(n_+^2-2n_-^2\right)+2n_+^2-n_-^2\right], \qquad (4.65)$$

$$\alpha^{(1)} = -\frac{9n_+^2n_-^2\left(n_+^2-n_-^2\right)}{4\left(n_+^2+n_-^2\right)^3}\left(a^2+1\right). \qquad (4.66)$$

In this section we have found solutions of special type, that exist together with

single wave ones for certain values of $k_\pm$. They will be further referred to as two–wave solutions.

4.5 Special case "3 to 1"

As it was pointed out earlier when the pair $\{k_1, k_2\}$ takes a value $\{3, 1\}$, single-wave solution (4.31)–(4.35), (4.39), (4.40) and (4.41)–(4.45) becomes invalid. Moreover, it is not a two-wave type solution regime, that was examined in the previous chapter either. See (4.52), (4.53). And, therefore, an individual analysis of this situation should be carried out.

We follow the routine of the previous section. Let

$$k_\pm^{(0)} = n_\pm. \tag{4.67}$$

We can put

$$n_+ = 3, \qquad n_- = 1. \tag{4.68}$$

We seek solutions of a form

$$\phi_+^{(0)} = a\cos\left(3x + \theta\right), \qquad \phi_-^{(0)} = \cos x. \tag{4.69}$$

Then, considering (4.55), (4.56), and using (4.60) and (4.68), periodic solution can only exist when

$$2n_+ k_+^{(1)} a = \left(\frac{3}{2}a + \frac{3}{4}a^3 + \frac{1}{4}\right) n_+^2, \qquad \theta = 2\pi n, \quad n \in \mathbb{N},$$

$$2n_- k_-^{(1)} = -\left(\frac{3}{4}a + \frac{3}{2}a^2 + \frac{3}{4}\right) n_-^2, \qquad \theta = 2\pi n, \quad n \in \mathbb{N},$$

hence, we can set

$$\theta = 0, \tag{4.70}$$

and we obtain

$$k_+^{(1)} = \left(\frac{3}{4} + \frac{3}{8}a^2 + \frac{1}{8a}\right) n_+, \tag{4.71}$$

$$k_-^{(1)} = -\left(\frac{3}{8}a + \frac{3}{4}a^2 + \frac{3}{8}\right) n_-. \tag{4.72}$$

Now using (4.65), (4.66) and (4.68), we find

$$\lambda^{(1)} = \frac{3\pi\left(7a^3 - a^2 + 17a + 3\right)}{4\sqrt{10}a}, \tag{4.73}$$

$$\alpha^{(1)} = -\frac{9\left(9a^3 + 3a^2 + 9a + 1\right)}{500a}. \tag{4.74}$$

Treating (4.73)–(4.74) as a curve on the $\left(\alpha^{(1)}, \lambda^{(1)}\right)$ plane we can find the region where solutions of form (4.69) exist. A tangent line to this curve is defined by the following

$$\left(\alpha^{(1)} - \alpha^{(1)}(a_0)\right) \frac{\mathrm{d}\lambda^{(1)}}{\mathrm{d}a}\bigg|_{a=a_0} = \left(\lambda^{(1)} - \lambda^{(1)}(a_0)\right) \frac{\mathrm{d}\alpha^{(1)}}{\mathrm{d}a}|_{a=a_0}, \tag{4.75}$$

where a_0 is a value of a at the point we are looking for tangents to. We want to find those tangent lines that pass through the origin $(0,0)$ (that will give boundaries of the region where solutions exist)

$$\begin{aligned} & \left[0 + \frac{9\left(9a_0^3 + 3a_0^2 + 9a_0 + 1\right)}{500a_0}\right] \cdot \frac{3\pi\left(14a_0 - 1 - \frac{3}{a_0^2}\right)}{4\sqrt{10}} \\ = & \left[0 - \frac{3\pi\left(7a_0^3 - a_0^2 + 17a_0 + 3\right)}{4\sqrt{10}a_0}\right] \cdot \frac{-9\left(18a_0 + 3 - \frac{1}{a_0^2}\right)}{500}, \end{aligned}$$

hence,

$$3a_0^4 - 18a_0^3 - 12a_0^2 - 2a_0 - 1 = 0,$$

which has two real roots

$$a_0 \approx -0.58292,\ 6.62054. \tag{4.76}$$

Substituting the result (4.76) into (4.75) we find the borderlines in the case "3 to 1" with assumption of weak–nonlinearity on a (λ, α)–plane

$$\lambda = -71.3738\alpha + 26.2928, \tag{4.77}$$

$$\lambda = -31.0493\alpha + 22.6636. \tag{4.78}$$

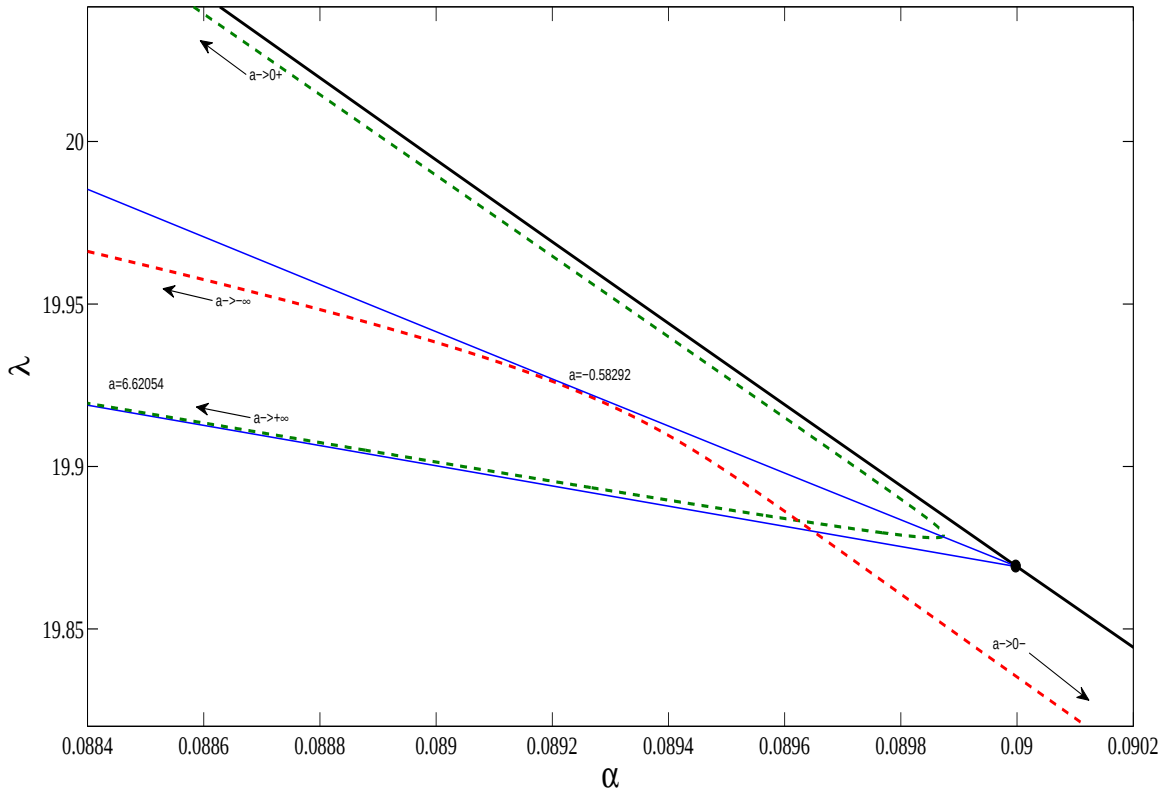

Figure 4.3: Case "3 to 1" region of existence in weak nonlinear case. Dotted lines are given by (4.73), (4.74). Borderline of solutions with $a > 0$ corresponds to the upper tangent line.

Let us address Fig. 4.3 now. If we draw a straight line from the "3 to 1" point inside the existence region, this line can either have three or one intersections with (4.73), (4.74) or one intersection and one tangency (such tangents form a sector). There are values of a corresponding for each of the above situations. And, hence, either three different solutions exist (for three values of a defined by intersections) when (α, λ) is inside the sector, or only one solution when (α, λ) is outside the sector. When a is small and positive, such solution is situated above the tangent to the line given by (4.77). When a is small and negative there is only one solution as well and it lies below the tangent to the line given by (4.78). There exist three different

solutions for different values of a (two for positive a and one for negative or vice versa) in the region bounded by (4.77)–(4.78). Asymptotic behavior near singular points ($a \to \pm\infty$, $a \to \pm 0$) is also shown in the figure. The above analysis helps to find the boundaries of the region of existence of "3 to 1" solutions in the weak nonlinear case.

4.6 Critical case $\alpha \simeq \frac{1}{4}$

As it was mentioned before in Section 4.2 it is only possible to transform Eq.(4.11) to (4.23), (4.24) only if $\alpha \neq \frac{1}{4}$. In this section we will derive a solution of Eq.(4.11) for α close to $\frac{1}{4}$. We start with rescaling x to eliminate parameter λ from the boundary condition and make solutions 2π–periodic. We introduce

$$\phi = \delta\phi_{new}, \qquad x_{new} = \sqrt{\kappa}x, \qquad \kappa = \sqrt{\frac{2\pi}{\lambda}}, \qquad \delta = \sqrt{\varepsilon}. \tag{4.79}$$

Substituting (4.79) into (4.11), (4.4) and omitting $_{new}$, we obtain the following equation

$$\kappa\frac{\partial^2}{\partial x^2}\left(\phi + \kappa\frac{\partial^2}{\partial x^2}\phi - \delta^2\phi^3\right) + \alpha\phi = 0, \tag{4.80}$$

with the following boundary condition

$$\phi(x + 2\pi) = \phi(x). \tag{4.81}$$

We expand ϕ, κ, α into series with small δ

$$\phi = \phi^{(0)} + \delta\phi^{(1)} + \delta^2\phi^{(2)} + \cdots, \tag{4.82}$$

$$\kappa = \kappa^{(0)} + \delta\kappa^{(1)} + \delta^2\kappa^{(2)} + \cdots, \tag{4.83}$$

$$\alpha = \alpha^{(0)} + \delta\alpha^{(1)} + \delta^2\alpha^{(2)} + \cdots, \tag{4.84}$$

Now, $\alpha^{(0)} = \frac{1}{4}$, using both (4.8) and (4.79) we find

$$\kappa^{(0)} = \frac{1}{2}. \tag{4.85}$$

Substituting (4.82)–(4.84) together with (4.85) into Eq.(4.80), in the zeroth order we have

$$\frac{1}{2}\left(\phi^{(0)}+\frac{1}{2}\phi^{(0)\prime\prime}\right)^{\prime\prime}+\frac{1}{4}\phi^{(0)}=0, \tag{4.86}$$

boundary condition (4.81) becomes

$$\phi^{(0)}(x+2\pi)=\phi^{(0)}(x), \tag{4.87}$$

hence, without loss of generality,

$$\phi^{(0)}=\cos x, \tag{4.88}$$

because the solution of (4.86) allows a shift along x and rescale of $\phi^{(0)}$. In the first order (4.80) with (4.82)–(4.84)

$$\frac{1}{2}\left(\phi^{(1)}+\frac{1}{2}\phi^{(1)\prime\prime}+\kappa^{(1)}\phi^{(0)\prime\prime}\right)^{\prime\prime}+\kappa^{(1)}\left(\phi^{(0)}+\frac{1}{2}\phi^{(0)\prime\prime}\right)^{\prime\prime}+\frac{1}{4}\phi^{(1)}+\alpha^{(1)}\phi^{(0)}=0,$$

hence, taking into account (4.88) we obtain

$$\frac{1}{2}\left(\phi^{(1)}+\frac{1}{2}\phi^{(1)\prime\prime}\right)^{\prime\prime}+\frac{1}{4}\phi^{(1)}+\alpha^{(1)}\cos x=0.$$

Boundary conditions are

$$\phi^{(1)}(x+2\pi)=\phi^{(1)}(x),$$

and, hence,

$$\alpha^{(1)}=0. \tag{4.89}$$

Without loss of generality, we can set

$$\phi^{(1)}=0. \tag{4.90}$$

In the second order of Eq.(4.80) with (4.82)–(4.84):

$$\frac{1}{2}\left(\phi^{(2)}+\frac{1}{2}\phi^{(2)\prime\prime}+\kappa^{(1)}\phi^{(1)\prime\prime}+\kappa^{(2)}\phi^{(0)\prime\prime}-\phi^{(0)3}\right)^{\prime\prime}+\kappa^{(1)}\left(\phi^{(1)}+\frac{1}{2}\phi^{(1)\prime\prime}+\kappa^{(1)}\phi^{(0)\prime\prime}\right)^{\prime\prime}$$
$$+\kappa^{(2)}\left(\phi^{(0)}+\frac{1}{2}\phi^{(0)\prime\prime}\right)^{\prime\prime}+\frac{1}{4}\phi^{(2)}+\alpha^{(2)}\phi^{(0)}=0,$$

hence, substituting already found solution (4.88), (4.89), (4.90) we get

$$\frac{1}{2}\left(\phi^{(2)}+\frac{1}{2}\phi^{(2)\prime\prime}\right)^{\prime\prime}+\frac{1}{4}\phi^{(2)}+\frac{9}{8}\cos 3x+\left(\frac{3}{8}+\kappa^{(1)2}+\alpha^{(2)}\right)\cos x=0, \qquad (4.91)$$

Boundary conditions (4.87) in the second order

$$\phi^{(2)}(x+2\pi)=\phi^{(2)}(x).$$

To satisfy the condition of periodicity the following must hold

$$\frac{3}{8}+\kappa^{(1)2}+\alpha^{(2)}=0. \qquad (4.92)$$

Using (4.92) we solve Eq.(4.91)

$$\phi^{(2)}=-\frac{9}{128}\cos 3x. \qquad (4.93)$$

One can see that solution (4.88)–(4.90), (4.92), (4.93) is of a 'single-wave' type and is similar to the one obtained in Section 4.3. However, the stability analysis of the present solution for $\alpha=\frac{1}{4}$ gives us completely different result compare to the general weak-nonlinear situation, which will be shown later.

4.7 Numerical simulations

4.7.1 Numerical methods description

In Section 4.2 we found the region (4.9) where periodic solutions exist. We also obtained analytical solutions of Eq.(2.29) in a specific situation, when nonlinearity is weak. In a more general case we use numeric simulations to find periodic steady states.

We consider a boundary value problem

$$\frac{\partial^2}{\partial x^2}\left(\phi - \phi^3 + \frac{\partial^2}{\partial x^2}\phi\right) + \alpha\phi = 0, \tag{4.94}$$

$$\phi(x+\lambda) = \phi(x). \tag{4.95}$$

The problem has two parameters, $\lambda \in [2\pi, +\infty)$ and $\alpha \in [0, \frac{1}{4}]$. We investigate existence of solutions of Eq.(4.94) in the full parameter space (λ, α). For rather small values of λ we used shooting method with 4-5 order Runge-Kutta integration implemented in Matlab. The step size of integration is automatically reduced to keep the desired accuracy. To find solutions for all values of the parameters, we define a simple rectangular mesh to fit in region (4.9). Starting from the border ((4.8) for instance), where an analytical solution has been found, and, therefore, initial values for shooting parameters are known, we move to the neighbor nodes, finding solutions there with the same initial shooting parameters. Then we can use the parameters found on the previous step (node) to find a solution in the next nodes expanding inside the area of existence.

Here we would like to give some details about how the shooting method was done. We are solving a fourth order ordinary differential equation with periodic boundary conditions. The system allows shifting along the space variable x, as there is no explicit dependence on x. Without loss of generality we can start integrating from some point x_0, where

$$\left.\frac{\partial\phi}{\partial x}\right|_{x_0} = 0. \tag{4.96}$$

It is easy to show by rewriting Eq.(4.94) as a system of four first-order equations,

that

$$\left.\frac{\partial^3\phi}{\partial x^3}\right|_{x_0} = 0. \tag{4.97}$$

We solve the problem on a half period interval as solution is symmetric in the following sense: if $\phi_0(x)$ is a solution, then $-\phi_0(x)$ is a solution as well. To make sure this condition holds, we request

$$\left.\frac{\partial\phi}{\partial x}\right|_{x_0+\frac{\lambda}{2}} = 0, \qquad \left.\frac{\partial^3\phi}{\partial x^3}\right|_{x_0+\frac{\lambda}{2}} = 0. \tag{4.98}$$

We integrate Eq.(4.94) from the starting point at x_0 to the ending point at $x_0 + \frac{\lambda}{2}$, with fixed values of λ and α and two initial conditions (4.96), (4.97). The two remaining initial conditions: values of the second and the fourth derivatives at x_0 are the shooting parameters and guess values for them can be obtained either from the known nearby numerical solution or from the known analytical solution from the previous step. The vector of misalignment is given by the following

$$\left(\left.\frac{\partial\phi}{\partial x}\right|_{x_0+\frac{\lambda}{2}}, \left.\frac{\partial^3\phi}{\partial x^3}\right|_{x_0+\frac{\lambda}{2}}\right). \tag{4.99}$$

Due to the fact that the equation is stiff this method works well only for not very large periods, once the domain of $\phi(x)$ has reached some sufficient value the method becomes slower and less precise.

At this point we switch to a relaxation method. We, first, discretize Eq.(4.94)

$$\begin{gathered}\frac{1}{h^4}\left(\phi_{i-2}^{(n+1)} - 4\phi_{i-1}^{(n+1)} + 6\phi_i^{(n+1)} - 4\phi_{i+1}^{(n+1)} + \phi_{i+2}^{(n+1)}\right) + \\ \frac{1}{12h^2}\left(\begin{array}{c} -\phi_{i-2}^{(n+1)}(1-3\phi_{i-2}^{(n)2}) + 16\phi_{i-1}^{(n+1)}(1-3\phi_{i-1}^{(n)2}) - 30\phi_i^{(n+1)}(1-3\phi_i^{(n)2}) \\ +16\phi_{i+1}^{(n+1)}(1-3\phi_{i+1}^{(n)2}) - \phi_{i+2}^{(n+1)}(1-3\phi_{i+2}^{(n)2}) \end{array}\right) \\ +\alpha\phi_i^{(n+1)} = \frac{1}{6h^2}\left(\phi_{i-2}^{(n)3} - 16\phi_{i-1}^{(n)3} + 30\phi_i^{(n)3} - 16\phi_{i+1}^{(n)3} + \phi_{i+2}^{(n)3}\right).\end{gathered} \tag{4.100}$$

Where for space discretization $\{x_i\}_{i=\overline{1,N}}$, $\quad x_i = h(i-1)$, with step $h = \frac{2\pi}{N-1}$. Discrete analog of the function $\phi(x)$ is $\phi_i = \phi(x_i)$. Superscript index $^{(n)}$ denotes to an order number of an iteration. A matrix equation $M\phi = b$ can be defined by (4.94),

where $\phi, b \in \mathbb{R}^N$, and $M \in \mathcal{M}(n, \mathbb{R})$ is a square five-diagonal matrix. Apparently, some terms of Eq.(4.94), those for which their index happen to be not in the range $\overline{1, N}$, are falling out of M. We use them in M to satisfy periodic boundary condition (4.95) in a way shown on Fig.4.4. When the matrix equation with implemented boundary conditions is constructed iteration process of finding a solution can be started. We guess a vector $\phi^{(0)} = (\phi_1^{(0)}, ..., \phi_N^{(0)}) \in \mathbb{R}^N$ to create $M^{(0)}$ and $b^{(0)}$. Then we solve $M^{(0)}\phi^{(1)} = b^{(0)}$ for $\phi^{(1)}$ and continue recurrent process $\phi^{(j+1)} = (M^{(j)})^{-1}b^{(j)}$. According to the general theory of relaxation methods (for reference see [39]) $\phi^{(j)}$ tends to solution of Eq.(4.94) as $j \to \infty$ and we stop the iterative process when $\left\|\phi^{(j+1)} - \phi^{(j)}\right\|$ is small enough.

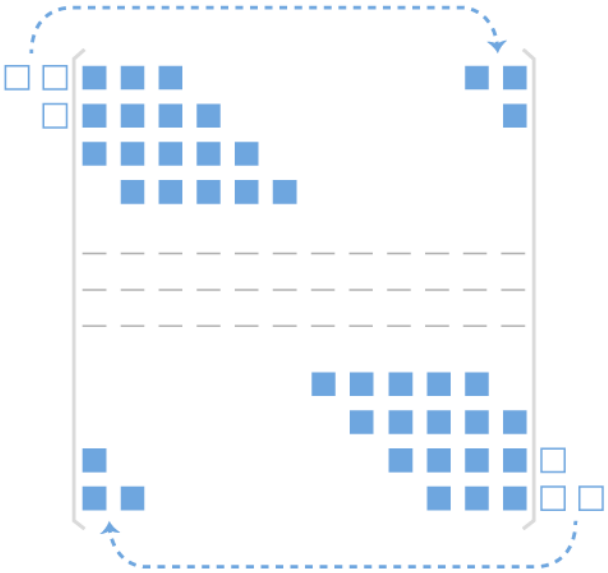

Figure 4.4: Discrete scheme. Boundary condition.

Moreover, the same problem (4.94), (4.95) were solved with COMSOL Multiphysics' '1–D General form PDE solver' to verify the results acquired earlier.

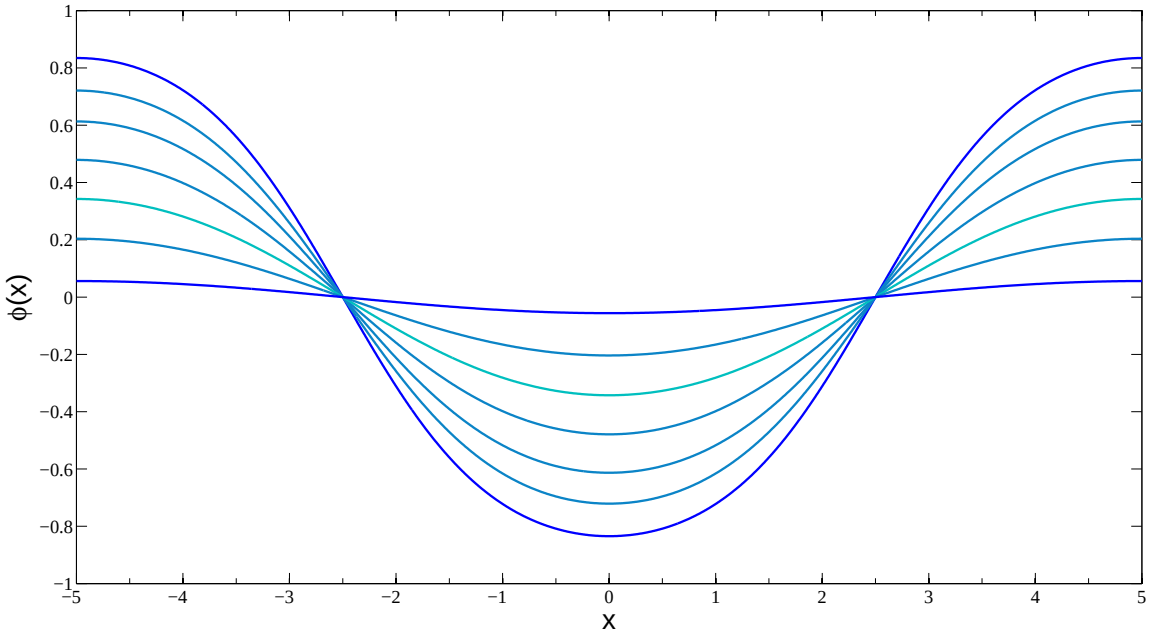

Figure 4.5: Single waves. Fixed $\lambda = 10$, $\alpha \in [0.01, 0.238]$. . As α increases amplitude of the solution decreases. At the critical α value point (when reaches borderlines (4.8)) solution becomes zero.

4.7.2 Single–wave solution

In this section we will discuss numerical solutions that are somehow related to single-wave solutions of the weak-nonlinear case. Starting with a known single-wave solution and changing initial conditions continuously we can get numerical solutions at any point on (λ, α), except the '3 to 1 case', which we will discuss later.

Even though we cannot call them single-wave anymore, because of strong nonlinearity and apparent influence of other frequency harmonics due to it, shapes of the graphs of such solutions resemble the single-wave ones for rather small periods. Like the Cahn–Hilliard equation solutions, when period increases the shapes of the graphs become more staged, as one can see on and Fig.4.6. When α increases the amplitude of the solution decreases and finally becomes zero at existence region boundary (4.8), for reference see Fig.4.5. In a similar way the results regarding single-wave solutions were obtained numerically by Liu and Goldenfeld [32].

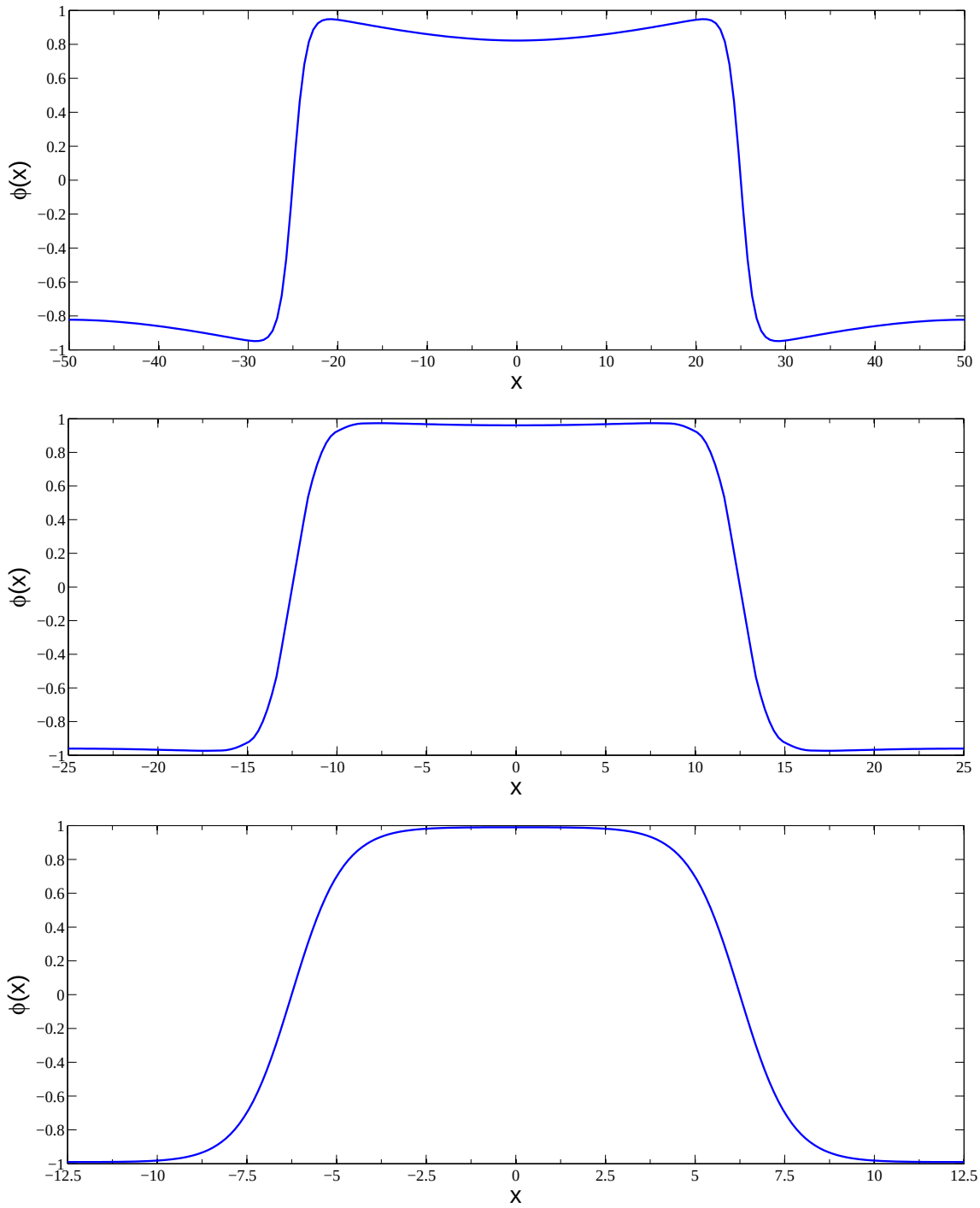

Figure 4.6: Shapes of single wave solutions for large periods, $\lambda = 100, 50, 25$, $\alpha = 0.001$ is fixed.

4.7.3 Two–wave solution

As an example of a two–wave solution we consider situations 2 to 1 and 4 to 1. Other cases are very similar and can be examined much in the same way. We start with

$$k_+ = n_+ = 2, \quad k_- = n_- = 1,$$

Hence, from (4.54) it follows

$$\lambda^{(0)} = 2\sqrt{5}\pi, \quad \alpha^{(0)} = 0.16, \tag{4.101}$$

moreover, using (4.65) and (4.66), we find

$$\lambda^{(1)} = \frac{3\pi}{4\sqrt{5}}(2a^2 + 7), \tag{4.102}$$

$$\alpha^{(1)} = -\frac{27}{125}\left(a^2 + 1\right), \tag{4.103}$$

where a is a relative amplitude of a high frequency oscillation to the low frequency one. We want to mention here that a can be both positive and negative. If a is positive two harmonics (k_+ and k_-) are added together, if a is negative, one is subtracted from another. Both solutions, with negative and positive a, coexist at the same point (λ, α) (one can see, that both $\lambda^{(1)}$ and $\alpha^{(1)}$ do not depend on sign of a), along with a general "single wave type" one. For the case "2 to 1" or "4 to 1" or any of those, where the ratio is an even number for that matter, there is no difference between two of them ($a > 0$ or $a < 0$), aside from that one is shifted with respect to another along x. In other cases, though, the shape of solution will depend on the sign of a.

We can treat a as an independent variable and plot a graph of $(\lambda^{(1)}(a), \alpha^{(1)}(a))$, see Fig.4.7 for reference. All possible values of $(\lambda^{(1)}, \alpha^{(1)})$ will correspond to straight lines (rays) that start at the origin and intersect the line $(\lambda^{(1)}(a), \alpha^{(1)}(a))$. A set of all possible (λ, α) or $(2\sqrt{5}\pi + \epsilon\lambda^{(1)}, 0.16 + \epsilon\alpha^{(1)})$ forms a sector with its vertex at $(\lambda^{(0)}, \alpha^{(0)})$. The upper borderline goes through $(2\sqrt{5}\pi, 0.16)$ and $(2\sqrt{5}\pi +$

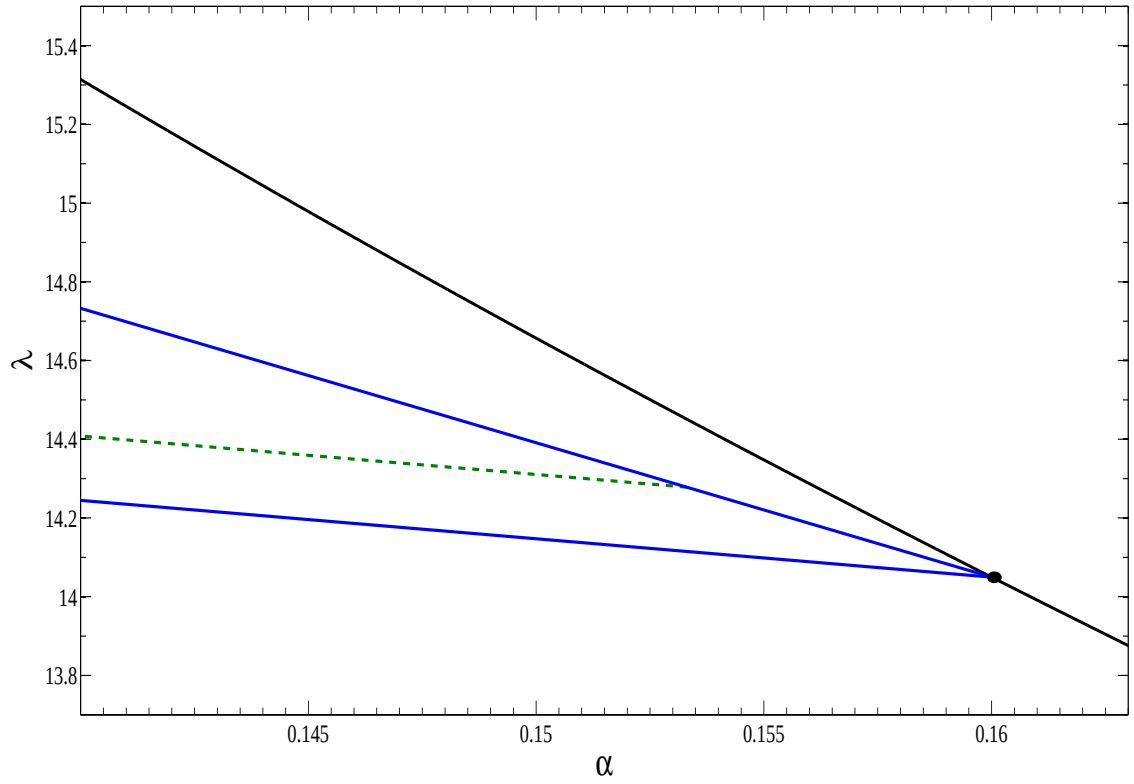

Figure 4.7: Case "2 to 1" region of existence in weak nonlinear case. Dotted line is given by (4.102) and (4.103). Region of existence of two–wave solutions is formed by a tangent to a dotted line ($a \to \pm\infty$) and a line that goes through the end of the dotted line ($a = 0$). Top line is the boundary of the region of existence of nontrivial periodic solutions.

$\epsilon\lambda^{(1)}(0), 0.16 + \epsilon\alpha^{(1)}(0))$ on a (λ, α)–plane, hence, its equation is

$$\lambda = -\frac{175\pi\sqrt{5}}{36}\alpha + \frac{25\pi\sqrt{5}}{9}.$$

The lower borderline starts at $(2\sqrt{5}\pi, 0.16)$ as well and is parallel to $(\lambda^{(1)}(a), \alpha^{(1)}(a))$, therefore, its equation is

$$\lambda = -\frac{25\pi\sqrt{5}}{18}\alpha + \frac{20\pi\sqrt{5}}{9}.$$

Numerical simulations allow us to examine existence of two–wave solutions in the most general case. The region of existence was found and the agreement between analytical results for weak nonlinearity and numerical ones is very good. Close to the lower border the relative amplitude a is large, this means that the higher frequency oscillation is a dominant one. As we move into the "2 to 1" region, a decreases, the contribution of lower frequency oscillation grows and, when close to the upper border, a is small and the low frequency oscillation prevails. Dependence of shapes of solutions on period is shown on a Fig.4.8. As α grows from 0 to its critical value, the amplitude of the solution decreases and becomes 0 at $(\frac{4}{25}, 2\pi\sqrt{5})$ in the same way single wave solutions do.

In the very same way we examine "4 to 1" case:

$$k_+ = n_+ = 4, \quad k_- = n_- = 1,$$

Hence, from (4.54) it follows

$$\lambda^{(0)} = 2\sqrt{17}\pi, \quad \alpha^{(0)} = \frac{16}{17^2}, \tag{4.104}$$

moreover, using (4.65) and (4.66), we find

$$\lambda^{(1)} = \frac{3\pi}{4\sqrt{17}}\left[14a^2 + 31\right], \tag{4.105}$$

$$\alpha^{(1)} = -\frac{540}{(17)^3}\left(a^2 + 1\right). \tag{4.106}$$

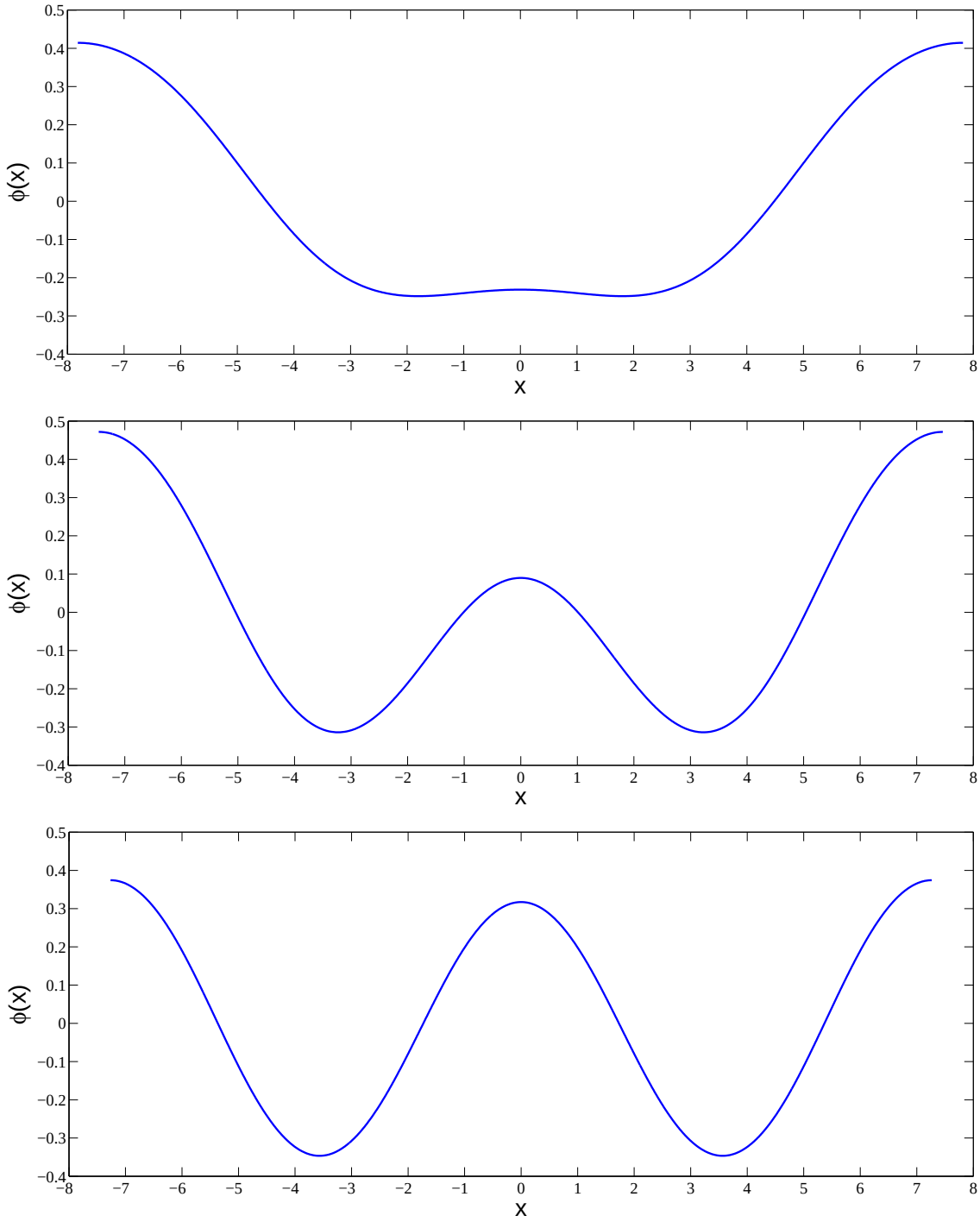

Figure 4.8: Shapes of "2 to 1" solutions depending on their periods, $\lambda = 15.8, 14.8, 14.4$, $\alpha = 0.14$ is fixed.

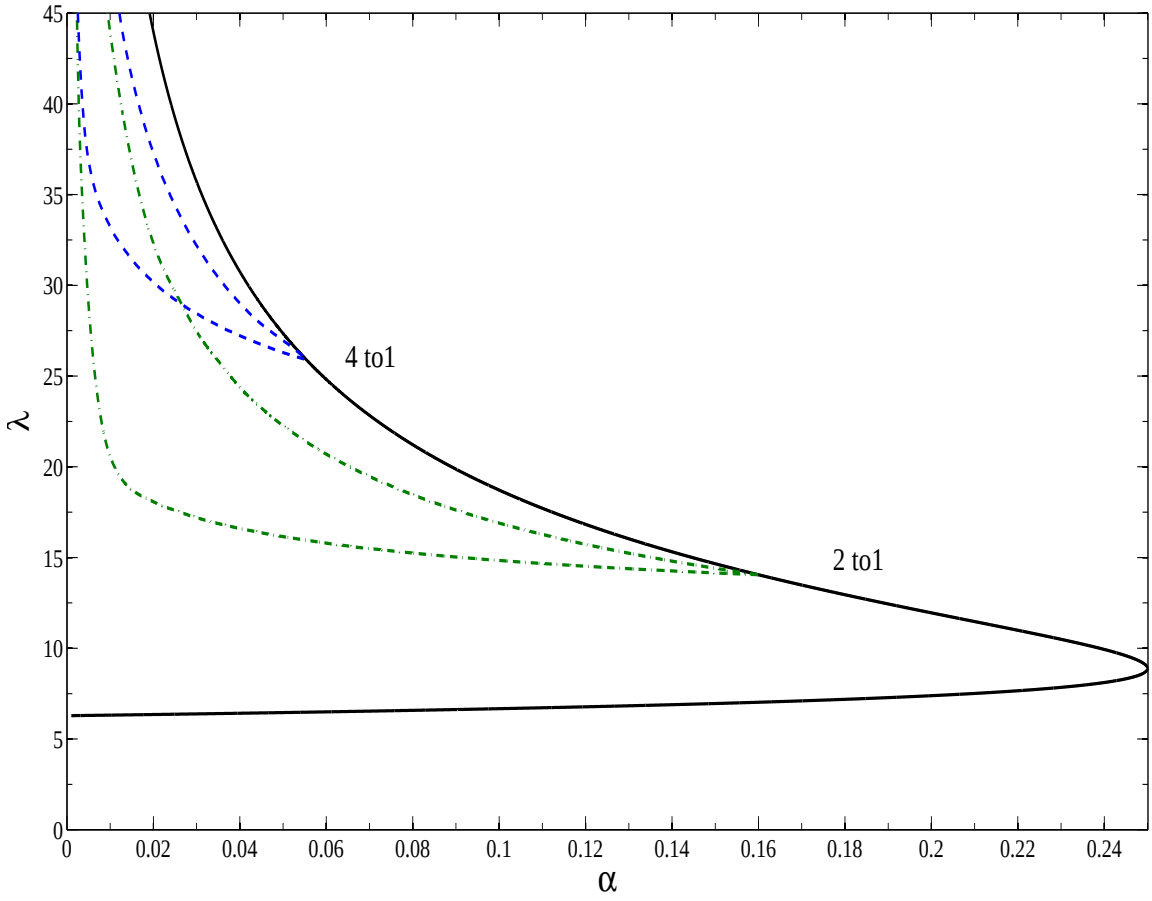

Figure 4.9: “2 to 1” and “4 to 1” regions on the existence diagram.

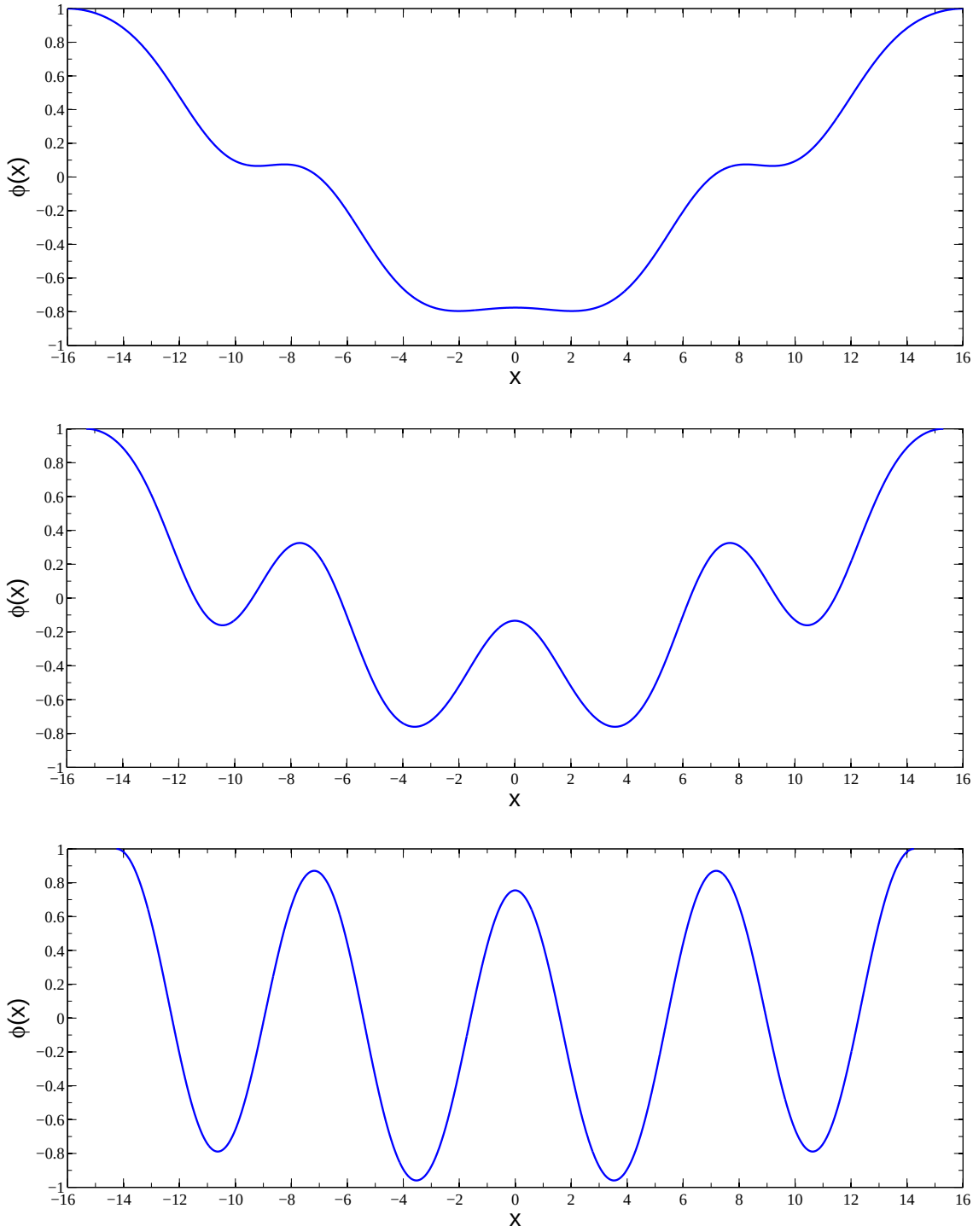

Figure 4.10: Shapes of "4 to 1" solutions depending on their period, $\lambda = 32, 30, 28$; $\alpha = 0.03$ is fixed.

Now we find the region of existence. The upper borderline goes through $(2\sqrt{17}\pi, \frac{16}{17^2})$ and $(2\sqrt{17}\pi + \lambda^{(1)}(0), \frac{16}{17^2} + \alpha^{(1)}(0))$ on a (λ, α)–plane, hence, its equation is

$$\lambda = -\frac{31\pi 17^2\sqrt{17}}{720}\alpha + \frac{121\pi\sqrt{17}}{45}.$$

The lower borderline starts at $(2\sqrt{17}\pi, \frac{16}{17^2})$ as well and is parallel to $(\lambda^{(1)}(a), \alpha^{(1)}(a))$, therefore, its equation is

$$\lambda = -\frac{7\pi 17^2\sqrt{17}}{360}\alpha + \frac{104\pi\sqrt{17}}{45}.$$

The region of existence of two wave solutions case "4 to 1" was found numerically, see Fig. 4.9. Likewise the previous case, close to the lower boundary high frequency oscillation has more impact on the shape of curve, whilst moving to the upper boundary low frequency oscillation becomes dominant as shown on Fig.4.10. As it was mentioned before there is a pair of solutions coexisting at the same time (one for positive value of a and one for negative). Approaching to the critical value of $\alpha = \frac{16}{17^2}$, both solutions vanish.

4.7.4 Case "3 to 1"

The analytical solutions of a case "3 to 1" for weak nonlinearity were found in Section 4.5. Let us now discuss numerical solutions of the same situation in general:

$$k_+ = n_+ = 3, \quad k_- = n_- = 1,$$

besides, (λ, α)–values of a "3 to 1" point can be found

$$\alpha^{(0)} = 0.09, \qquad \lambda^{(0)} = 2\pi\sqrt{10}. \tag{4.107}$$

We also found out that there is a region between lines given by (4.77)–(4.78) where three different solutions of form (4.69) coexist for three different values of a. Now we would like to find boundary lines of this region without weak-nonlinearity assumption. We find a solution well above supposed border line and move 'down' decreasing λ for a fixed value of α. See from Fig.4.11 that we are in situation of $a > 0$ and increasing a. That means that there are two leading oscillations, the low frequency

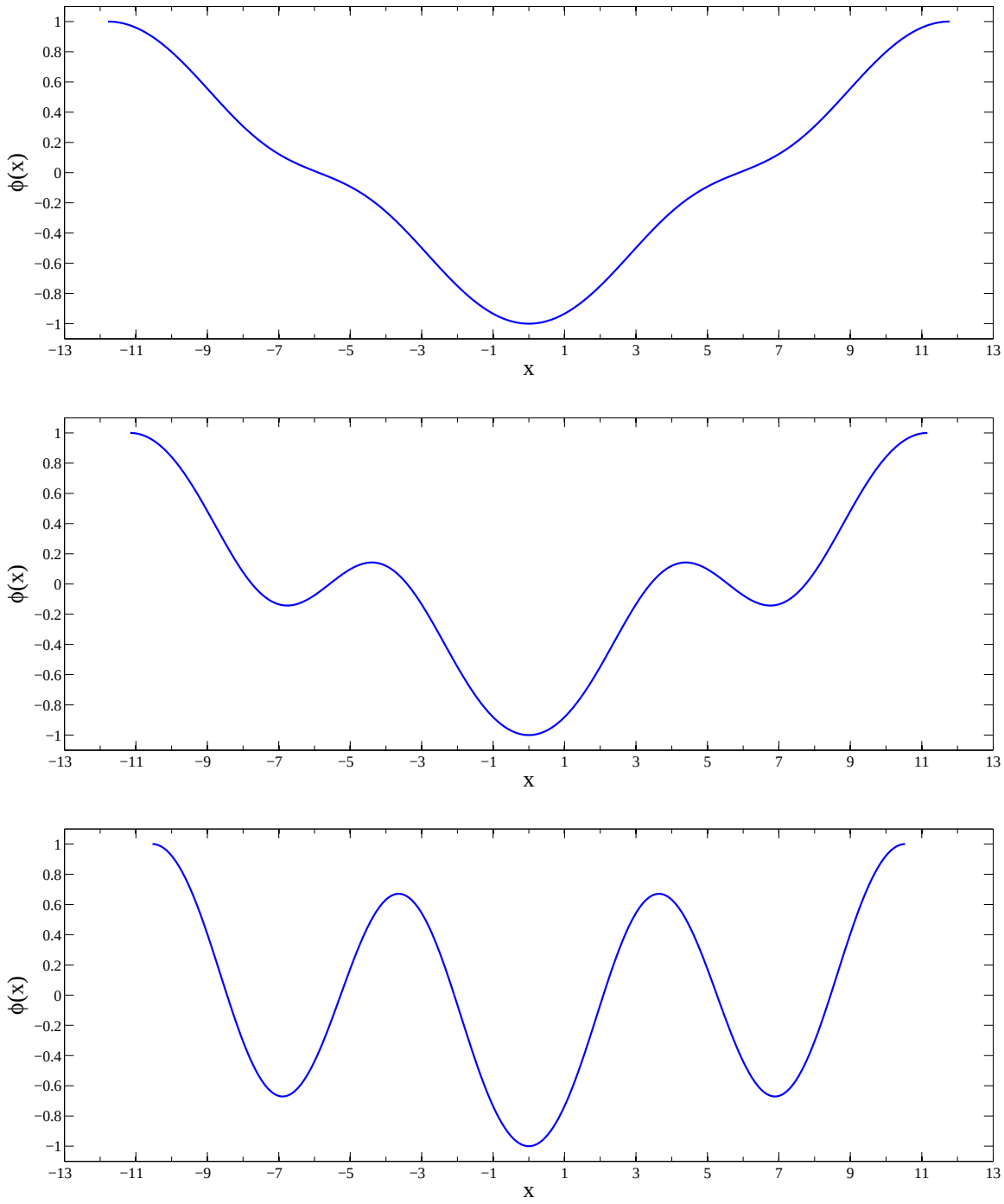

Figure 4.11: Shapes of "3 to 1" solutions depending on their period, $\lambda = 23.6, 22.2, 21$; $\alpha = 0.07$ is fixed, case of $a > 0$.

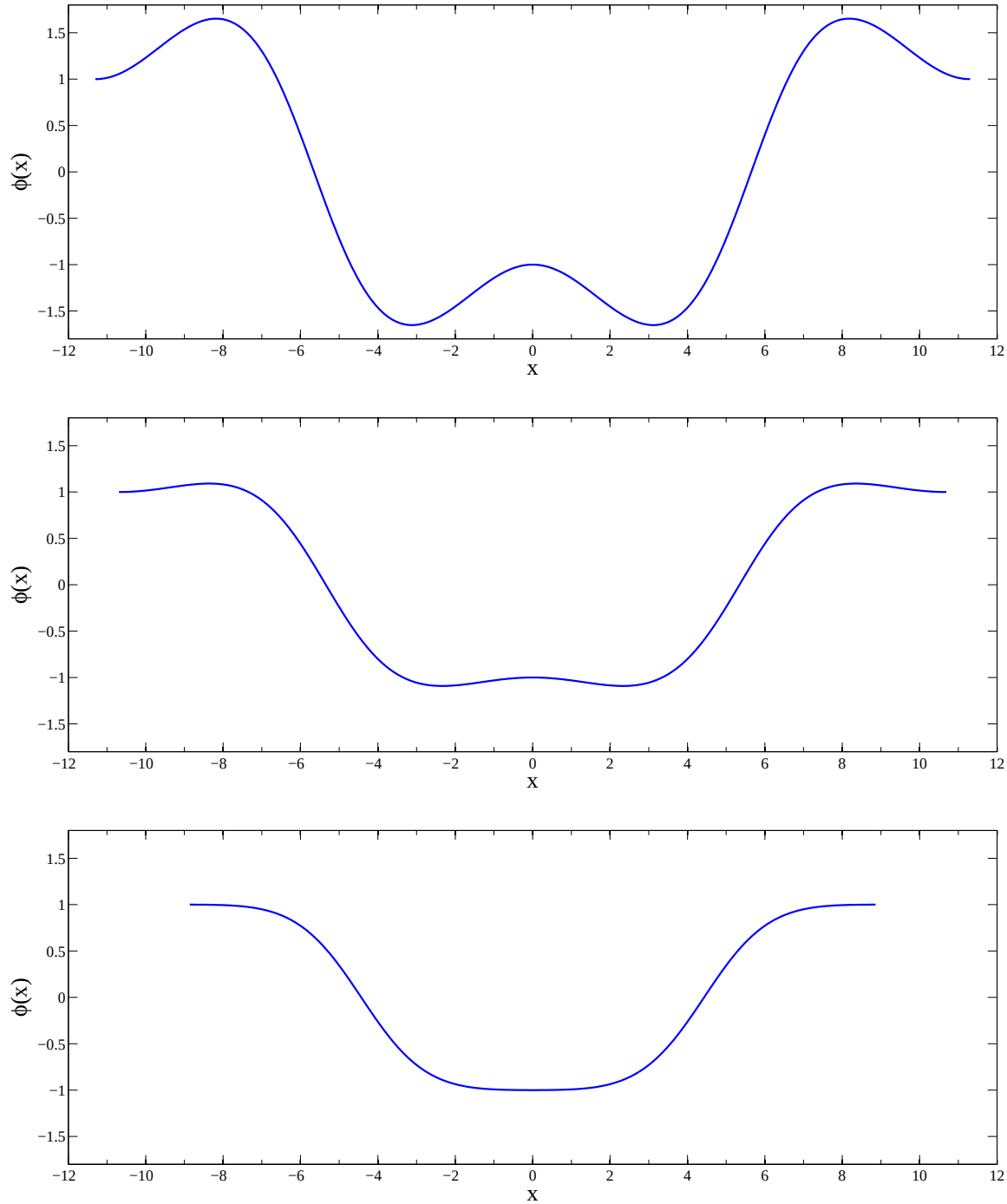

Figure 4.12: Shapes of "3 to 1" solutions depending on their period, $\lambda = 22.4, 21.5, 17.8$; $\alpha = 0.7$ is fixed, case of $a < 0$.

one is dominant but as we go 'down' decreasing λ the high frequency one becomes more significant. Its impact grows up until the moment when high frequency oscillation becomes dominant. That is where the lower border line lies. After that if we want to trace the evaluation of the solution we ought to start increasing λ. Soon enough a grows big and such solutions become very much alike simple single waves of a half period. We want to mention that nonlinearity might have crucial effect on the solutions and we cannot consider the solution as a sum of two frequencies in the leading order.

To find the upper boundary of the "3 to 1" region we find a solution at a point below the lower boundary, fix α and start increasing λ. We are in the mode when a is small and negative and a increases as we go 'up'. Likewise the previous situation low frequency oscillation is the dominant one but high frequency contribution becomes more and more significant. At the upper borderline fast oscillation becomes dominant. After this point we start to decrease λ in order to see what happen to the solution. Again a goes to $-\infty$ quickly and solutions resemble ones with a half period. The region where three solutions of form (4.69) coexist was found numerically (for reference see Fig. 4.13) in the manner described above.

4.8 Conclusions

In the present chapter, using perturbation method with some assumptions on a solution and using numerical simulations in general case, we described spatial periodic steady states of the extended Cahn–Hilliard equation. We found two main different types of solutions: single waves, two-wave solutions, depending on parameters of the problem α and λ. A situation when single waves do not exist were considered and "3 to 1" type solutions were found. Numerical simulations allowed to show diagrams of existence of the steady states. Variety of shapes of solutions were shown depending on the parameters of the problem. In the next chapter we will discuss stability of spatial periodic steady states.

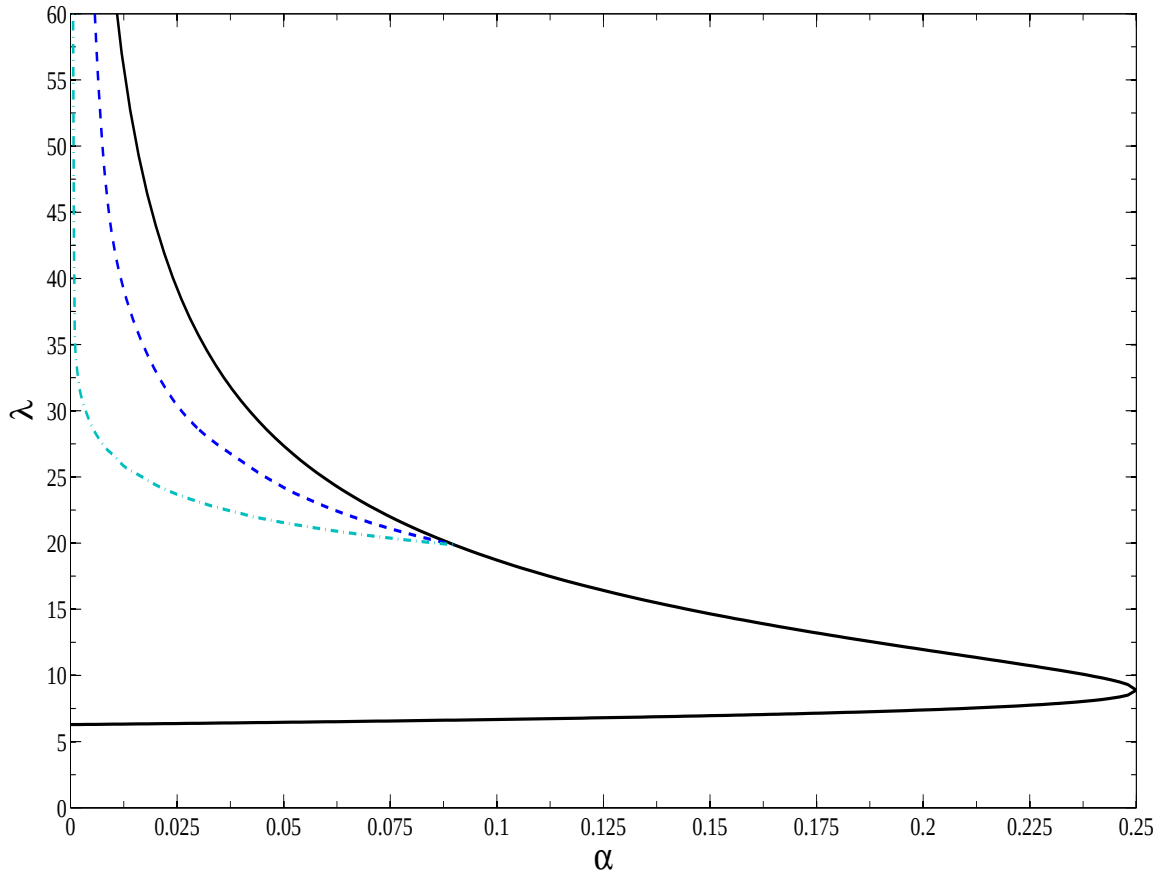

Figure 4.13: "3 to 1" region in the existence diagram. Upper of the dotted lines corresponds to the boundary of $a < 0$ solutions shown on Fig. 4.12, lower line corresponds to the boundary of $a > 0$ solutions shown on Fig. 4.11.

Chapter 5

Stability of periodic solutions of extended Cahn–Hilliard equation.

The second part of the discussion is to check if those periodic steady states found in the previous chapter are stable. We will add disturbance to the known solution and will treat it as a small parameter, linearize equation and solve an eigenvalue problem. The eigenvalue spectrum will tell us about the stability of the solution.

To allow perturbations with a different period to the unperturbed solution, the perturbation we apply Floquet boundary conditions. These must be used with caution however: in our derivation of the extended Cahn-Hilliard equation from the free energy functional we used periodic boundary conditions to eliminate the boundary term when integrating by parts. This means only perturbations with a period commensurate with the period of the unperturbed solution are allowed, (the ratio of the two periods must be a rational number). In our calculations we do not impose this condition and allow cases where the the periods are incommensurate (the ratio between the two periods may be irrational). We interpret the latter types of solutions as "local" i.e. domains embedded in a periodic solution with a period much larger than the size of the domains.

We consider Eq.(2.29) in a one–dimentional case.

$$\frac{\partial}{\partial t}\phi + \frac{\partial^2}{\partial x^2}(\phi - \phi^3 + \frac{\partial^2}{\partial x^2}\phi) + \alpha\phi = 0. \tag{5.1}$$

We make a substitution

$$x_{new} = kx, \qquad k = \frac{2\pi}{\lambda}, \tag{5.2}$$

to eliminate λ from boundary condition (4.4) and make steady states 2π– periodic. After substitution (5.2) into Eq.(5.1) we have

$$\frac{\partial}{\partial t}\phi + k^2\frac{\partial^2}{\partial x^2}(\phi - \phi^3 + k^2\frac{\partial^2}{\partial x^2}\phi) + \alpha\phi = 0. \tag{5.3}$$

Now we consider a known steady state, which is 2π–periodic denoted by Φ with a small disturbance $\psi \ll 1$

$$\phi = \Phi(x) + \psi(x,t). \tag{5.4}$$

Substituting (5.4) into Eq.(5.3) and linearizing, we have

$$\frac{\partial}{\partial t}\psi + k^2\frac{\partial^2}{\partial x^2}\left(\psi - 3\Phi^2\psi + k^2\frac{\partial^2}{\partial x^2}\psi\right) + \alpha\psi = 0. \tag{5.5}$$

Considering harmonic disturbances, we let

$$\psi(x,t) = \mathrm{e}^{st}\,\psi_{new}(x), \tag{5.6}$$

where s is a growth/decay rate. Substituting (5.6) into (5.5) and omitting $_{new}$, yields

$$s\psi + k^2\frac{\partial^2}{\partial x^2}(\psi - 3\Phi^2\psi + k^2\frac{\partial^2}{\partial x^2}\psi) + \alpha\psi = 0. \tag{5.7}$$

Eq.(5.7) is an eigenvalue problem, where s plays the role of an eigenvalue and ψ is a corresponding eigenfunction. We require that the disturbance is localized near the base solution

$$|\psi| < \text{const} \qquad \text{for all } x. \tag{5.8}$$

We choose to apply Floquet boundary conditions to satisfy (5.8)

$$\psi(x + 2\pi) = \psi(x)\,\mathrm{e}^{\mathrm{i}\theta}, \qquad \text{for any } \theta \in [0, 2\pi] \tag{5.9}$$

Floquet conditions restrict the disturbance ψ from growing infinitely, besides, changing parameter θ in the given interval allows us to examine stability with respect to

multiple period disturbances.

5.1 Stability in a weak nonlinear case

In this section we analytically examine the stability in a weak nonlinear case. We consider Eq.(5.7) in a weak nonlinear regime

$$s\psi + k^2\frac{\partial^2}{\partial x^2}(\psi - 3\Phi^2\psi + k^2\frac{\partial^2}{\partial x^2}\psi) + \alpha\psi = 0. \tag{5.10}$$

We examine a single-wave solution (4.31)–(4.35), (4.39), (4.40) and (4.41)–(4.45), which in the current variables is of form

$$\Phi(x) = \epsilon\cos x + \ldots, \qquad k = \sqrt{\frac{1}{2} \pm \sqrt{\frac{1}{4} - \alpha}} + \ldots . \tag{5.11}$$

In the zeroth order of (5.10) with (5.11) we have

$$s\psi + k^2\psi'' + k^4\psi'''' + \alpha\psi = 0. \tag{5.12}$$

We consider disturbance ψ of the form

$$\psi = e^{ix},$$

and substituting it into (5.12) we have

$$s - k^2 + k^4 + \alpha = 0, \tag{5.13}$$

The above equation shows, that if considered a zero solution from the existence region boundary with $k = \sqrt{\frac{1}{2} \pm \sqrt{\frac{1}{4} - \alpha}}$, then s is zero. Now, let us see what happens if we choose a solution close to the zero one, but from the region of existence. Its wavenumber is given by

$$k = \sqrt{\frac{1}{2} \pm \sqrt{\frac{1}{4} - \alpha} \mp \Delta}, \tag{5.14}$$

where Δ is a small "step" into the region of existence. Substituting (5.14) into (5.13), taking into account that Δ is small and neglecting terms of the order higher than linear, we obtain

$$s = 4\Delta\sqrt{\frac{1}{2} \pm \sqrt{\frac{1}{4} - \alpha}} \cdot \sqrt{\frac{1}{4} - \alpha} > 0, \tag{5.15}$$

which proves instability in the weak nonlinear case. When $\alpha = \frac{1}{4}$, this analysis is invalid and such case should be examined separately.

5.2 Critical case $\alpha \simeq \frac{1}{4}$

Let us now examine the case of α close to $\frac{1}{4}$. Assuming the base solution is small ($\phi = \delta\phi_{new}$), we rewrite Eq.(5.7)

$$s\psi + k^2\left(\psi + k^2\psi'' - 3\delta^2\phi^2\psi\right)'' + \alpha\psi = 0, \tag{5.16}$$

$$|\psi| < \text{const} \qquad \text{for all } x, \qquad \delta \ll 1, \tag{5.17}$$

and steady states were found in the Section 4.6

$$\phi = \cos x - \frac{9\delta^2}{128}\cos 3x + \mathrm{O}(\delta^3), \tag{5.18}$$

we are also looking for k and α in a form

$$k^2 = \frac{1}{2} + \delta\kappa^{(1)} + \delta^2\kappa^{(2)} + \mathrm{O}(\delta^3), \tag{5.19}$$

$$\alpha = \frac{1}{4} + \delta^2\alpha^{(2)} + \mathrm{O}(\delta^3), \tag{5.20}$$

and we already have obtained the following relation between $\kappa^{(1)}$ and $\alpha^{(2)}$

$$\frac{3}{8} + \kappa^{(1)2} + \alpha^{(2)} = 0. \tag{5.21}$$

Disturbance $\psi(x)$ should satisfy Floquet boundary condition. It is easy to show that Floquet boundary condition in the form (5.9) are equivalent to the following

$$\psi = \psi_{new}\, \mathrm{e}^{\mathrm{i}\tau x}, \qquad \tau = \frac{\theta}{2\pi}, \qquad \tau \in [0, 2], \tag{5.22}$$

where ψ_{new} is a 2π– periodic function of x. One can see that ψ from (5.22) satisfies Floquet condition (5.9) and one can decompose function ψ that satisfies (5.9) in a form (5.22). We choose to write disturbance in the form

$$\psi = \psi_{new}\, \mathrm{e}^{\mathrm{i}\delta q x}, \tag{5.23}$$

where

$$\psi_{new}(x + 2\pi) = \psi_{new}(x). \tag{5.24}$$

Then substituting (5.23) into (5.16) and (5.17) and omitting $_{new}$, we have

$$\begin{aligned} &s\psi + k^2\left(\psi + k^2\psi'' - 3\delta^2\phi^2\psi\right)'' + \mathrm{i}\delta q k^2\left(2\psi' + 4k^2\psi'''\right) \\ &-\delta^2 q^2 k^2\left(\psi + 6k^2\psi''\right) + \mathrm{O}(\delta^3) + \alpha\psi = 0, \end{aligned} \tag{5.25}$$

Seek a solution in the form

$$\psi = \psi^{(0)} + \delta\psi^{(1)} + \delta^2\psi^{(2)} + \cdots, \tag{5.26}$$

$$s = \delta s^{(1)} + \delta^2 s^{(2)} + \cdots. \tag{5.27}$$

In the zeroth order of (5.16) together with (5.19), (5.20) and (5.26), (5.27)

$$\frac{1}{2}\left(\psi^{(0)} + \frac{1}{2}\psi^{(0)\prime\prime}\right)'' + \frac{1}{4}\psi^{(0)} = 0,$$

$$\psi^{(0)}(x + 2\pi) = \psi^{(0)}(x),$$

hence,

$$\psi^{(0)} = S\sin x + C\cos x. \tag{5.28}$$

In the first order of (5.16) together with ((5.19), (5.20) and (5.26), (5.27)

$$s^{(1)}\psi^{(0)} + \frac{1}{2}\left(\psi^{(1)\prime\prime} + \frac{1}{2}\psi^{(1)\prime\prime\prime\prime} + \kappa^{(1)}\psi^{(0)\prime\prime\prime\prime}\right) + \kappa^{(1)}\left(\psi^{(0)\prime\prime} + \frac{1}{2}\psi^{(0)\prime\prime\prime\prime}\right)$$
$$+\mathrm{i}q\frac{1}{2}\left(2\psi^{(0)\prime} + 4\frac{1}{2}\psi^{(0)\prime\prime\prime}\right) + \frac{1}{4}\psi^{(1)} = 0,$$

hence, taking into account (5.28), we have

$$\frac{1}{2}\left(\psi^{(1)\prime\prime} + \frac{1}{2}\psi^{(1)\prime\prime\prime\prime}\right) + \frac{1}{4}\psi^{(1)} + s^{(1)}\left(S\sin x + C\cos x\right) = 0. \tag{5.29}$$

Disturbance $\psi^{(1)}(x)$ should be 2π–periodic, hence $\left|\psi^{(1)}\right| < \text{const}$, for all x, and hence,

$$s^{(1)} = 0, \qquad \psi^{(1)} = 0. \tag{5.30}$$

In the second order of (5.16) together with (5.18), (5.19), (5.20), (5.26) (5.27)and (5.30)

$$s^{(2)}\psi^{(0)} + \frac{1}{2}\left[\psi^{(2)} + \frac{1}{2}\psi^{(2)\prime\prime} + \kappa^{(2)}\psi^{(0)\prime\prime} - 3\left(\cos x\right)^2\psi^{(0)}\right]^{\prime\prime} + \kappa^{(1)}\left(\kappa^{(1)}\psi^{(0)\prime\prime}\right)^{\prime\prime}$$
$$+\kappa^{(2)}\left(\psi^{(0)} + \frac{1}{2}\psi^{(0)\prime\prime}\right)^{\prime\prime} + \mathrm{i}q\kappa^{(1)}\left(2\psi^{(0)\prime} + 4\frac{1}{2}\psi^{(0)\prime\prime\prime}\right) + \mathrm{i}q\frac{1}{2}\left(4\kappa^{(1)}\psi^{(0)\prime\prime\prime}\right)$$
$$-q^2\frac{1}{2}\left(\psi^{(0)} + 6\frac{1}{2}\psi^{(0)\prime\prime}\right) + \frac{1}{4}\psi^{(2)} + \alpha^{(2)}\psi^{(0)} = 0,$$

hence, taking into account (5.28) and (5.21), we obtain

$$\frac{1}{2}\left(\psi^{(2)\prime\prime} + \frac{1}{2}\psi^{(2)\prime\prime\prime\prime}\right) + \frac{1}{4}\psi^{(2)}$$
$$+\frac{3}{4}\left[S\sin x + C\cos x + \frac{S}{2}\left(3\sin 3x - \sin x\right) + \frac{C}{2}\left(3\cos 3x + \cos x\right)\right]$$
$$+\left(s^{(2)} + q^2 - \frac{3}{8}\right)\left(S\sin x + C\cos x\right) - 2\mathrm{i}q\kappa^{(1)}\left(S\cos x - C\sin x\right) = 0.$$

Disturbance $\psi^{(2)}(x)$ should be 2π–periodic and therefore bounded

$$\left|\psi^{(2)}\right| < \text{const} \qquad \text{for all } x,$$

which holds if and only if

$$\frac{3}{4}\frac{S}{2} + \left(s^{(2)} + q^2 - \frac{3}{8}\right) S + 2\mathrm{i}q\kappa^{(1)} C = 0,$$

$$\frac{3}{4}\frac{3C}{2} + \left(s^{(2)} + q^2 - \frac{3}{8}\right) C - 2\mathrm{i}q\kappa^{(1)} S = 0,$$

hence, we have a homogenous linear system of two equations. It has a nontrivial solution when its determinant is zero, which yields

$$\left(s^{(2)} + q^2\right)\left(s^{(2)} + q^2 + \frac{3}{4}\right) - 4q^2\kappa^{(1)2} = 0,$$

which is a quadratic equation for $s^{(2)}$, and has a root such that $\operatorname{Re} s^{(2)} > 0$ only if

$$q^2 + \frac{3}{4} - 4\kappa^{(1)2} < 0,$$

hence, we obtain

$$\kappa^{(1)2} > \frac{1}{4}\left(q^2 + \frac{3}{4}\right).$$

Thus, instability occurs for some q if

$$\kappa^{(1)2} > \frac{3}{16}. \tag{5.31}$$

To rewrite this criterion in terms k and α, we do the following. Using (5.19), (5.20) and (5.21) we can rewrite (5.31) in the form

$$\frac{\left(k^2 - \frac{1}{2}\right)^2}{\frac{8}{3}\left[\left(\frac{1}{4} - \alpha\right) - \left(k^2 - \frac{1}{2}\right)^2\right]} \gtrsim \frac{3}{16},$$

hence, it follows

$$3\left(k^2 - \frac{1}{2}\right)^2 \gtrsim \frac{1}{4} - \alpha \gtrsim \left(k^2 - \frac{1}{2}\right)^2. \tag{5.32}$$

Using (5.19) to estimate $\delta\kappa^{(1)}$ and substituting the result into (5.32) we obtain

$$6\left(k - \frac{1}{\sqrt{2}}\right)^2 \gtrsim \frac{1}{4} - \alpha \gtrsim 2\left(k - \frac{1}{\sqrt{2}}\right)^2,$$

and finally using $\lambda \simeq 2\sqrt{2}\pi$, we obtain the estimates for the instability region for α close to $\frac{1}{4}$

$$\frac{3}{8\pi^2}\left(\lambda - 2\sqrt{2}\pi\right)^2 \gtrsim \frac{1}{4} - \alpha \gtrsim \frac{1}{8\pi^2}\left(\lambda - 2\sqrt{2}\pi\right)^2.$$

The expression on the left-hand side is, with some error, the same as the borderline of the region of existence (4.8). Solutions are stable when

$$\alpha \gtrsim \frac{1}{4} - \frac{1}{8\pi^2}\left(\lambda - 2\sqrt{2}\pi\right)^2,$$

and α is close to $\frac{1}{4}$.

In the present section we have found out that in weak nonlinear case all periodic solutions are unstable, except at some part of a neighborhood of the point $(2\sqrt{2}\pi, \frac{1}{4})$, where the stability region touches the existence borderline given by (4.8).

5.3 Numerical results

In this chapter we will discuss numerical simulations that were done to examine the stability of periodic spatial solutions of the extended Cahn-Hilliard equation. For a general case of a steady state of Eq.(5.1) we need to solve problem (5.7)–(5.8) numerically. Unlike we did for Cahn-Hilliard in Section 3.7, here we use shooting method with 4-5 order Runge-Kutta integration implemented in Matlab. Likewise Section 4.7.1 there is a mesh on an (λ, α)– plane and a base solution is known at each node as well as an interval of integration. We write Eq.(5.7) as a system of four first-order equations

$$\begin{aligned}
\psi_1' &= \psi_2 \\
\psi_2' &= \psi_3 \\
\psi_3' &= \psi_4 \\
\psi_4' &= -\psi_3(1 - 3\Phi^2) - 12\psi_2\Phi\Phi' - 6\psi_1(\Phi'^2 + \Phi\Phi'') + s\psi_1
\end{aligned} \tag{5.33}$$

Integrating (5.33) four times with initial conditions of the form

$$\psi_i^j(x_0) = \delta_i^j, \qquad i, j = \overline{1, 4},$$

where $\delta_{i,j}$ is a Kronecker delta and index j denotes to the order number of integration, we obtain a general solution of (5.33). To satisfy Floquet boundary condition

$$\psi_i(x + 2\pi) = \psi_i(x_0)\, \mathrm{e}^{\mathrm{i}\theta}, \qquad i = \overline{1,4},$$

the Evans function should be zero

$$\det \left\{ \psi_i^j(x_0 + 2\pi, s) - \delta_i^j\, \mathrm{e}^{\mathrm{i}\theta} \right\} = 0, \qquad i,j = \overline{1,4}. \tag{5.34}$$

System (5.33) and, hence, condition (5.34) depend on eigenvalue s, which is a shooting parameter of the problem. Starting with different initial guess and changing Floquet parameter θ from 0 to 2π it is possible to obtain various eigenvalues of (5.33). On Fig. 5.1 several maximal eigenvalues are shown depending on θ for a certain steady state, which happen to be unstable as there are positive eigenvalues present. If all the eigenvalues are negative a steady state is stable, if even one positive eigenvalue was found, that yields instability. To find the boundary of the region of stability we find a set of such steady states for which the maximal eigenvalue is zero.

The results are presented on Fig.5.2. The region of stability was found numerically. It agrees well with all analytical results obtained in previous sections of this chapter.

- solutions are unstable for $\alpha = 0$, that is the main result of chapter one
- in weak-nonlinear case steady states are unstable as well, which is confirmed in Section 5.1
- there is a contact point at $\alpha = \frac{1}{4}$, where the region of stability touches the existence region's boundary. The shape of the stability region, analytically found in Section 5.2, agrees with the numerical results presented in the present section
- all double-wave solutions are unstable

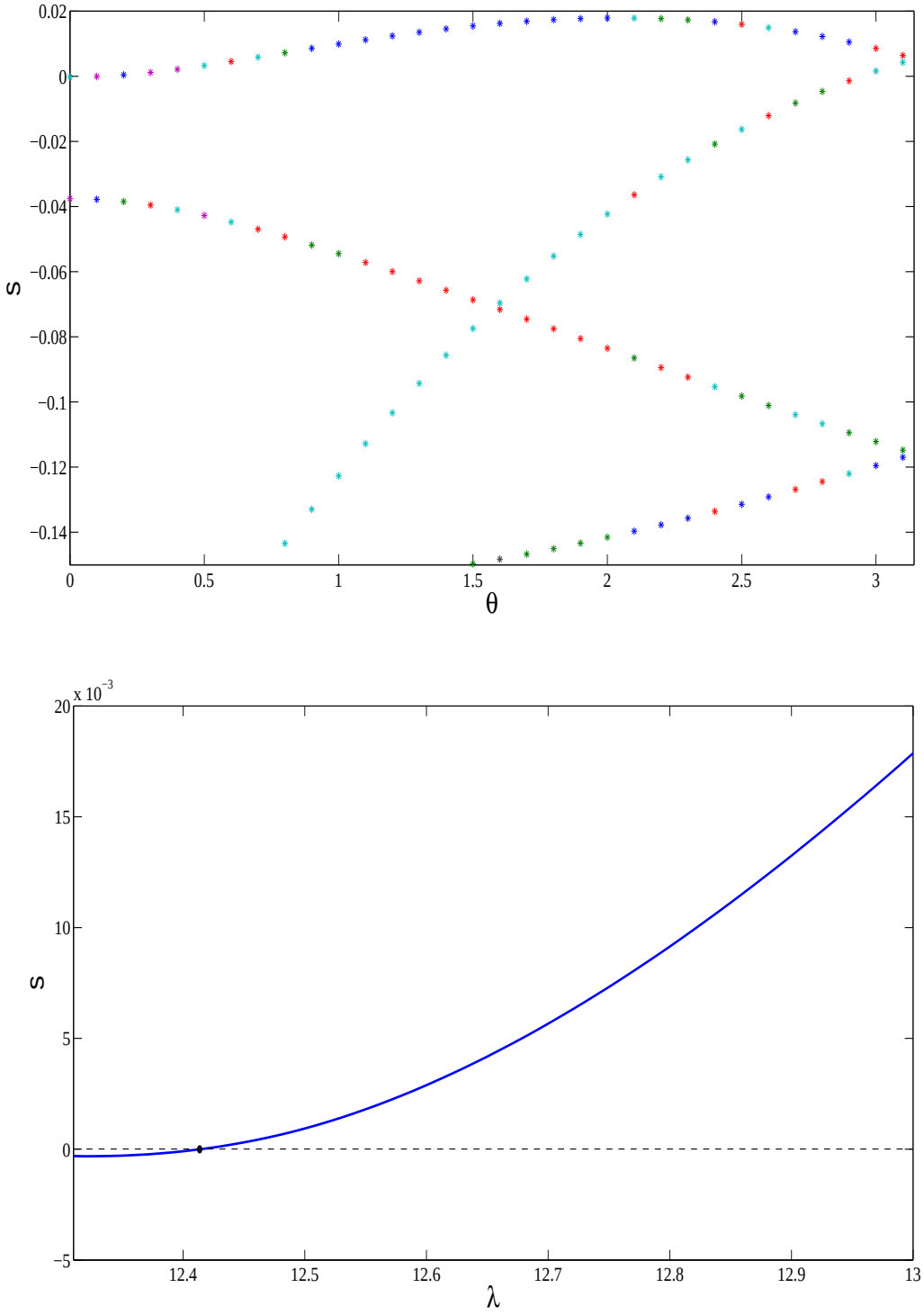

Figure 5.1: In the top figure dependence of several maximal eigenvalues on Floquet parameter θ is shown for a steady state $\alpha = 0.15, \quad \lambda = 13$. In the bottom figure dependence of maximal eigenvalue on the period of a steady state is shown, $\alpha = 0.15$. Dot corresponds to the transition to stable solutions.

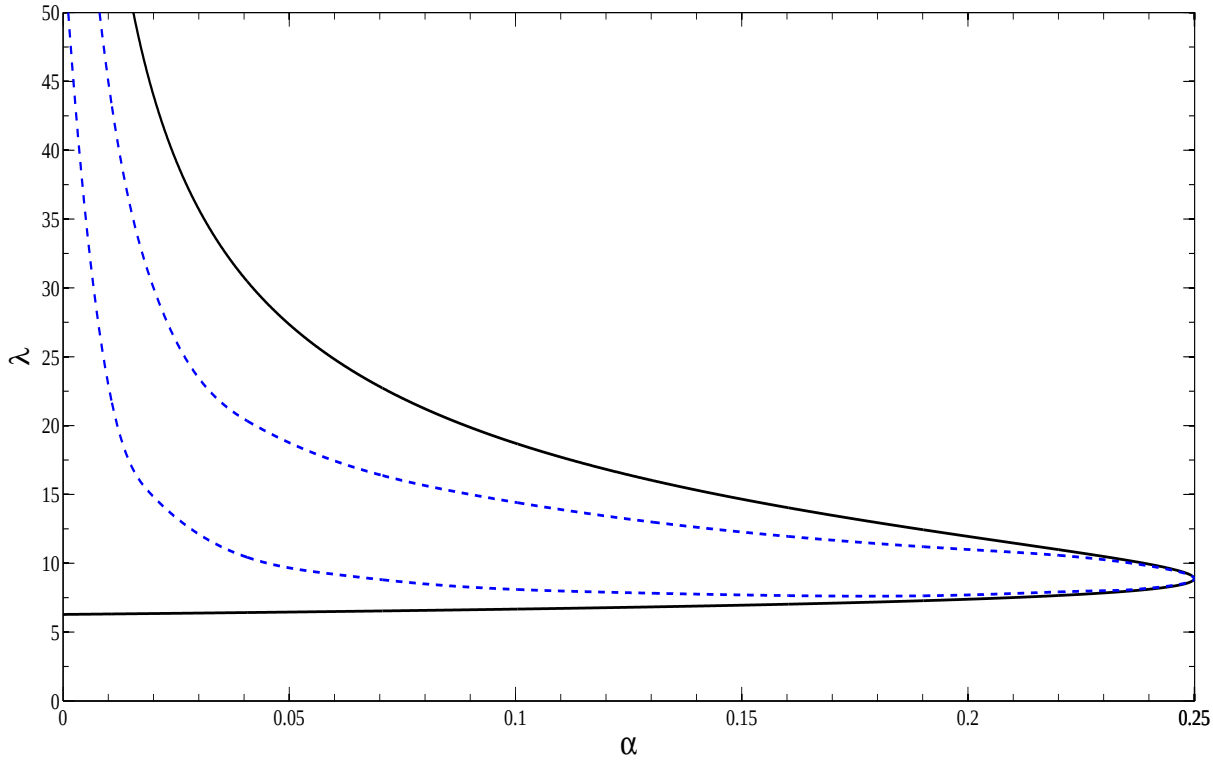

Figure 5.2: Stability region boundary corresponds to the dotted line. Periodic solutions inside the dotted contour are stable. Stability region boundary and existence region boundary have equal tangents at $(0.25, 2\sqrt{2}\pi)$.

5.4 Conclusions

In the present chapter we examined stability of spatial periodic steady states of the extended Cahn–Hilliard equation. We considered steady states with small disturbances and used linear stability analysis to proceed. An eigenvalue problem was obtained and solved for all types of steady states. In the case of weak nonlinearity the eigenvalue problem was solved analytically using perturbation theory. All steady states happen to be unstable, except for the neighborhood of point $(0.25, 2\pi\sqrt{2})$, where the stability region boundary touches the existence region boundary. In the situation of arbitrary parameters α and λ numerical investigation was carried out. The stability diagram was obtained. Stable steady states can be only of single wave type and they exist for any $\alpha \in (0, 0.25]$ and specific λ.

5.5 Comparison with Liu and Goldenfeld results

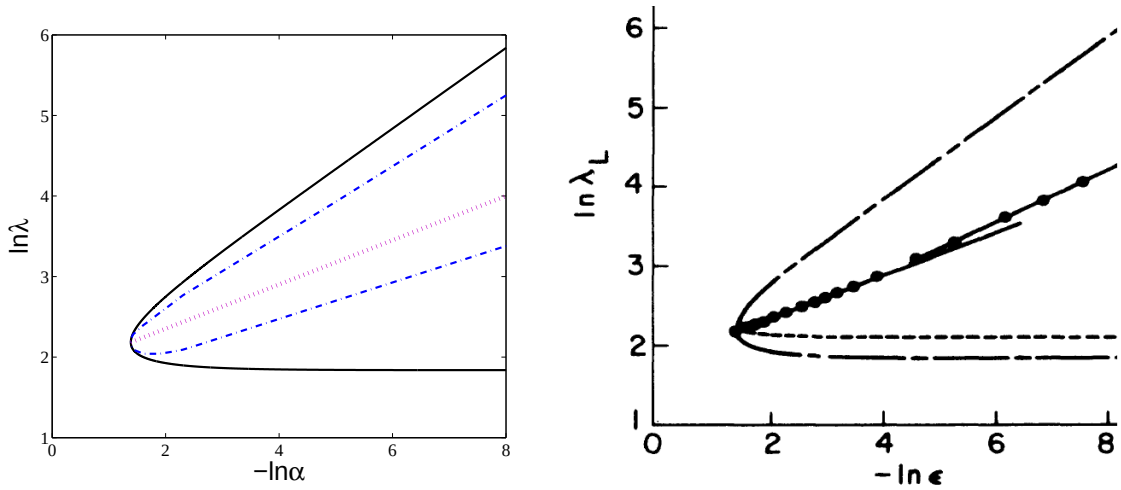

Figure 5.3: Comparison of stability results. In Fig. 5.3(a) the region of stability is shown with dashed lines, dotted line corresponds to the stable solutions from [32]. In Fig. 5.3(b) the original [32] diagram is shown. Parameters α and ϵ are the same.

In Fig.5.3 we compare obtained in this work stability results with the ones obtained in [32]. Liu and Goldenfeld minimized a corresponding to (5.1) free energy functional, given by Eq.(1.3) with respect to a period of the solution. For a fixed α

they found which of the possible nontrivial steady states gives a minima to the free energy, and such solutions are marked with dots on their stability diagram. We see a contradiction with our result, that shows an entire region of stable solutions (instead just a curve) in the the region of existence. What might be an explanation is that there might be another integral, another decreasing in time functional (besides the energy functional) that makes it impossible for any disturbance to change the period of a steady state. Hence, if we consider two steady states (let them be stable in terms of our analysis) for a fixed α and one of them gives a smaller value to free energy functional (1.3), that does not mean that the other state is unstable, because there is no such small disturbance (both Liu and Goldenfeld and us use linear stability analysis) that can transfer a steady state with larger energy to a steady state with smaller energy. To check that, we solved an evolutionary extended Cahn–Hilliard for an arbitrary stable (in our analysis) steady state with disturbances of the form of Liu and Goldenfeld's stable steady states and the system relaxes back to the initial steady state with higher energy.

Chapter 6

Conclusions

6.1 Summary and concluding remarks

In the thesis we examined Cahn–Hilliard equation and its extension. Though, results for Cahn–Hilliard equation are not new we considered it to build up a certain methodology to apply afterwards to the extension of the equation.

In the first part of the thesis we discussed the existence of spatial periodic steady states of the Cahn–Hilliard equation in the full parameter space. We verified the results by examining the phase diagram of the equation, as the system has a first integral that can easily be found. Three regions of existence were found. One with no nontrivial solutions, one with one nontrivial solution (notice that the system allows shifting along the spatial x–axis and we do not consider two solutions being different if one can be derived from another by shifting along the spatial coordinate) and a region where two different nontrivial solutions exist for the same values of parameters λ and a. We also proved that all periodic solutions of Cahn–Hilliard equation are unstable. There is a reasonable explanation to that as Cahn–Hilliard equation governs a global phase segregation of binary melts, therefore, local segregation patterns may exist but not for a long time, as such system tends to attain a complete separation of two components of a melt.

In the second part of the thesis we considered the extended Cahn-Hilliard equation which is more suitable to describe local phase separation. We first examined existence of spatial periodic steady states with respect to parameters of the equation:

λ–period and α– controlling parameter of local segregation. Unlike Cahn–Hilliard equation, extended version has a variety of different regimes of such solutions. It happens that the uniform periodic patterns, where there is a clear alternation of phases present, occur only for either rather small periods or rather large (see Fig.4.5). Inbetween we are in the situation of 3 to 1 waves (see Fig. 4.11) for which complete local segregation does not occur. Moreover, it was found out that all over the (λ, α)–plane there exist an infinite number of regions with extra solutions, which we called two-wave solutions, as they have two different oscillations in the leading order when nonlinearity is weak. Such solutions do not show complete segregation either (see Fig. 4.8). Analytical solutions of all types of steady states mentioned above were found in the case of weak nonlinearity and numerical calculations were done in the general case.

The stability analysis was carried out for all types of periodic steady states of the extension of Cahn–Hilliard equation. It was shown analytically by solving an eigenvalue problem that all steady states in the weak nonlinear case are unstable, except for the neighborhood of the point $(2\sqrt{2}\pi, \frac{1}{4})$. Without an assumption about weak nonlinearity stability analysis were done numerically. The region of stability was found. Only steady states with clear separation of phases can be stable. We can make the following conclusions that are related to the phase separation in diblock copolymers

- the extended Cahn–Hilliard equation shows lamellae spatial periodic patterns in the process of phase separation
- there are limitations to possible geometries of patterns that can be observed for a sufficient period of time, i.e. stable.
- for a particular system with fixed external parameters (α is fixed) there is set of steady states, with periods varying in some range, that system can tend to. It is unclear how to control which steady state the system will stabilize at.

6.2 Future work

In this thesis we examined spatial periodic steady states of the extended Cahn–Hilliard equation, which governs the process of phase transition in diblock copolymer melts, in 1–D. We particulary studied the case of symmetrical polymers (fraction of alike monomers in a molecule $f = 0.5$). There are a number of possible suggestions for future work.

Firstly, it is interesting to study periodic solutions for 2– and 3–D cases. That will give more insight into the process of phase separation. Once this is accomplished, we can think of how the system picks a steady state to tend to, because now for fixed parameters of the system (α is fixed) we have an infinite number of steady states with a range of periods and it is unclear how to pick initial conditions to show a solution with a priori chosen period. For instance, Chen and Chakrabarti proposed to induce a particular pattern using chemically active substrates [10].

Secondly, the model can be extended (for reference see [36]) to the case of non–symmetrical copolymers.

$$\frac{\partial \phi}{\partial t} = M\nabla^2 \left(-b\phi + u\phi^4 + \kappa\nabla^2\phi\right) - B(\phi - 1 + 2f). \tag{6.1}$$

This will allow us to show periodic spherical and cylindrical patterns and their dependence on weight ratio f.

Bibliography

[1] Bahiana, N., Oono, Y. 1990: Cell dynamical system approach to block copolymers. *Phys. Rev. A,* **41**, 6763-6771.

[2] Bates, F.S., Fredrickson, G.H. 1990: Block copolymer thermodynamics – Theory and experiment. *Annu. Rev. of Phys. Chem.,* **41**, 525-557.

[3] Benilov, E.S., Chugunova, M. 2010: Waves in liquid films on vibrating substrates. *Phys. Rev. E,* **81**, 036302.

[4] Brown, G., Chakrabarti, A. 1994: Surface-induced ordering in block copolymer melts. *Journal of Chem. Phys.,* **101**, 3310-3317.

[5] Brown, G., Chakrabarti, A. 1994: Ordering of block copolymer melts in confined geometry. *Journal of Chem. Phys.,* **102**, 1440-1448.

[6] Cahn, J.W. 1961: On spinodal decomposition. *Acta Metallurgica,* **9**, 795-801.

[7] Cahn, J.W., Hilliard, J.E. 1958: Free energy of a non-uniform system. I. Interfacial free energy. *Journal of Chem. Phys.,* **28**, 258-267.

[8] Cahn, J.W. 1959: Free energy of a non-uniform system. II. Thermodynamic basis. *Journal of Chem. Phys.,* **30**, 1121-1124.

[9] Cahn, J.W., Hilliard, J.E. 1959: Free energy of a non-uniform system. III. Nucleation in a two–component incompressible fluid. *Journal of Chem. Phys.,* **31**, 688-699.

[10] Chen, H., Chakrabarti, A. 1998: Morphology of thin block copolymer films on chemically patterned substrates. *Journal of Chem. Phys.,* **108**, 6897-6905.

[11] Choksi, R., Peletier, M., Williams, J.F. 2009: On the phase diagram for microphase separation of dyblock copolymers: an approach via a nonlocal Cahn-Hilliard functional. *SIAM Journal of Applied Math.,* **69**, 17121738.

[12] Choksi, R., Maras, M., Williams, J.F. 2011: 2D phase diagram for minimizers of a Cahn–Hilliard functional with long–range interactions. *SIAM Journal of Applied Dynamical Systems.* **10**, 13441362.

[13] "Spin-coating on nanoscale topography and phase separation of diblock copolymers" 2008. *http://www.macsi.ul.ie/2/esgi70/crann.pdf.*

[14] Douy, A., Gallot, B.R. 1971: Study of liquid-crystalline structures of polystyrene-poolybutadine block copolymers by small angle X-ray scattering and electron microscopy. *Mol. Cryst. and Liq. Cryst.,* **14**, 191-208

[15] Developments in Block Copolymer. 1982, edited by I Goodman.

[16] Developments in Block Copolymer. Science and Technology 2004, edited by Ian W. Hamley.

[17] Helfand, E., Tagami, Y. 1971: Theory of interface between immisible polymers. *Journal of Polym. Science. Part B. Polymer Letters.,* **9**, 741-758.

[18] Helfand, E. 1975: Block co–polymer theory. III. Statistical mechanics of the microdomain structure. *Macromolecules,* **8**, 552-556.

[19] Helfand, E., Wasserman, Z.R. 1976: Block co–polymer theory. IV. Narrow interphase approximation. *Macromolecules,* **9**, 879-888.

[20] Helfand, E., Wasserman, Z.R. 1978: Block co–polymer theory. V. Spherical domains. *Macromolecules,* **11**, 960-966.

[21] Helfand, E., Wasserman, Z.R. 1980: Block co–polymer theory. VI. Cylindrycal domains. *Macromolecules,* **13**, 994-998.

[22] Howard, P. 2009: Spectral analysis of stationary solutions of the Cahn–Hilliard equation. *Adv. Differential Equations,* **14**, 23-55.

[23] Hillert, M. 1961: A solid-solution model for inhomogeneous systems. *Acta Metallurgica,* **9**, 525-535.

[24] Grant, C.P. 1993: Spinoidal decomposition for the Cahn–Hilliard equation. *Commun in Partial Differential Equations,* **18**, 453-490.

[25] Kawasaki, T. 1978: Kinetic–behavior of a double Ising system – Application to phase separation in magnetic binary–alloys. *Progress of Theor. Phys.,* **59**, 1812-1824.

[26] Landau, L.D., Lifshitz, E.M. 1951: Course of Theoretical Physics, Volume 5.

[27] Langer, J.S. 1971: Theory of spinodal decomposition in alloys. *Annals of Physics,* **65**, 53-86.

[28] Laugesen, R.S., Pugh, M.C. 2000: Linear stability of steady states for thin film and Cahn–Hilliard type equations. *Archive for Rational Mechanics and Analysis,* **154**, 3-51.

[29] Lebowitz, J.L., Kalos, M.H. 1976: Computer-simulation of phase separation in a quenched binary alloy. *Scripta Metallurgia,* **10**, 9-12.

[30] Lee, W.T., Delaney, M., Vynnycky, M., Morris, M.A. 2012: Ordering of block copolymer microstructures in corner geometries. Submitted to *Soft Condensed Matter.*

[31] Leibler, L. 1980: Theory of microphase separation in block copolymers. *Macromolecules,* **13**, 1602-1617.

[32] Liu, F., Goldfend, N. 1988: Dynamics of phase separation in block copolymer melts. *Phys. Rev. A,* **39**, 4805-4810.

[33] Matsen, M. W., Schick, M. 1993: Stable and unstable phases of a diblock copolymer melt. *Phys. Rev. Letters,* **72**, 2660-2663.

[34] Novick–Cohen, A., Segel, L., A. 1982: Nonlinear aspects of the Cahn–Hilliard equation. *Physica D,* **10**, 277-298.

[35] Ohta, T., Kawasaki, K. 1986: Equilibrium morphology of block copolymer melts. *Macromolecules,* **19**, 2621-2632.

[36] Oono, Y., Shiwa, Y. 1987: Computationally efficient modeling of block copolymer and Benard pattern formation. *Modern Phys. Lett. B,* **1**, 49-55.

[37] Oono, Y., Puri, S. 1987: Computationally efficient modeling of ordering of quenched phases. *Phys. Rev. Lett.,* **58**, 836-839.

[38] Oono, Y., Bahiana, N. 1988: $\frac{2}{3}$-power law for copolymer lamellar thickness implies a $\frac{1}{3}$-power law for spinodal decomposition. *Phys. Rev. Lett.,* **61**, 1109-1111.

[39] Temple, G. 1938: The general theory of relaxation methods applied to linear systems. *Proceedings of the Royal Society of London. Ser. A, Math. and Phys. Sciences,* **169**, 476-500.